EFFECT OF *TRANS*-CINNAMALDEHYDE-ENCAPSULATED ZEOLITIC IMIDAZOLATE FRAMEWORK-8 NANOPARTICLE COMPLEXES SOLUTIONS ON THE GROWTH OF *E.COLI* O157:H7 AND QUALITY OF FRESH SPINACH LEAVES

A Thesis

by

XIAOYING YANG

Submitted to the Graduate and Professional School of
Texas A&M University
in partial fulfillment of the requirements for the degree of

MASTER OF SCIENCE

Chair of Committee,	Elena Castell-Perez
Committee Members,	Alejandro Castillo
	Rosana Moreira
Head of Department,	Bhimanagouda Patil

December 2021

Major Subject: Food Science and Technology

ABSTRACT

A zeolitic Imidazolate Framework-8 (ZIF-8) is a metal-organic framework (MOF) with good drug delivery capability. This study synthesized and characterized ZIF-8 nanoparticles encapsulated with *trans*-cinnamaldehyde oil (TC) and tested the antimicrobial effect of TC-encapsulated ZIF-8 nanoparticle complexes with 0.1mg/mL poly lysine (PL) coating (TC@ZIF-8_PL) against *Escherichia coli (E.coli)* O157:H7 on fresh spinach.

Several experiments were carried out to determine the antimicrobial activity of different mass ratios of TC-encapsulated ZIF-8. The optimal mass ratio of TC to ZIF-8 for nanoparticles complexes (0.5TC@ZIF-8_PL) was used for the studies. *E.coli* O157:H7 (ATCC 43895) strain, the most reported Gram-negative microorganism associated with foodborne outbreaks in spinach, was used as the target pathogen. Spinach samples were treated with 0.5TC@ZIF-8_PL nanoparticle complexes solution, 200 ppm chlorine, free TC, and sterilized distilled water (control). All sample groups were rinsed for 1 min, dried in a biosafety cabinet, weighted and packed in sample bags, and stored at 4°C for up to 15 days for shelf-life studies. The quality of spinach samples was assessed by monitoring changes in were moisture content (MC), water activity (Aw), color, pH, texture (firmness and work), vitamin C content, total carotenoid, and chlorophyll content.

Throughout the 15 days of storage at 4ºC, spinach treated with 0.5TC@ZIF-8_PL had less ($p<0.05$) water loss, loss of total chlorophyll and total carotenoid, and change in

pH. However, treatments did not prevent the reduction of vitamin C content and color degradation ($p>0.05$) and adversely affected spinach firmness.

DEDICATION

This work is dedicated to my family, my friends, and all people who supported me and enlightened me through my graduate study and life at TAMU.

ACKNOWLEDGMENTS

I would like to express my gratitude to Dr. Castell-Perez, my graduate advisor and the chair of my thesis committee for her kindness, patience, and support in enlightening and guiding me through my research work. And also, thanks to my committee members Dr. Moreira and Dr. Castillo for their valuable opinions on my work.

Thanks also go to Dr. King, Dr. Fulvio, and Dr. Rusyn for their kind support and help with my research experiments.

Finally, thanks to my friends and lab members and the department faculty and staff for making my time at Texas A&M University a great experience.

CONTRIBUTORS AND FUNDING SOURCES

Contributors

This work was supervised by a thesis committee consisting of Dr. Elena Castell-Perez [Chair] and Dr. Rosana Moreira [Member] of the Department of Biological and Agricultural Engineering and Dr. Alejandro Castillo [Member] of the Department of Food Science and Technology.

The data analysis for Chapter 3.1.5 was conducted partly by Lucie Ford of the Department of Veterinary Integrative Biosciences.

All other work conducted for the thesis was completed by the student independently.

Funding Sources

All research work was completed without outside financial support.

NOMENCLATURE

°C	Degree Celsius
°F	Degree Fahrenheit
2-mim	2-methylimidazole
2TSB	Double Strength Tryptic Soy Broth
ATCC	American Type Culture Collection
Aw	Water Activity
CDC	Centers for Disease Control and Prevention
CDT	Chemodynamic Therapy
DI	Deionized
DMEM	Dulbecco's Modified Eagle Medium
E.coli	*Escherichia coli*
EE	Encapsulation Efficiency
EtOH	Ethanol
FBS	Fetal Bovine Serum
FDA	U.S Food and Drug Administration
FMI	Food Industry Association
GFP	Green Fluorescent Protein
GRAS	Generally Recorded as Safe
h	Hour
HCl	Hydrochloric acid

HPCD	Hydroxypropyl-β-cyclodextrin
HUS	Hemolytic-uremic Syndrome
L	Liter
LB	Luria Bertani
LEO	Lavender Essential Oil
MC	Moisture Content
MIC	Minimum Inhibitory Concentration
min	Minute
mL	Milliliter
MOF	Metal-Organic Framework
nm	Nanometer
NP	Nanoparticles
PBS	Phosphate Buffered Saline
PDL	α-poly-D-lysine
PDT	Photodynamic Therapy
pH	Potential of Hydrogen
PL	Poly-lysine
PLL	α-poly-L-lysine
psi	Pounds per Square Inch
PTT	Photothermal Therapy
PW	Peptone Water
RPM	Rotates per Minute

SEM	Scanning Electron Microscope
SMAC	MacConkey Agar containing Sorbitol
STEC	Shiga toxin-producing *Escherichia coli*
TAB	Tetrabutylammonium Bromide
TC	*trans*-Cinnamaldehyde
TSA	Tryptic Soy Agar
TSB	Tryptic Soy Broth
USDA	U.S. Department of Agriculture
UV-Vis	Ultraviolet visible
w/v	Weight/volume
ZIF	Zeolitic Imidazolate Framework
ZIF-8	Zeolitic Imidazolate Framework-8
μg	Microgram
μL	Microliter
μM	Micromolar

TABLE OF CONTENTS

Page

LIST OF FIGURES

Page

LIST OF TABLES

Page

1. INTRODUCTION

Fresh produce is an excellent source of many essential nutrients, such as vitamins, minerals, and fiber, and their consumption is associated with decreased risk of chronic diseases such as cardiovascular disease, type 2 diabetes, and cancer (Slavin & Lloyd, 2012). As people pay more and more attention to healthy food and nutrition, the sales of fresh produce have increased significantly especially during the pandemic of COVID-19, as a healthy diet might reduce the risk of negative outcomes from virus infection (Zabetakis et al., 2020; Iddir et al., 2020). According to "Agricultural Products Power in 2021" made by the Food Industry Association (FMI), the sales of the fresh product will reach 69.6 billion U.S. dollars, an increase of 11.4% compared with 2020, and at the same time, consumers purchased more fresh agricultural products than before the COVID-19 pandemic, with more fresh fruits (8.9% increase) and vegetables (14.2% increase) (FMI, 2021).

Spinach has high nutritional value because it contains various kinds of vitamins (especially C, E, β-carotene), folic acid, mineral components (especially the high concentration of magnesium for 55±16 mg ca/100 g) (Kawashima & Soares, 2003), and dietary fiber (Lisiewska et al., 2009) as well as high antioxidant capacity compared to all vegetables (Jaworska, 2005). The U.S. per capita consumption of spinach was more than 2.26 pounds in 2020 (Shahbandeh, 2021). Although not as large as onions and potatoes, leafy vegetables are more susceptible to pathogens than roots (Sinha et al., 2005). Once the leaf tissues are damaged, there might be multiple changes to shorten shelf life such as

the increased respiration rate, accelerated moisture loss, and the wounded lettuce cells provide an easier way for microorganisms to penetrate (Kim et al., 2010).

Foodborne illnesses account for a large part of the annual disease outbreaks in the United States, especially those related to fresh produce. According to the Centers for Disease Control and Prevention (CDC) reports (CDC, 2020), there have been more than 40 outbreaks of diseases related to fresh food in the last ten years, and hundreds of cases have been reported in recent five years related to fresh spinach. Even though the CDC has published a series of regulations and plans for the safe consumption of spinach, it is impossible to measure whether they can be implemented in every step from the farm to the table.

With the development of food preservation technology becoming more and more mature, compounds with antibacterial functions are used in food preservation. Among them, natural substances extracted from herbs or plants have become an interest in replacing traditional chemical additives (Nychas, 1995) as their functionalities are mostly gained from essential oil fractions (Deans & Ritchie, 1987). Multiple types of essential oils have antibacterial and antifungal activities, such as *thymol* (Pandey et al., 2021), eugenol, and *trans*-Cinnamaldehyde (TC) (Pateiro et al., 2021), whose activities have been proven with different types of microorganisms. However, as an antibacterial agent, essential oils have limited application in foods due to their high volatility, poor water solubility, and even bring bad flavor to foods (Kalemba & Kunicka, 2003).

Nanoparticles are defined as particle dispersions or solid particles with a size in the range of 10-1000 nm. The dissolution, retention, encapsulation, or attachment of drugs,

especially essential oils, to the nanoparticle matrix, can prevent the sensory properties from being transferred to the food, increase its water solubility, reduce its volatility, and provide pathogens with effective antibacterial properties (Mohanraj and Chen, 2006; Hill, 2014). Metal-organic frameworks (MOFs) are crystalline materials composed of metal ions or clusters bridged by organic ligands to form an infinite one, two, or three-dimensional network and are becoming one of the fastest-growing fields in the fields of chemistry and materials science (Lin et al., 2014). ZIF-8 is a special member of ZIFs, which have specific thermal and chemical stability and have been used in various drug delivery studies (Ho et al., 2020). However, research on the direct application of drug-encapsulated ZIF-8 particles to foods, especially leafy greens is lacking.

The main goal of this study was to test the effectiveness of encapsulating a natural antimicrobial, *trans*-Cinnamaldehyde (TC), using ZIF-8 nanoparticles, and its suitability for use in fresh produce safety applications. The specific objectives to achieve the main goal were to:

1. Develop and optimize a method to synthesize and characterize the ZIF-8 nanoparticles to encapsulate TC.

2. Test the efficacy of application methods of solutions of ZIF-8 nanoparticles with entrapped TC to inactivate *E.coli* O157:H7 on fresh spinach leaves.

3. Determine whether the applied ZIF-8 nanoparticles with entrapped TC have a detrimental effect on the quality and shelf life of fresh spinach leaves.

2. LITERATURE REVIEW

2.1. Foodborne Illness Related to Leafy Greens

According to the Centers for Disease Control and Prevention (CDC), around 48 million Americans are affected by foodborne diseases each year, resulting in 128,000 hospitalizations and 3,000 deaths (CDC, 2018a). The CDC has received more and more outbreak reports related to foodborne pathogens in the past ten years. From 1998 to 2008, 46% of foodborne diseases were caused by agricultural products such as fruits, nuts, fungi, leafy vegetables, root vegetables, sprout vegetables, and cane vegetables. Between 2005 and 2011, outbreaks caused by agricultural products were more prominent, with more disease cases than outbreaks related to other non-leafy-green agricultural produce (Olaimat and Holley, 2012; Painter et al., 2013). This difference may be since many fresh produce products, especially leafy greens, are eaten raw, and there is no opportunity for pathogen-killing steps (Turner et al., 2019).

Besides, leafy vegetables were the second and fifth most common causes of hospitalization and death from foodborne diseases (Painter et al., 2013). In the infections linked to fresh spinach in 2006, 199 persons got infected from 26 states with 51% hospitalization, and 16% developed a type of kidney failure named hemolytic-uremic syndrome (HUS) (CDC, 2006). There was also a recall of the Organic Spinach and Spring Mix blend due to *E. coli* O157:H7 contamination in 2012 (CDC, 2012).

Agricultural products are distributed over large geographic areas in the United States; therefore, the incidence of outbreaks is relatively low (Turner et al., 2019). At the

same time, the short shelf life and rapid turnover of agricultural products make it challenging to trace contaminated before the end of the epidemic, as harvesting and distribution are usually completed before the affected fields are identified (Arnade et al., 2009; Lynch et al., 2009). However, since most pathogens associated with foodborne diseases are related to several different types of agricultural products, historical data on pathogen strains can help identify possible sources of contamination more quickly. At the same time, the outbreak of foodborne diseases also relates to the season to a certain extent: it usually peaks in spring, and the second smaller peak occurs in autumn. (Sivapalasingam et al., 2004).

In the United States, bacterial pathogens such as *Escherichia coli*, *Salmonella*, and *Listeria monocytogenes* have been identified as common causes of foodborne illness. Shiga toxin-producing *Escherichia coli* (STEC) is one of the most often causes illness transmitted by leafy vegetables according to the Centers for Disease Control and Prevention (CDC) analysis in the United States from 1973-2012 (Herman et al., 2015), and the STEC serogroup found most commonly in U.S. patients is *E. coli* O157. Of the approximately 265,000 STEC infections in the United States each year, 36% are caused by *E.coli* infection (CDC, 2018b). There are many contamination factors in fresh vegetables such as soil, improperly composted animal manure (Whipps et al., 2008), domestic animals and wildlife (Stuart et al., 2006; Berger et al., 2010), seasons (Lynchs et al., 2009), irrigated water (Getting et al., 2011) and also some postharvest processing as storage conditions and packaging. As for leafy vegetables, contaminated water was a common source of pollution (Luna-Guevara et al., 2019).

Microbial contamination can be controlled by proper cleaning and disinfection in the food industry. The use of sterile water, the design of the equipment, regular monitoring of microbial growth can help to detect the existence of pathogens (Chatterjee & Abraham, 2018). Some physical and chemical methods are also widely used during food processing but are not suitable for fresh leafy produce. The natural and effective technology for inhibiting pathogen growth and increased shelf and qualities is still beginning.

2.2. The Application of Essential Oils as Natural Antimicrobials

2.2.1. Essential Oils as Natural Antimicrobial

Due to the abuse and improper handling of antibiotics and consumer awareness of health, the use of natural antimicrobial compounds in food preservation has attracted widespread attention from consumers and the food industry (Gyawali & Ibrahim, 2014). Antimicrobial agents can be added directly to product formulations, coated on their surface, or incorporated into packaging materials to inhibit the growth of undesirable microorganisms in food (Appendini & Hotchkiss, 2002; Hanušová et al., 2009). The main natural compounds are essential oils derived from plants, enzymes obtained from animal sources, bacteriocins from microbial sources, organic acids, and natural polymers (Del Nobile et al., 2012).

Plant essential oils have received widespread attention in the food industry due to their potential as detergents and are Generally Recorded as Safe (GRAS) (Del Nobile et al., 2012). The active ingredients are ubiquitous in essential oil fractions, and most of them have broad-spectrum antibacterial activity against food-borne pathogens and spoilage bacteria (Gutierrez et al., 2009), especially for Gram-positive bacteria (Marino et al.,

2001). The chemical structure of plant essential oil components determines their antibacterial activity, especially the presence of hydrophilic functional groups, such as the hydroxyl groups of phenolic components or the lipophilicity of some essential oil components (Dorman & Deans, 2000). Besides, by-product produced by natural plants can also be used as a source of antibacterial compounds, significantly saving production costs (Gyawali & Ibrahim, 2014). Generally, thyme oil, clove oil, sage oil, and other compounds with phenolic groups are the most effective (Skandamis et al., 2002).

Additionally, essential oils were also reported in other areas which benefit human beings besides antimicrobial effects. Nigella sativa L, the essential oil of black cumin seeds, has the potential to treat inflammatory diseases because of its radical scavenging capacity (Burits & Bucar, 2000). The lavender essential oil can be effectively used in cosmetic and therapeutic settings due to its biological activities (Cavanagh & Wilkinson, 2002). Besides its potent antimicrobial and antifungal effect, the function of Eucalyptus in insect repellent, herbicidal, acaricidal, and nematocidal can also be widely used (Barish et al., 2008).

2.2.2. *trans*-Cinnamaldehyde as Natural Antimicrobial

Cinnamon spice is obtained from the inner bark of trees within the genus *Cinnamomum* and contains about 250 species (Vasconcelos et al., 2018). The most common species are *C. cassia* (Chinese assia, usually called Cassia) and *C. verum* (also known as *C. zeylanicum*, often called true cinnamon), they contain up to 85.3% and 90.5% of cinnamaldehyde, respectively (Shreaz et al., 2016). It is well known that cinnamaldehyde has a variety of bioactive properties that many therapists claim that

cinnamaldehyde can effectively lower blood sugar levels (Qin et al., 2003) and promote blood lipid-lowering effects (Kannappan et al., 2006). Moleyar & Narasimham (1992) tested fifteen essential oil components towards foodborne *Staphylococcus* sp., *Micrococcus* sp., *Bacillus* sp., and *Enterobacter* sp. and found that cinnamic aldehyde was the most effective one that it can completely inhibit the bacterial growth for more than a month at 30℃ at a concentration of 500 μg/mL.

The trans isomer of cinnamaldehyde was naturally the main structure as Figure 2.1 shows, which becomes the source of flavor and odor of cinnamon (Transport Information Service, 2021). Generally Recognized as Safe (GRAS) by the United States Food and Drug Administration (FDA), it is also the main component why cinnamon spice has antibacterial properties (Baskaran et al., 2010; Gill & Holley, 2004; Kwon et al., 2003; Visvalingam et al., 2013). *Trans*-Cinnamaldehyde (TC) can not only effectively inhibit the growth of a series of microorganisms (such as bacteria, molds, and yeasts), but also inhibit the toxins produced by microorganisms (Kwon et al., 2003; Gill & Holley, 2006; Yossa et al., 2012; Friedman, 2017).

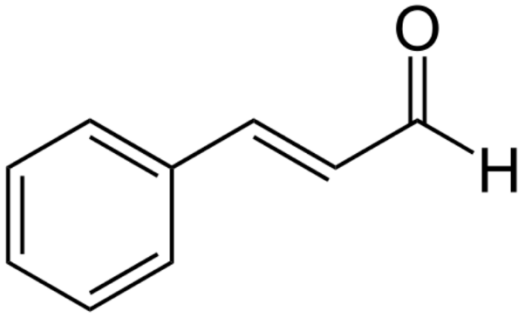

Figure 2.1 Chemical structure of *trans*-cinnamaldehyde.

However, the application of TC has been restricted for the following reasons: 1) its special and unique flavor and taste (Moleyar & Narasimham, 1992), sometimes may influence other components; 2) the lower solubility in water with approximately 1.1g/L at room temperature (Ashakirin et al., 2017); 3) very sensitive to air and light which may influence its function when long-time exposure (Ashakirin et al., 2017) and 4) TC needs to be decomposed into cinnamic acid under the catalysis of enzymes in the body to exert its antibacterial activity so that it may be unstable in the blood (Vasconcelos et al., 2018). Not only TC, but the low solubility of essential oil components in water significantly affects their antibacterial activity, as their antibacterial ability is reflected in the solubility of phospholipid double layer of the cell membrane, and low water solubility inhibits its penetration of bacteria or fungal cells (Knobloch et al., 1989). Thus, a method or technology which can help enhance their delivery is urgently needed and widely interested.

2.3. Metal-Organic Framework Nanoparticles

Metal-organic frameworks (MOF) are a 3D order composed of inorganic clusters linked with organic units through strong bonds (Furukawa et al., 2013; Wang et al., 2018). When inorganic units containing metal, which will result in higher porosity, greater surface area, variability and diversity of porous, high thermal and chemical stability of MOF structure (Furukawa et al., 2013). These functionalities let them apply in various range of areas such as gas storage and separations (Eddaoudi et al., 2002), chemical sensing (Kreno et al., 2010), membranes (Bae et al., 2010), catalysis (Lee et al., 2009), and drug delivery (Horcajada et al., 2010).

Nanoscale form of MOF, also known as MOF nanoparticles (NPs), can be precisely controlled with predictable size and shape and show significant potential in use in the areas of catalysis, separations, nanomedicine, and membranes (Furukawa et al., 2013; Wang et al., 2018). The characteristics of NPs are highly related to their size and surface (Khan et al., 2019), while the uniformed size and well-defined surface chemistry of MOF NPs (Wang et al., 2018) can not only provide themselves with substantial structural diversity, the porous nature caused by thein composition also contributes to the reloadability and release of drugs (Wuttke et al., 2017). The interactions between the particles and the drug are limited to the inside of the particle, while the outside of the particle handles the physiological interaction and global targeting (Wuttke et al., 2017). In addition, the high loading capacity and low toxicity results of MOF NPs in mouse phagocytosis assays (Horcajada et al., 2010) also provide ideas for their safe application in food.

The dissolution, retention, encapsulation, or attachment of drugs, especially essential oils, to the nanoparticle matrix, can prevent the sensory properties such as color, odor and taste from being transferred to the food, increase its water solubility, reduce its volatility, and provide pathogens with effective antibacterial properties (Mohanraj & Chen 2006; Hill, 2014). Besides, MOF NPs are also widely used in the area of clinical medicine, and they can be used as multifunctional nanomedicine of cancer (Rowe et al., 2009), as a member of photodynamic therapy (PDT) of cancer (Lismont et al., 2017) and also for Magnetic Resonance Imaging (MRI) (Peller et al., 2018).

2.3.1. Zeolitic Imidazolate Framework

Zeolitic Imidazolate Framework (ZIF) is one of the subclass members of MOF, composed of imidazolate linkers and metal ions metal, among them, the divalent metal cation is connected to the tetrahedral framework that often has a zeolite topology through the imidazolium anion as (Cravillon et al., 2009; Chen et al., 2014; Yao & Wang, 2014; Ho et al., 2020). ZIFs have the advantages of zeolitic and MOFs, including crystallinity, micro-porosity, high surface area, specific thermal and chemical stability, and have been widely used in drug delivery (Venna et al., 2010; Yao & Wang, 2014; Ho et al., 2020). ZIFs can exist in powder base or ZIF-based films and membranes (Chen et al., 2014). The framework of ZIFs compounds are very similar to that of zeolite, that is, T-O-T bridge (T = Si, Al, P) in zeolite is replaced by M-Im-M bridge (M = Zn, Co), and coincidentally, the two joint angles is 145° (Venna et al., 2010), which provides structural support for its outstanding properties and functions, especially in some emerging functional applications such as gas separation (Venna & Carreon, 2010), catalysis(Jiang et al., 2009), and sensing (Lu & Hupp, 2010).

2.3.2. Zeolitic Imidazolate Framework-8

Zeolitic Imidazolate Framework-8 (ZIF-8) is a particular member of ZIFs. The large pores, large inner crystallite surface area, and the exceptional thermal and chemical stability have made ZIF-8 one of the most widely applied and established ZIFs materials (Cravillon et al., 2009; Venna & Carreon, 2010). The following advantages: 1) composition of ZIF-8 (Zn^{2+} and 2-methylimidazole) are all bio-friendly, 2) simplicity of

nano-scale preparation, 3) high loading capacity, and 4) its biodegradability at pH < 6 make them highly applicated to drug delivery system (Li et al., 2018).

The formation mechanism of the zeolite imidazolate framework is fundamental to improving the structure and morphology control in synthesizing these new materials. Venna et al. (2010) explored the evolution of the ZIF-8 structure over time at room temperature (Figure 2.2). The authors determined the formation of ZIF-8 at different stages: 1) 0 < t <10 minutes, the nucleation of the ZIF-8 phase requires a specific incubation time, which corresponds to the nucleation stage, 2) After nucleation, there is a growth stage, and the relative crystallinity of ZIF-8 increases with time during this period and reaches its maximum in about 60 minutes, and 3) in the stationary phase (t> 60 minutes), the relative crystallization rate of ZIF-8 remains relatively constant with the consumption of the metastable phase.

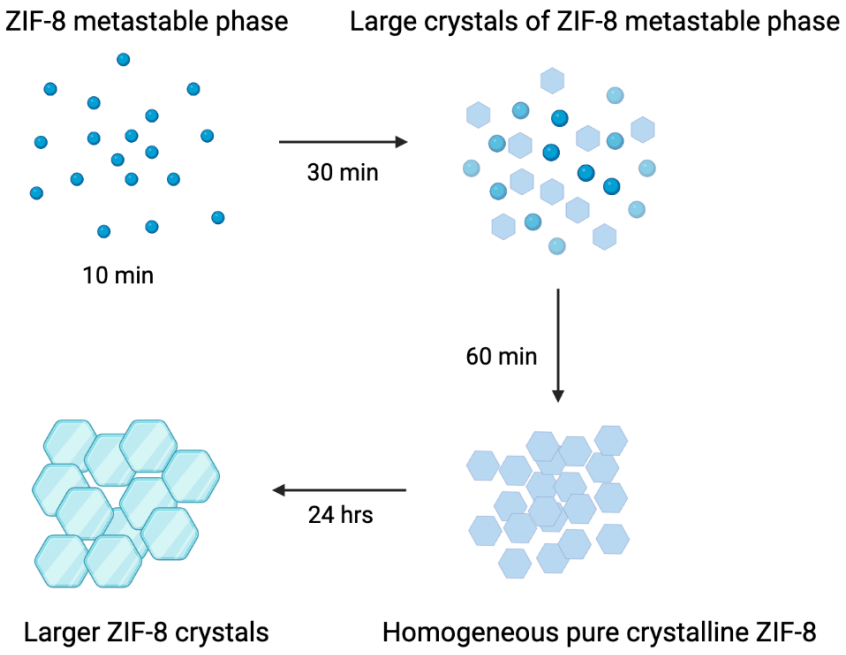

Figure 2.2 Proposed formation pathway of ZIF-8 as a function of synthesis time.

The synthesis of ZIF-8 has been achieved by hydrothermal in water or solvothermal synthesis in organic solvents, with varied temperature and time (Tranchemontagne et al., 2008). ZIF-8 mainly exists in particles made by de-solvation or separated from other mixtures (Chen et al., 2014). In the field of solvent synthesis, organic solvents (Yaghi et al., 2006) are usually used as the reaction medium, especially methanol, which can not only adjust the crystal size (Cravillon et al., 2011) but also can rapidly yield crystallization with the use of additives (such as the ligand sodium formate) (Cravillon et al., 2012). However, organic solvents are expensive and not environmentally friendly.

Production of ZIF-8 in aqueous solution at room temperature was initiated by Pan et al. (2011) and Tanaka et al. (2012). Ionic thermal methods are also commonly used for the synthesis of ZIF-8, ionic liquids are used as solvents and template agents (structure directing agents) (Parnham & Morris, 2007). Green solvents, such as ionic liquids (Martins et al., 2010; Yang and Lu, 2012), are commonly used, which can be used not only as solvents (Parnham and Morris, 2007), but also recycled. Sonochemical methods are also used in the synthesis of ZIF-8 contributing to the uniform dispersion and nucleation of nanoparticles (Qin et al., 2010). However, considering cost and efficiency issues, solvent minimization has become more acceptable (Garay et al., 2007; Stock and Biswas, 2012). For example, Lin et al. (2011) can efficiently prepare porous/zeolitic metal azelate skeletons by heating a mixture of metal oxides/hydroxides and azole ligands, with water as the only by-product; Cliffe et al. (2012) describe an "accelerated aging" method for the synthesis of metal-organic materials. In a static, non-stirred reaction mixture, ZnO is catalytically and topologically specific converted to an unusual dense stacked zeolite

imidazole ester skeleton (ZIF) species. ZIF-8 can also be synthesized mechanochemically, especially by hand grinding (Fernández-Bertrán et al., 2012). The authors used imidazole and oxide in stoichiometric amounts was carried out by hand milling of small samples for 20 min.

2.3.3. Applications of ZIF-8 in Drug Delivery

ZIF-8 has many relevant properties, such as good dispersibility, high loading capacity, excellent thermal and chemical stability, and pH-sensitive degradation as mentioned above. sun et al. (2012) reported that ZIF-8 has a high surface area (BET: 1630 $m^2 \bullet g^{-1}$) and large pores (11.6 Å). Since both Zn ions and MIM are physiological components, ZIF-8 composed of them is pH sensitive (Lu et al., 2012; Venna et al., 2010). pH triggered activation of ZIF-8 is attributed to protonation of imidazole, which leads to disintegration of ZIF-8. High thermal and chemical stability of ZIF-8 has also been reported (Park et al., 2006). All these properties make ZIF-8 a suitable carrier for drug delivery.

The pH of the tumor tissue region (pH 5.5-6.0) is more acidic than in blood and normal tissue (pH 7.4), and the use of pH-responsive drug carriers can enhance the effective release of antitumor drugs into the tumor tissue or cells (Sun et al., 2012). Due to the pH-sensitive nature of ZIF-8 (rapid breakdown in acidic solutions), it can be used as an attractive pH-responsive drug delivery system at tumor sites. For instance, Zheng et al. (2016) entrapped the doxorubicin (DOX) in ZIF-8 at pH 7.4 while the drug was gradually released in the tumor site rather in blood.

The high loading capacity of ZIF-8 also makes it a potential choice for drug encapsulation. Zhang et al. (2016) obtained a capacity of up to 20% (wt) for DOX-encapsulated ZIF-8, while Liédana et al, (2012) encapsulated caffeine in ZIF-8 and observed a higher drug loading (~28 wt%).

In the field of cancer treatment, ZIF-8 has also shown great potential as a nanocarrier for multiple therapeutic agents such as photothermal therapy (PTT), photodynamic therapy (PDT), and chemodynamic therapy (CDT) (Feng et al., 2021). The biodegradable property and no long-term toxicity made ZIF-8 a suitable carrier for photothermal agents (Feng et al., 2021). Li et al. (2018) loaded Cyanine (Cy) into ZIF-8 to exhibit excellent photothermal conversion efficiency. The same was observed with the ZIF-8-based Indocyanine Green (ICG) theragnostic system made by Wang et al. (2018), which showed a favorable photothermal killing capacity.

ZnPc@ZIF-8 can be a good choice in photodynamic therapy (PDT) as their monomeric state can prevent self-aggregation. The particles can be completely degraded after therapy due to their pH-sensitive property (Xu et al., 2018). Chen et al. (2019) prepared the hybrid nanocarrier NaClO@ZIF-8@Pluronic F68. Through the synergistic effect of nanocarriers and ascorbic acid, the production of intracellular singlet oxygen was confirmed in 4T1 cells, thereby inducing significant cell apoptosis.

In protein and genome edit, ZIF-8 can also be a good choice of carrier. Encapsulating the protein in ZIF-8 can protect the protein from conformational changes under adverse conditions (Liang et al., 2015). As mentioned above, ZIF-8 has a unique

pH-sensitive ability and shows the potential to evade the endocytic pathway (Li et al., 2015), thus providing an effective method for the delivery of gene-editing tools.

Nevertheless, as a drug delivery carrier, ZIF-8 may have the following disadvantages: (1) The ZIF-8 material needs to be biocompatible in medicine, and (2) the biodegradability of ZIF-8 may affect the efficacy and therapeutic effect of the drug (Feng et al., 2021).

2.4. Poly-lysine Coated Nanoparticles

Although use of nanoparticles in drug delivery approach is not a new concept, no matter which method is used to synthesize, the increased surface energy caused by the surface interaction can make the nanoparticles aggregate into a more thermodynamically stable state (Merisko & Liversidge, 2008). Poly-lysine (PL) is a polymer from the homopolymers group produced due to differences in stereochemistry and connection positions. Figure 2.3 illustrates the polymerization at the α-carbon position produces α-Polylysine, and the difference in the chirality of the central carbon atom results in α-poly-L-lysine (PLL) and α-poly-D-lysine (PDL) (Hiraki, 1995).).

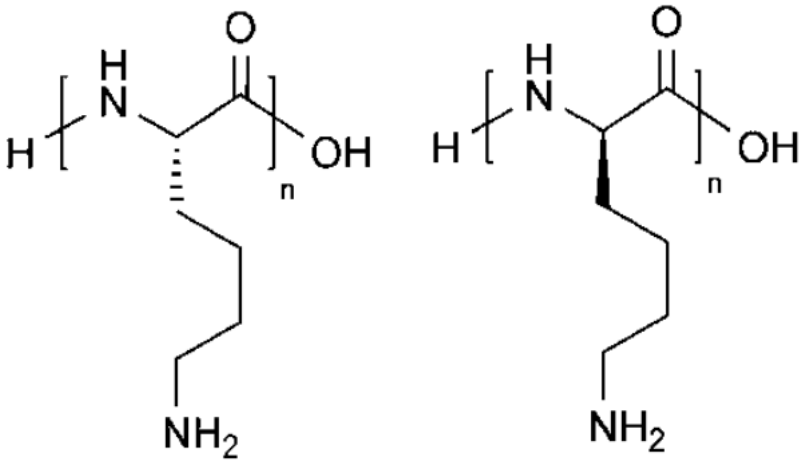

Figure 2.3 Chemical structure of alpha-poly-L-lysine (PLL) (right) and alpha-poly-D-lysine (PDL) (left).

Poly-L-lysine (PLL) has a flexible structural framework and many active amino groups, which provide good biocompatibility and relatively good solubility in water and thus promotes drug delivery and cell adhesion (Shan et al., 2009). Considering this, the application of PLL in nanoparticles as stabilizers and surfactants is no longer novel. Singn et al. (2010) observed that PLL can help improve the stability of bovine serum albumin (BSA) nanoparticles in an aggressive protein hydrolysis environment. PL-coated copper nanoparticles (CuNPs) showed excellent water-solubility and made this dispersion stable for more than 3 months (Ouyang et al., 2013).

PL has also been reported to have antimicrobial activity. Stored at 12°C for 6 days, PL exhibited antibacterial activity against *E. coli* O157:H7, *Salmonella* typhimurium and *Listeria monocytogenes* in six foods (milk, beef, rice, bologna, broccoli, cauliflower) and broth (Georgnaras et al., 2007). In addition to the antimicrobial activity itself, PL coating

reported to enhance the antimicrobial activity of the nanoparticles. For instance, PL-coated silver nanoparticles (AgNPs) have enhanced antimicrobial effect both for Gram-positive (*S. aureus*) and Gram-negative (*P. aeruginosa*) microorganisms which is high enough to achieve a bactericidal effect (Ghilini et al., 2018). PL-coated CuNPs can also help to disrupt the ion solution inside the cells and thus increase the antimicrobial effect on both *Escherichia coli* and *Staphylococcus aureus* (Ouyang et al., 2013).

2.5. The Application of Encapsulated Nanoparticles as Antimicrobials

Nanotechnology is a method for improving the efficiency of antimicrobial treatments (Yuan et al., 2018). Nanomaterials and nanoparticles, in particular, have demonstrated antimicrobial activity against both Gram-negative and Gram-positive bacteria, mycobacteria, fungi, viruses, bacteriophages, broad-spectrum protozoa, and algae (Luksiene, 2017; Wang et al., 2017; Fernando et al., 2018). Nanoparticles as antimicrobial agents are carried out mainly by two aspects, including the antimicrobial action of the nanoparticles themselves or as carriers for the delivery of other antimicrobial agents (Srividya et al. 2017; Wang et al. 2017; Varier et al. 2019). In particular, as carriers aimed at delivery systems to improve the function of natural antimicrobial agents (Rafiee et al., 2019).

Through encapsulation technology, natural antimicrobial agents are packed into particles. The wall material protects the target compounds from harsh conditions and controls their release, thus enhancing the antimicrobial activity (Yousefi et al. 2019; Dima et al., 2020). As for essential oils, the nano-encapsulation technology can improve their bioavailability, protect them from degradation phenomena, increase solubility and

physical stability, reduce volatility, and mask the strong aroma (Weiss et al., 2009; Ferreira & Nunes, 2019; Liao et al., 2021). For example, low water solubility and low stability are two harmful properties of lavender essential oil (LEO), which limit its antibacterial activity. When LEO is encapsulated in hydroxypropyl-β-cyclodextrin (HPCD), its antibacterial activity against *Escherichia coli*, *Candida albicans*, and *Staphylococcus aureus* is increased by about 3 times (Yuan et al., 2019).

It has been proven that nanoparticles can destroy microbial cell membranes by penetration and abrasion and then induce intracellular antibacterial effects, such as the production of reactive oxygen species (Wang et al., 2017), interaction with DNA/RNA and proteins (Fernando et al., 2018), inactivating enzymes (Varier et al., 2019), reducing the permeability of cells (Abduraimova et al., 2021), releasing metal ions (Liu et al., 2019), and hindering the formation of biofilms (Fernando et al., 2018). The antibacterial activity of nanoparticles is directly affected by variables such as chemistry, particle size and shape, surface area to volume ratio, and zeta potential (Lam et al., 2018).

ZIF-8 and ZIF-8-based composite materials have great antibacterial potential (Kohsari et al., 2016; Wang et al., 2016; Zhang et al., 2019) due to their inherent highly porous structure (Figure 2.4) and the interaction of zinc ions (Au-Duong & Lee, 2017). As an effective antimicrobial agent, zinc ions can form a series of effects on cells and cause bacterial growth inhibition or death, such as cell deformation, cell wall rupture leading to cytoplasmic leakage, formation of an alkaline microenvironment (Wang et al., 2014; Tan et al., 2018). The antibacterial properties of ZIF-8 have found their use in many

applications, such as implant coatings (Tao et al., 2020), water filtration (Wang et al., 2016), and multifunctional fabrics (Yang et al., 2020).

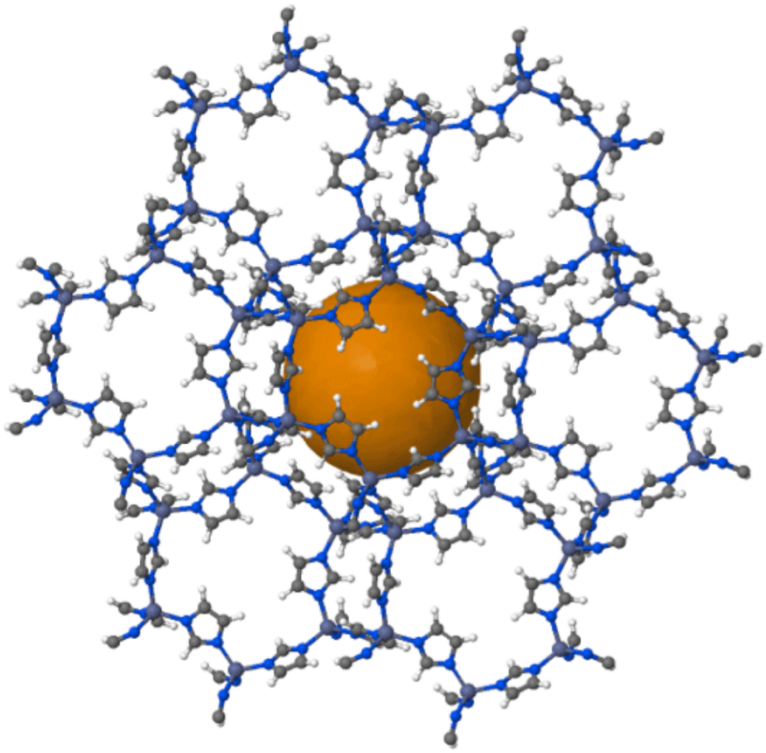

Figure 2.4 ZIF-8 Structure (Retrieved from ChemTube3D).

Wei et al. (2020) investigated the antibacterial effect of ZIF-8 nanosheets on *A. hydrophila* colonies using a plate count method. *A. hydrophil*a was co-cultured with 1.0 mg ml -1 concentration of ZIF-8 for 8 h and no *A. hydrophila* bacteria were found. Taheri et al. (2021) reported the stability and antimicrobial behavior of ZIF-8 nanoparticles in bacterial culture media, which showed higher antibacterial efficacy compared to ZnO. And Kathuria et al. (2021) even simulated the application of PLLA-15% ZIF-8 MOF composites in acidic foods and high alcohol foods, however, the studied composite films

were not suitable for direct food contact in its current form due to the high mobility of metal ions.

2.5.1. Minimum Inhibitory Concentration (MIC)

The minimum inhibitory concentration (MIC) of a compound is defined as the lowest concentration of an antibiotic or antimicrobial that inhibits the visible growth of microorganisms after overnight incubation (Andrews, 2001). MIC can be determined mainly by two methods, by dilution in agar solids or liquids, and with strips impregnated with a predetermined concentration gradient of antimicrobials (Kowalska-Krochmal & Dudek-Wicher, 2021).

Broth dilution is the primary dilution method according to the recommendations of The European Committee on Antimicrobial Susceptibility Testing (EUCAST, 1998) and the US Clinical and Laboratory Standards Institute (CLSI, 2018). The antimicrobial substance needs to be pre-dissolved to obtain a stock solution and then diluted to obtain the appropriate starting concentration to determine the MIC (Andrew et al., 2001). Water is the most common and readily available solvent and diluent (Kowalska-Krochmal & Dudek-Wicher, 2021) and can dissolve most β-lactams, fluoroquinolones, and aminoglycosides. Notably, although the determination of MIC using gradient methods is more straightforward and faster than dilution methods, disc diffusion methods using strips have decreased significantly in recent years because of their inconsistent results, often yielding lower MIC values than the broth microdilution method (EUCAST, 2020).

MIC values must be compared with MIC clinical breakpoints due to the susceptibility and resistance of the strain to the antimicrobial agent. MIC values are not

constant, and they are updated periodically as microorganisms and dosing rules change. Although the same MIC value may be obtained in a study, it sometimes varies, so it is necessary to consider the effect of cumulative data when determining MIC values (Kowalska-Krochmal & Dudek-Wicher, 2021).

2.6. The Antimicrobial Effects of Chlorine on Leafy Greens

Green leafy vegetables are always eaten raw, thus, disinfection and cleaning is the most practical way to clean these products. Chlorination, whether in the form of chlorine, sodium hypochlorite (NaClO), calcium hypochlorite ($Ca(ClO)_2$), or chlorine dioxide (ClO_2), is cheaper and were widely used than ultraviolet radiation, ozone, or peracetic acid treatments (Garrett et al., 2003). In the processing of fresh commercial produce, chlorine rinsing is often used, with concentrations ranging from 50 to 200 ppm within 2 mins (Parish et al., 2003). As a source of free chlorine, NaClO is attractive as an antibacterial agent in recycled wash water during the processing of green leafy vegetables and can significantly reduce or prevent pathogen cross-contamination in water (Luo et al., 2011; Gombas et al., 2017). However, the efficacy of NaClO is limited by the concentration of free or available chlorine, the presence of organic matter, pH, temperature, and porous and rough sample surfaces (Sapers, 2001; Fukuzaki, 2006; Van et. al, 2015).

Studies have shown that chlorine rinsing can reduce the bacterial load on green leaves ranging from <1 log CFU/g to 3.15 log CFU/g depend on the inoculation method, chlorine concentration, application time, and the target bacteria tested (Burnett et al., 2004; Akbas & Olmez，2006; Nthenge et al., 2007; López-Gálvez et al., 2010). However, the antibacterial efficacy of chlorine rinsing on different green leaf varieties may be different.

Take lettuce, for example, the log reduction achieved by Beuchar (1999) and Nthenge et al. (2007) is comparable to the log reduction caused by water washing.

Chlorine-based sanitizers are widely used on fresh produce for their low cost and sanitary effectiveness in food processing (Petri et al, 2021). It is critical to actively maintain adequate levels of free chlorine in the wash water; however, the dynamic characteristics of the wash water can affect the effectiveness of the added antimicrobial agent. Among other things, the accumulation of organic and inorganic substances during the washing process can lead to a significant decrease in the concentration of free chlorine, thus reducing its antimicrobial efficiency (Deborde & von Gunten, 2008; Gombas et al, 2017).

One of the main problems with the use of chlorine is its reaction with organic matter, producing potentially health-hazardous disinfection by-products such as teratogenic trihalomethanes and haloacetic acids (Hrudey, 2009; Li & Huang, 2019; Banach et al., 2020), leading to a reduction in its efficacy in inactivating microorganisms (Gómez-López et al, 2013; Gómez-López et al., 2014). In some European countries, including Germany, Switzerland, the Netherlands and Belgium, the use of chlorine in food processing has been banned (Bachelli et al., 2013; Petri et al., 2015); therefore, there is a trend to eliminate chlorine from the disinfection process

3. METHODOLOGY

3.1. ZIF-8 Nanoparticles Synthesis and Characteristics

3.1.1. Zeolitic Imidazolate Framework-8 (ZIF-8) Particles

Synthesis of Zeolitic Imidazolate Framework-8(ZIF-8) particles was based on modifications of a method developed by Ho et al. (2020) (Figure 3.1).

Approximately 0.94 g of zinc nitrate hexahydrate ($Zn(NO_3)_2 \cdot 6H_2O$, 98%, Strem Chemicals, Newburyport, MA, USA) and 3.3 g of 2-methylimidazole (2-mim, $C_4H_6N_2$, 99%, Acros Organics, Geel, Belgium) were dissolved separately in an Erlenmeyer flask containing 20 mL of absolute ethanol (EtOH, EMPLURA®, Supelco®, Bellefonte, PA, USA) and stirred for 15 min until completely dissolved. The two Erlenmeyer flasks were placed in an ultrasonic cleanser with ultrasound frequency 42 kHz ± 6% and power consumption total 70 W (1510R-MT, Bransonic Ultrasonic Corp., Danbury, CT, USA) for 5 min. The 2-mim ligand solution was then quickly added to the zinc nitrate solution and sonicated for 60 min. The molar ratio of EtOH/Zn after mixing the two solutions was 333. The milky solution was then centrifugated (Allegra TM 25R Centrifuge, Beckman Coulter, Brea, CA, USA) at 9000 rpm for 10 minutes and washed thrice with 40 mL of EtOH, respectively. After washing, the ZIF-8 solution was vacuum dried (Vacuum oven with Welch 1376 DuoSeal Vacuum Pump, Thomas Industries Inc., Skokie, IL, USA) at 35 °C for 2 h. The resultant nanoparticles were collected with a size of approximately 101.800 ± 4.904 nm (Sevimli-Yurttas et al., 2021), and then placed in a desiccator, and stored at room temperature for future testing, approximately within two weeks.

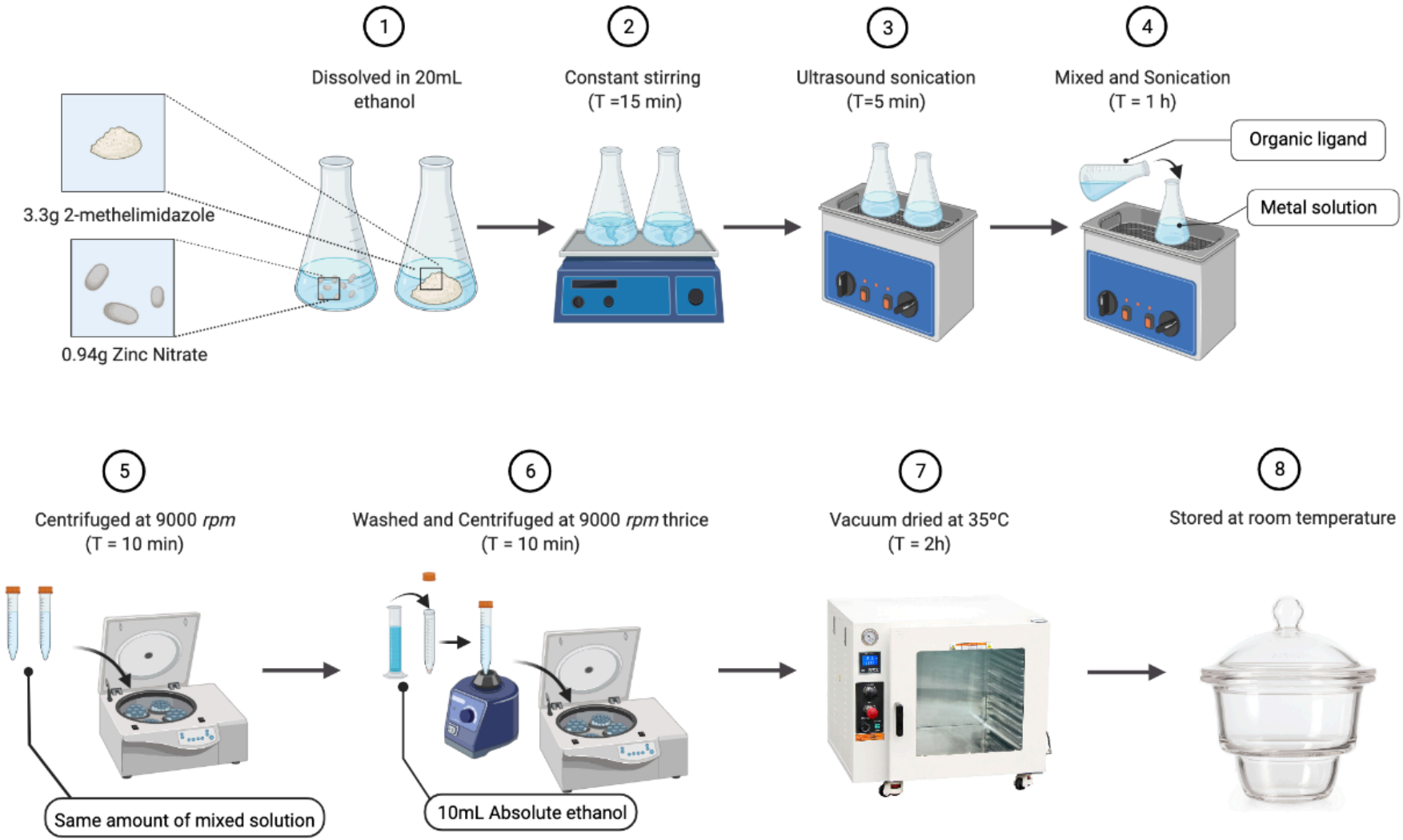

Figure 3.1 Schematic illustration of ZIF-8 synthesis procedure.

Encapsulation of *trans*-Cinnamaldehyde (TC) (C_9H_8O, 99%, Acros Organics, Geel, Belgium) in the ZIF-8 nanoparticles was performed by the one-pot synthesis in which a given amount of TC was added together with 2-methylimidazole when preparing the solution of the organic ligand (Ho et al., 2020). Mass ratios of TC per total solid component were 0.10, 0.25, 0.5 and 0.75, and the TC-encapsulated ZIF-8 were denoted as 0.1TC@ZIF-8, 0.25TC@ZIF-8, 0.5TC@ZIF-8 and 0.75TC@ZIF-8, respectively.

3.1.2. ZIF-8 Nanoparticles Coated with Poly-lysine

To obtain good aqueous stability to avoid sedimentation and aggregation of ZIF-8 nanoparticles, coating of nanoparticles with poly-lysine (PL) was carried out based on preliminary studies conducted in our laboratory (Sevimli-Yurttas et al., 2021) (Figure 3.2). Approximately 30 mg of ZIF-8 or TC@ZIF-8 nanoparticles were suspended in 30 mL 0.1 mg/mL of poly-lysine at a ratio of 1:1 (mg/mL), followed by vortexing until fully dissolved and sonicated with ultrasound at a frequency of 42 kHz ± 6% and power consumption of 70 W for 5 min. The samples were then freeze-dried (FreeZone ^{6}, Labconco Corp., Kansas City, MO， USA) for 48h. The PL-coated ZIF-8 and TC@ZIF-8 particles were collected, placed in a desiccator, and stored at room temperature for future testing, approximately within two weeks.

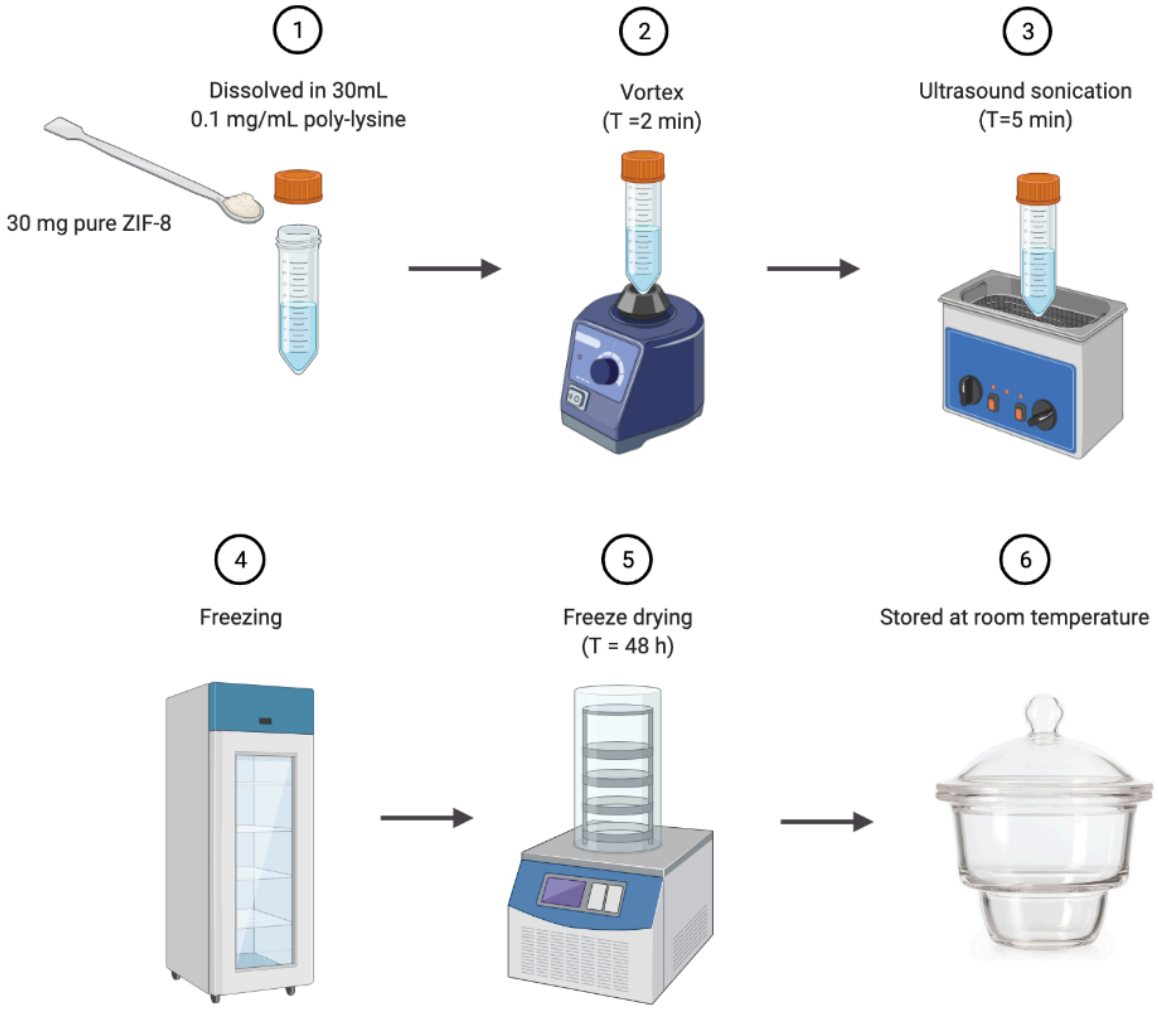

Figure 3.2 Schematic illustration of poly-lysine coated ZIF-8 synthesis procedure.

3.1.3. Encapsulation Efficiency of TC@ZIF-8 Nanoparticle Complexes

The amount (percentage) of entrapped TC in the ZIF-8 (TC@ZIF-8) nanoparticles was determined by UV-Visible spectrophotometry (Genesys 10S UV-Vis Spectrophotometer, Thermo Fisher Scientific, Madison, WI, USA). A blank solution was prepared by dissolving 5 mg ZIF-8 nanoparticles in 10mL 0.1 M HCl at a concentration of 0.5 mg/mL. Approximately 5 mg of TC@ZIF-8 were dissolved in 10 mL 0.1 M HCl acid as sample solutions (dilute from Hydrochloric Acid, Acid Chlorhydrique, 34-37%, VWR Chemicals BDH®, Radnor, PA, USA) at a concentration of 0.5 mg/mL and mixed thoroughly. The suspension was left for 15 min under constant agitation and then placed in the UV-Visible spectrophotometer at 295 nm. The wavelength was determined as the maximum absorbance in preliminary tests by scanning the UV–Vis spectra of TC dissolved in 0.1 M HCI) (Appendix A) in triplicate. Blanks and sample solutions were diluted with 0.1 M HCl for proper spectrophotometric readings to make the absorbances within a linear range (Gomes et al., 2011; Hill et al., 2013).

Encapsulation efficiency (EE%) of the ZIF-8 nanoparticles was determined as:

$$EE(\%) = \frac{amount\ of\ active\ compound\ entrapped}{inital\ active\ compound\ amount} \times 100 \qquad 3.1$$

where the “amount of active compound entrapped” is the amount of compound (TC in this study) present in the ZIF-8 particles in (mg/mL) / (mg/mL), and the “initial active compound amount” indicates the amount of compound (TC) initially used to manufacture the particles (g/g).

A calibration curve was obtained for TC dissolved in the 0.1M HCl solution ranging from 0.5 μg/mL to 6.0 μg/mL in 295nm (Appendix B).

3.2. Antimicrobial test against *Escherichia coli (E. coli)* O157:H7

3.2.1. Bacterial Culture Preparation

Escherichia coli O157:H7 (ATCC 43895) was obtained from the Texas A&M University Food Microbiology Laboratory culture collection (Department of Animal Science, College Station, TX USA).

One loop of *E.coli* O157:H7 was resuscitated in TSB (DifcoTM Tryptic Soy Broth, Soybean-Casein Digest Medium, BD, Franklin Lakes, NJ, USA) by identical duplicate transfers and incubated aerobically for 24 h at 35℃ in an incubator (Symphony Forced Air General Incubator, VWR, Radnor, PA, USA). From this, the T strike method was used to plated on TSA (Difco™ Tryptic Soy Agar, Soybean-Casein Digest Medium, BD, Franklin Lakes, NJ, USA) for isolating colonies. A single colony was transferred to the Trypticase Soy Agar Slant (Becton, Dickinson and Company, Spark, MD, USA) and incubated 24 h at 35°C, then the slant was stored in a refrigerator at 4°C for future use no more than three months (Figure 3.3). Pathogen isolates were maintained, revived, and handled under biosafety level (BSL) 2 containment at all times according to Texas A&M University System Institutional Biosafety Committee (IBC) policy, and operations were carried out in a fume hood (Purifier Biological Safety Cabinet®, Labconco Corporation, Kansas City, MO, USA). All of the tips, media, containers were sterilized in a High-pressure Steam Sterilizer (MLS-3781L Labo Autoclave, Sanyo Electric Co., Ltd., Osaka, Japan).

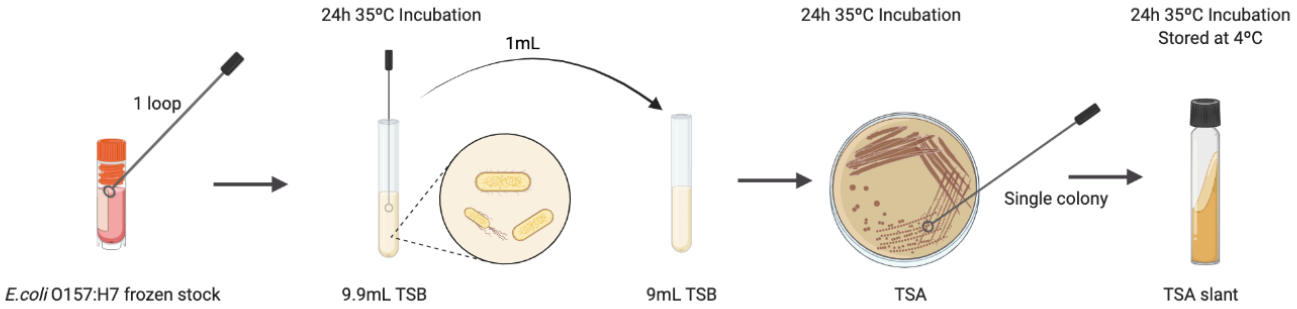

Figure 3.3 Schematic illustration of *E.coli* O157:H7 resuscitation.

3.2.2. Minimum Inhibitory Concentration (MIC)

The minimum inhibitory concentrations (MIC) of ZIF-8 and 0.5TC@ZIF-8 nanoparticles, both with and without 0.1mg/mL poly lysine coating were determined using a broth dilution assay (Brandt et al., 2010), where 0.5TC@ZIF-8_PL was the most effective TC encapsulated ZIF-8 particle determined by preliminary experiments.

Bacterial cultures were incubated at 35°C for 24 h and then diluted and transferred to 9.0 mL double-strength TSB (2xTSB) for an initial inoculum of approximately 5.0 log10 CFU/mL in each sample well. Enumeration of the inoculum was completed by serial dilution in sterile 0.1% peptone water (w/v) (Buffered Peptone Water, CRITERION™ Dehydrated Culture Media, New York, NY, USA) and spread plating 100 µL on Petri dishes (VWR® Disposable Sterile Petri Dishes, 100x15mm, Radnor, PA, USA) containing TSA, aliquots of 100 µL of all antimicrobial solutions and solvents blanks were spread plated to ensure sterility, all plates were incubated for 24 h at 35°C (Figure 3.4).

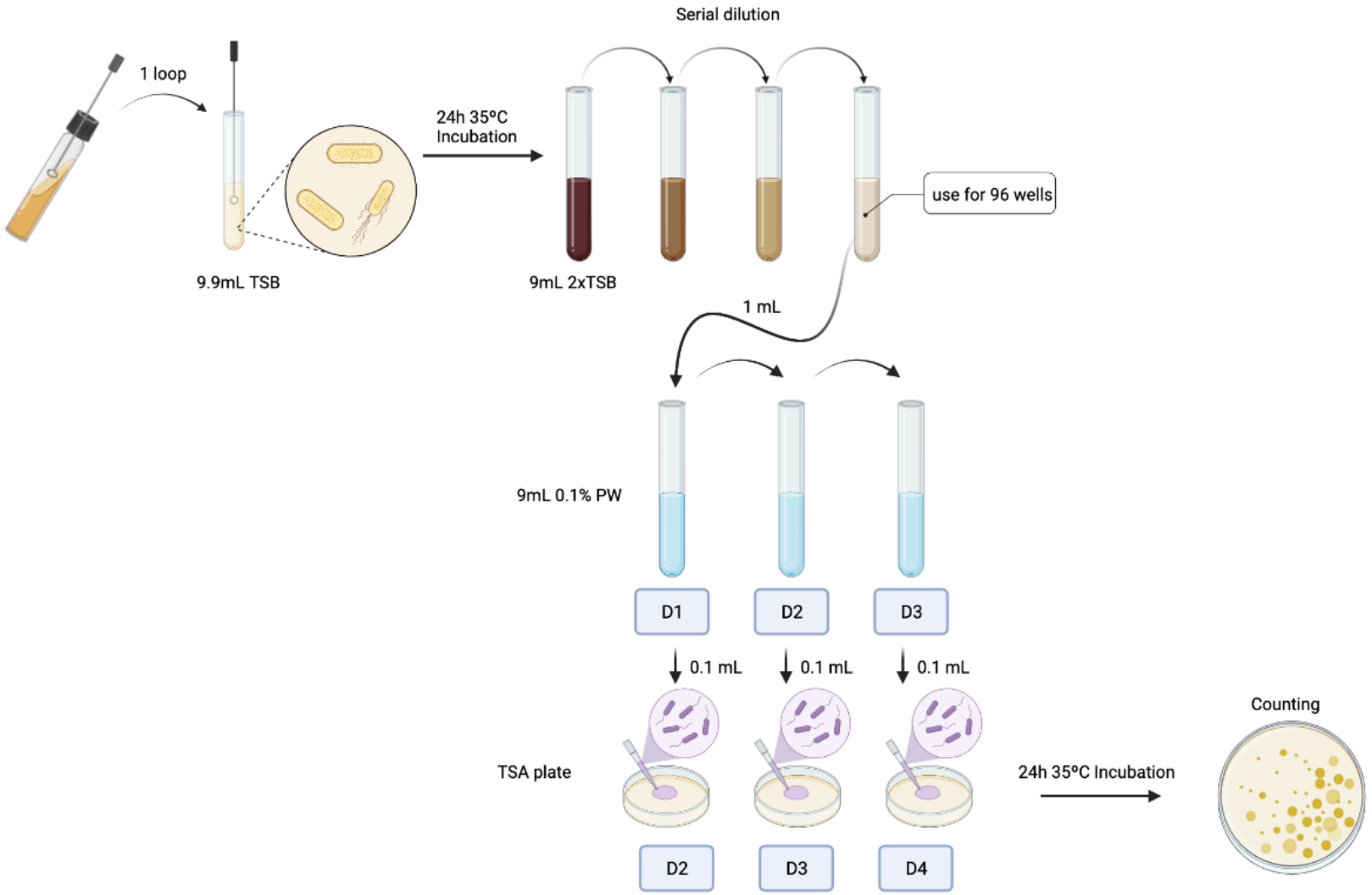

Figure 3.4 Schematic illustration of preparation and counting of MIC bacterial inoculum.

The ZIF-8, ZIF-8_PL, 0.5TC@ZIF-8, and 0.5TC@ZIF-8_PL nanoparticle solutions were added to the microtiter plates as aqueous suspensions of different concentrations ranging from 1250-10000 µg/mL and 250-2000 µg/mL for *E.coli* O157:H7 (ATCC 43895) (Kalemba and Kunicka, 2003). TC was added as an aqueous solution containing 1.0 g/100 g acetonitrile (H_3CCN, HPLC LC-MS grade, VWR, Radnor, PA, USA) and 0.01 g/100 g Tween 20® ($C_{58}H_{114}O_{26}$, Reagent Grade, VWR, Radnor, PA, USA) with concentrations ranging from 62.5 - 2000 µg/mL; poly-lysine was added at the range of 0.1 to 0.5 mg/mL (Table 3.1).

Table 3.1 Treatments for determination of minimum inhibitory concentration of *E.coli* O157:H7

Antimicrobial Compounds*	Concentration Range [µg/mL]
ZIF-8	1250-10000
0.5TC@ZIF-8	250-2000
ZIF-8_PL	1250-10000
0.5TC@ZIF-8_PL	250-2000
TC	62.5-2000
PL	100-500

* TC = *trans*-Cinnamaldehyde; PL = poly lysine

Equivalent volumes (100 µL) of the different treatment solutions and bacterial inoculum in 2×broth was loaded into each test well, noted as sample group (SPL) in 96 well microtiter plates (Nunclon™ Delta Surface 96-wells, Thermo Scientific, Waltham, MA, USA). Negative controls (NEG) were prepared with 100 µL sterilized water and 100 µL 2×TSB to account for baseline OD630 readings. Sample controls (SPLC) were composed of 100 µL antimicrobial solution and 100 µL 2×TSB to cancel the solution background color. Positive controls (POS) were also prepared containing 100 µL

inoculum in 2×TSB and 100 μL sterilized water to ensure that the liquid which dilutes the particles has no inhibitory effect on bacterial growth (Table 3.2).

Figure 3.5 illustrates the setup of 96 wells for each treatment groups. SPL and SPLC groups were added the initial concentration of antimicrobial solution to the first and sixth column, respectively, and then serial dilution with 100 μL sterilized distilled water. The pipette was drawn and dispensed multiple times during each mixing to ensure a uniform solution. Eight replicates were performed for each concentration of SPL and SPLC.

Table 3.2 Setup of 96 wells of antimicrobial treatment groups

Treatment Groups *	Composition [200 μL total]
SPL	100 μL treatment solutions 100 μL *E.coli* O157:H7 inoculum in 2 x TSB
SPLC	100 μL treatment solutions 100 μL 2 x TSB
NEG	100 μL sterilized water 100 μL 2 x TSB
POS	100 μL sterilized water 100 μL *E.coli* O157:H7 inoculum in 2 x TSB
BLK	N/A

* SPL = Sample Groups; SPLC = Sample Control Groups; NEG = Negative Controls; POS = Positive Controls; BLK = Blank.

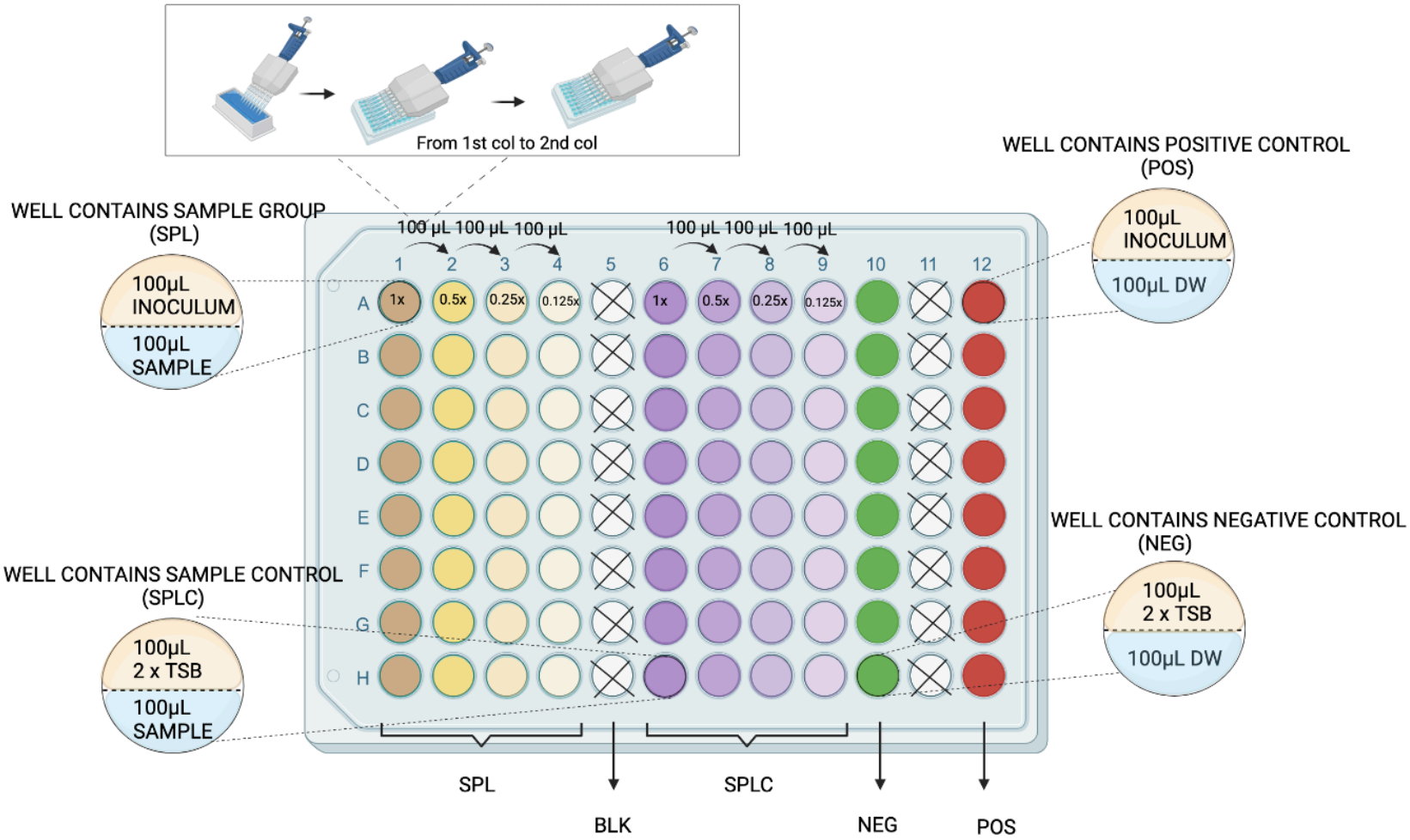

Figure 3.5 Schematic illustration of MIC procedures and 96 well plate setup.

Once the plate was prepared, it was covered with a Mylar plate sealer (Thermo Scientific, Waltham, MA, USA), incubated at 37°C, and shaken gently in an ELISA (Synergy H1 Microplate Reader, BioTek, Winooski, VT, USA) before each reading. The optical density (OD) at 630 was recorded every 30 mins for 24 h with a total of 49 readings in Gen 5 Microplate Plate and Imager Software Version 3.00 (BioTek, Winooski, VT, USA). Next, all the OD630 (SPL) were normalized by using the OD630 (BLANK) values of the sample control with the equations below (Hill, 2014):

$$\left(0_h OD_{630,SPL}\right) - \left(0_h OD_{630,SPLC}\right) = 0_h OD_{630,Normalized} \qquad 3.2$$

$$\left(24_h OD_{630,SPL}\right) - \left(24_h OD_{630,SPLC}\right) = 24_h OD_{630,Normalized} \qquad 3.3$$

$$\left(24_h OD_{630,Normalized}\right) - \left(0_h OD_{630,Normalized}\right) = \Delta OD_{630} \qquad 3.4$$

Any antimicrobial sample well that showed ≤ OD_{NEG} was considered to be effectively inhibited by the antimicrobial, with no growth of *E.coli* O157:H7. The MICs were determined as the lowest concentration of an antimicrobial that inhibited growth for all test replicates for all microorganisms, respectively (Brandt et al., 2010).

3.2.3. Effects of Antimicrobial Treatment Applications Method on the Total Aerobic Plate Count (APC) of Fresh Spinach Leaves

Thoroughly washed whole leaves of spinach were purchased from a local grocery (H.E.B., TX) and kept refrigerated (4°C) until needed (within 24 hours). All leaves showing signs of decay, cuts, or bruises were removed. The antibacterial treatment on the surface of spinach leaves was carried out by spraying and rinsing with a 0.5TC@ZIF-8_PL nanoparticle complexes solution at its MIC (3000 μg/mL).

3.2.3.1. Spraying Method

A 3000 μg/mL of 0.5TC@ZIF-8_PL nanoparticle solution was sprayed into the leaves twice using the sprayer bottles two times (~1mL) on each side of a leaf at a distance of 10 cm, followed by 15min drying in a fume hood (Purifier Biological Safety Cabinet®, Labconco Corporation, Kansas City, MO, USA). Around 200 g spinach leaves were used in this experiment. A group of leaves sprayed the same way with sterilized distilled water saved as the control group.

3.2.3.2. Rinsing

Another group of spinach leaves (200 g) was rinsed in 3000 μg/mL 0.5TC@ZIF-8_PL nanoparticles solution for 30 s, and the leaves rinsed the same way with sterilized distilled water (control group). Spinach leaves from each application treatment were then weighted (10g), placed in a sterilized Whirl-Pk™ Stand-Up Sample Bag (Nasco Education, LLC, Fort Atkinson, WI, USA) and stored in the fume hood at room temperature for 5 days.

Total Aerobic Plate Counts (APC) testing was conducted on days 0, 1, 3, and 5 at room temperature (~21℃). 90 mL of 0.1% peptone water was added to 10 g of spinach leaves in sample bags. Squeezed and grounded by hand for 2 minutes, and then the homogenous were serially diluted and enumerated on 3M™ Petrifilm™ Aerobic Count Plate (3M aerobic plate count, St. Paul, MN, USA). Petrifilms™ were then put into the microbiological incubator for 48 hours at 35°C before counting the colony growth (Figure 3.6). This experiment was completed in triplicate, and all replicate samples were plated in duplicate (Hill, 2014; Zhang, 2020). Results were reported as CFU/g of spinach.

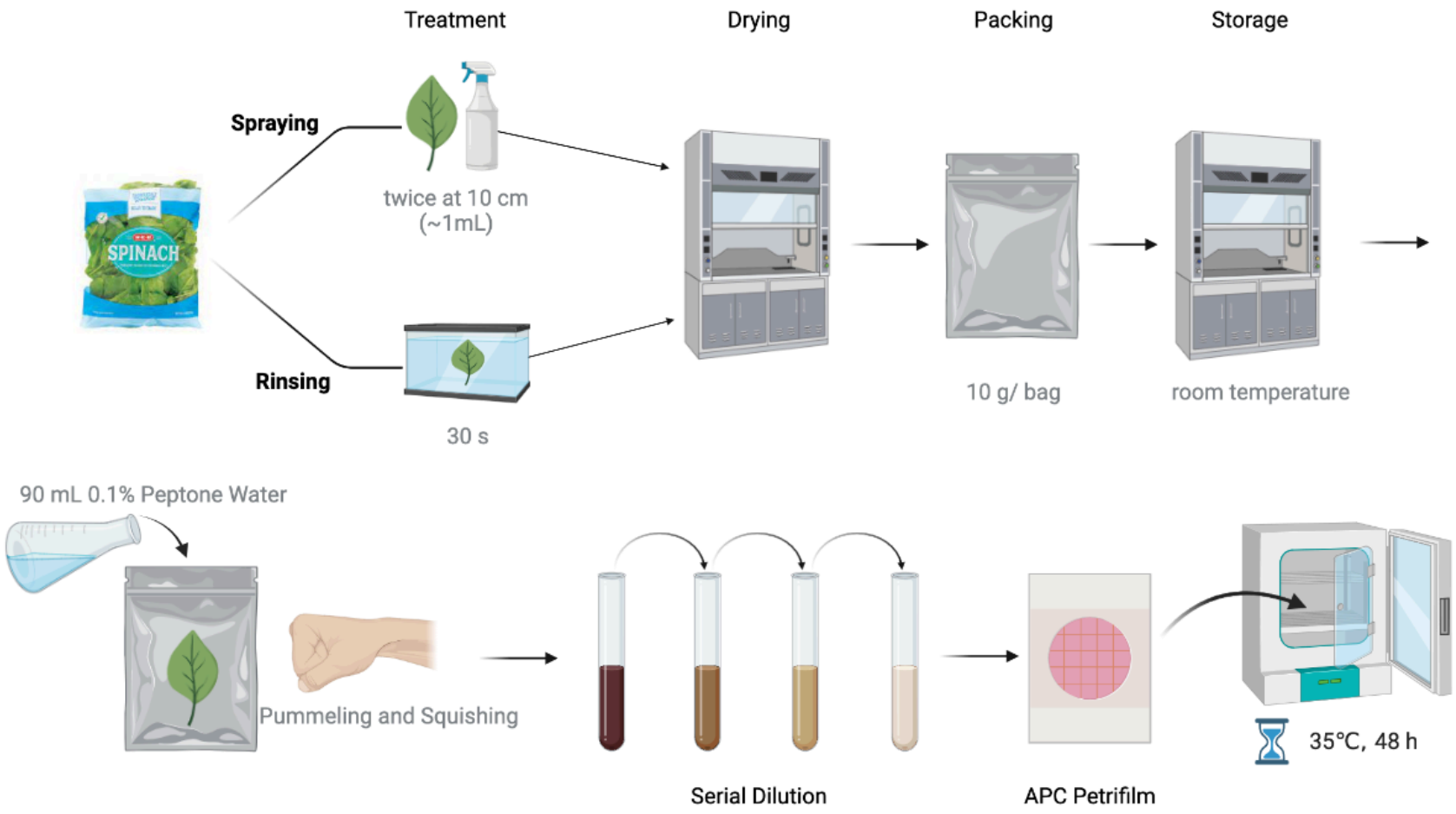

Figure 3.6 Schematic illustration of Total Aerobic Plate Count procedure.

3.2.4. Antimicrobial Dose-Response Application

Dose-dependent antimicrobial effects of the ZIF-8 and TC@ZIF-8 nanoparticles were studied using the plate dilution method modified from Taheri et al. (2011). At specific concentrations of ZIF-8 (0.1, 1, 1.5, 2.5 mg/mL), the dose concentration of TC@ZIF-8 was determined by Equation 3.5:

$$\text{Dose} = \frac{Concentration\ of\ ZIF{-}8}{1{-}EE\%} \qquad 3.5$$

Where the "dose" is the concentration of TC@ZIF-8 applied to *E.coli* O157:H7 (mg/mL), the "concentration of ZIF-8" is the concentration of ZIF-8 in TC@ZIF-8 (mg/mL), and the "EE%" is the encapsulation efficiency of the different mass ratios of TC@ZIF-8, calculated using equation 3.1.

All nanoparticles were dispersed in TSB medium containing ~10^5 cells/mL of *E.coli* O157:H7 in falcon tubes (15mL, PP, 17000g, Conical-Bottom, Sterilized, VWR, Radnor, PA, USA) and then incubated at 35℃. After 24 h incubation, the solution in each tube was plate-diluted and the number of live bacteria was determined. Enumeration was completed by serial dilution in sterile 0.1% peptone water (w/v) and spread plating 100 µL on TSA plate, aliquots of 100 µL of all antimicrobial solutions, and solvents blanks were spread plated to ensure sterility, all plates were incubated for 24 h at 35°C (Figure 3.7). All concentrations were conducted three repetitions and each repetition was plated by three duplications.

Antimicrobial dose-response was determined by the log reduction of the bacterial load:

$$\text{Log Reduction Bacterial Load} = log_{10}(\frac{N_0}{N}) \qquad 3.6$$

Where the "log reduction bacterial load" is the log reduction of *E. coli* O157:H7 after 24h treatment with the antimicrobial nanoparticle complexes at 35ºC (CFU/mL), "N_0" is the initial population of *E. coli* O157:H7, 10^9 CFU/mL in this study, and "N" is the population of *E. coli* O157:H7 after 24h treatment at 35ºC (CFU/mL).

3.2.5. Inhibition of the growth of *E.coli* O157:H7 attached to the surface of spinach leaves by antimicrobial treatments

Thoroughly washed whole leaves of spinach were purchased from a local grocery (H.E.B., TX) and kept refrigerated (4°C) until needed (within 24 hours). The advertised sell-by date was 14 days after packaging. All leaves showing signs of decay, cuts, or bruises were removed.

Briefly, the prewashed spinach was directly inoculated with *E.coli* O157:H7 culture to minimize bacterial internalization. The bacteria were diluted in sterile 0.1% (v/v) peptone water to achieve an inoculum of approximately 5 log10 CFU/mL. Spinach leaves were submerged in the inoculum for 10 mins and then placed on a metal drying rack inside a biosafety cabinet to air dry for 30 mins for bacterial attachment onto the leaves (Hill, 2014).

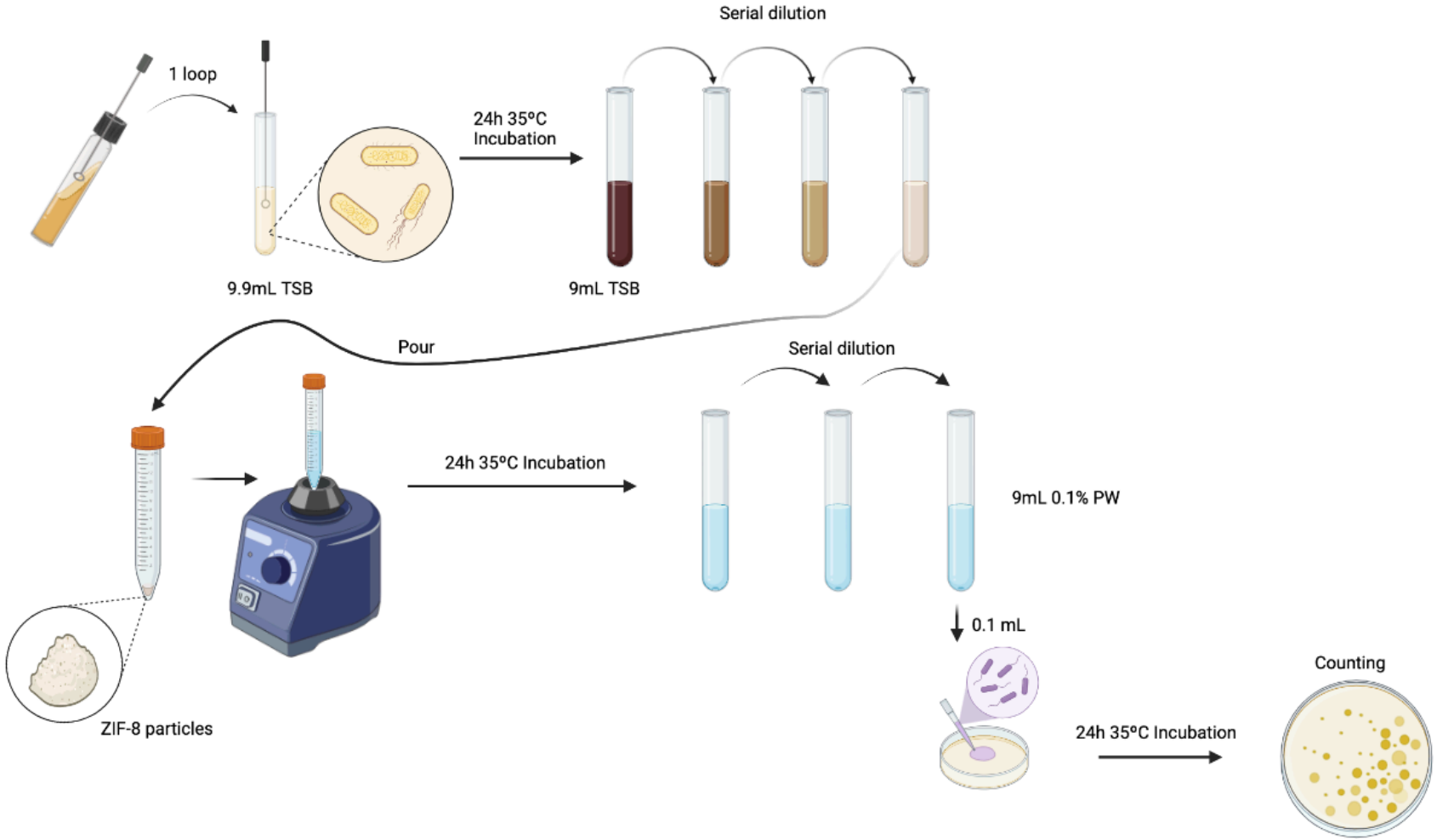

Figure 3.7 Schematic illustration of antimicrobial dose-response procedure.

Results from spraying versus rinsing application, the rinsing method was more effective of the antimicrobial nanoparticles (Section 3.2.3) in inhibiting APC, so the rinsing method was applied to the subsequent treatments. Spinach leaves were rinsed in 3.68mg/mL of 0.5TC@ZIF-8_PL in PBS (pH 7.4) for 1, 5, 10, and 20 min, respectively, and the optimum rinsing time was determined by the number of *E.coli* O157:H7 inhibited. 3.68mg/mL 0.5TC@ZIF-8_PL was selected as the most effective antimicrobial compound ($p<0.05$), from Section 3.2.4. Next, 200 ppm chlorine solutions (500 ml) were made immediately before use for the purpose of comparison with the 0.5TC@ZIF-8_PL nanoparticle solution, by diluting 7.4% sodium hypochlorite (Clorox Concentrated Disinfecting Bleach, Clorox, Oakland, CA, USA) in deionized water. The concentration of chlorine was verified with chlorine concentration test strips (Free Chlorine Test Strips, 0-600 mg/L, Hach, Loveland, CO, USA). Spinach leaves rinsed by sterilized distilled water for the same time (1, 5, 10, 20 min) were used as the negative control group.

The spinach leaves from all groups were placed on a metal drying rack and uniformly dried for 15 minutes on each side in a biological safety cabinet, weighed into 10 g samples, packed in a sterilized Whirl-Pak™ Stand-Up Sample Bags (Nasco Education, LLC, Fort Atkinson, WI, USA), and diluted with 90 mL of sterile 0.1% w/v peptone before squeezing. Blended samples were serially diluted using 0.1% w/v peptone water and spread plated onto MacConkey Agar containing Sorbitol (SMAC) (BBL™ MacConkey Agar, BD, Franklin Lakes, NJ, USA) to enumerate the bacteria. Figure 3.8 shows the treatments of the spinach leaves.

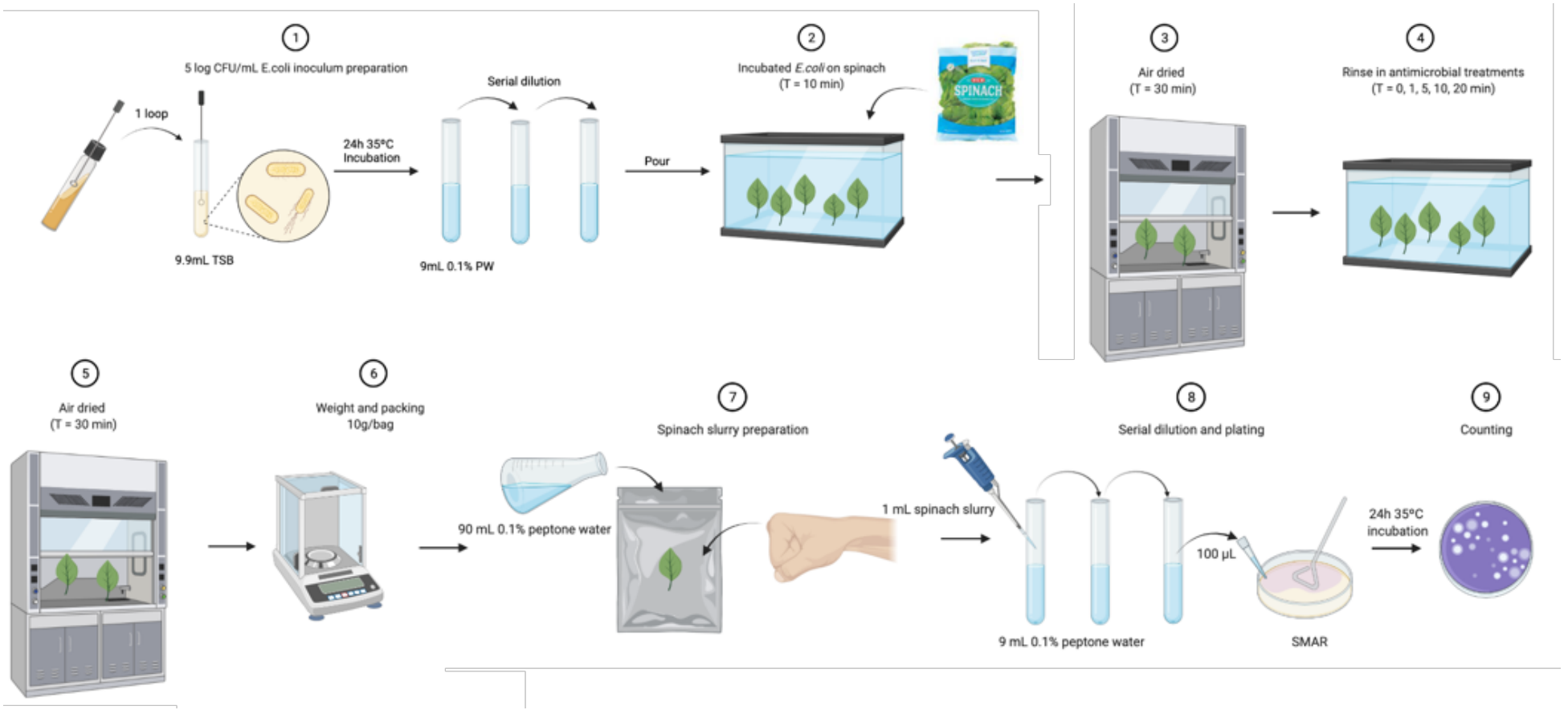

Figure 3.8 Schematic illustration of inhibition of antibacterial treatments on *E.coli* O157:H7 attached to the surface of spinach leaves.

To enumerate background microflora, negative controls were spread plated onto standard TSA. Plates were incubated for 24 hours at 35°C before counting the colony growth. This experiment was completed in triplicate and all replicate samples were plated in duplicate (Keskinen et al. 2009; Pan & Nakano, 2014). Killed *E.coli* O157:H7 were calculated by the difference between the surviving *E.coli* O157:H7 in the control group and the surviving *E.coli* O157:H7 after treatment with the antimicrobial treatments and results were reported as CFU/mL.

3.3. Spinach Shelf Life and Quality Study

3.3.1. Sample Preparation

Spinach samples were prepared the same way as described in section 3.2.5 (Figure 3.9) without *E.coli* O157:H7 incubation. According to the results in section 3.2.5, 1 min rinsing time was the most effective time ($p<0.05$) for 0.5TC@ZIF-8_PL nanoparticle solution in inhibiting the growth of *E.coli* O157:H7, thus all spinach leaves were rinsed in the antimicrobial solution for 1 min and dried in a biosafety cabinet for 15 min on each side. Next, 10 g of leaves were weighted and sealed in a sterilized Stand-Up sample bag, placed in biosafety cabinet, and stored at 4°C. Quality attributes were analyzed on the day of sample preparation (day 0), and then after 5, 10, and 15 days of storage at room temperature within 2 h after preparation. Spinach leaves rinsed 1 min in sterilized distilled water were used as a negative control (Table 3.3)

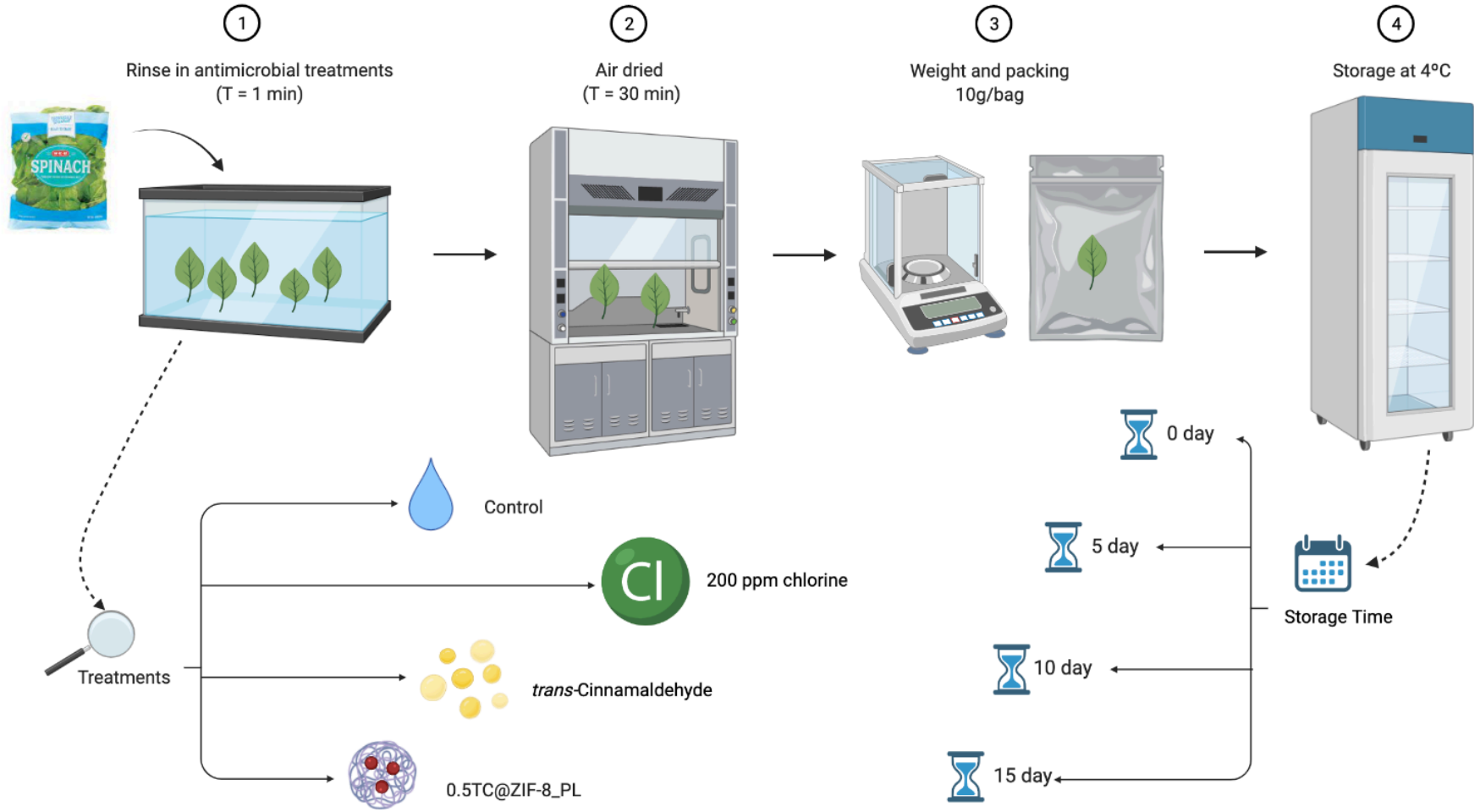

Figure 3.9 Flow chart of spinach sample preparation for shelf life study.

Table 3.3 Spinach shelf life and quality study at 4ºC.

	Storage Time			
Treatment	0 day	5 day	10 day	15 day
Negative Control	N_0	N_5	N_10	N_15
200 ppm Chlorine	C_0	C_5	C_10	C_15
trans-Cinnamaldehyde	TC_0	TC_5	TC_10	TC_15
0.5TC@ZIF-8_PL	S_0	S_5	S_10	S_15

N, C, TC, and S stand for the negative control group, chlorine-treated group, *trans*-Cinnamaldehyde-treated group, and 0.5TC@ZIF-8_PL treated group, respectively;
The numbers 0, 5, 10 and 15 after the underscore are the time points of each quality study during storage.

Moisture content (MC), water activity (Aw), pH, color, texture, vitamin C, chlorophyll, and total carotenoid content were selected physical and chemical quality attributes of spinach to be monitored throughout the 15-day study (Figure 3.10).

3.3.2. Moisture Content

Moisture content of the spinach leaves on a wet basis (MC) was measured by the reduced weight before and after drying:

$$MC\ (\%) = \frac{w-d}{w} \times 100 \qquad 3.7$$

where *w* is the wet weight (g) of spinach samples before drying and *d* indicates the dry wet (g) after drying.

About 10 g of spinach were dried at 60-65 °C in a vacuum oven (<13.3 kPa) (Vacuum Oven with Welch 1376 DuoSeal Vacuum Pump, Thomas Industries Inc., Skokie, IL, USA) for 12-14 hours at once, until constant weights were achieved, following AOAC method 930.04 (Helrich, 1990). Three duplications were made for each treatment at each storage time (0, 5, 10, 15 days) (Hill, 2014).

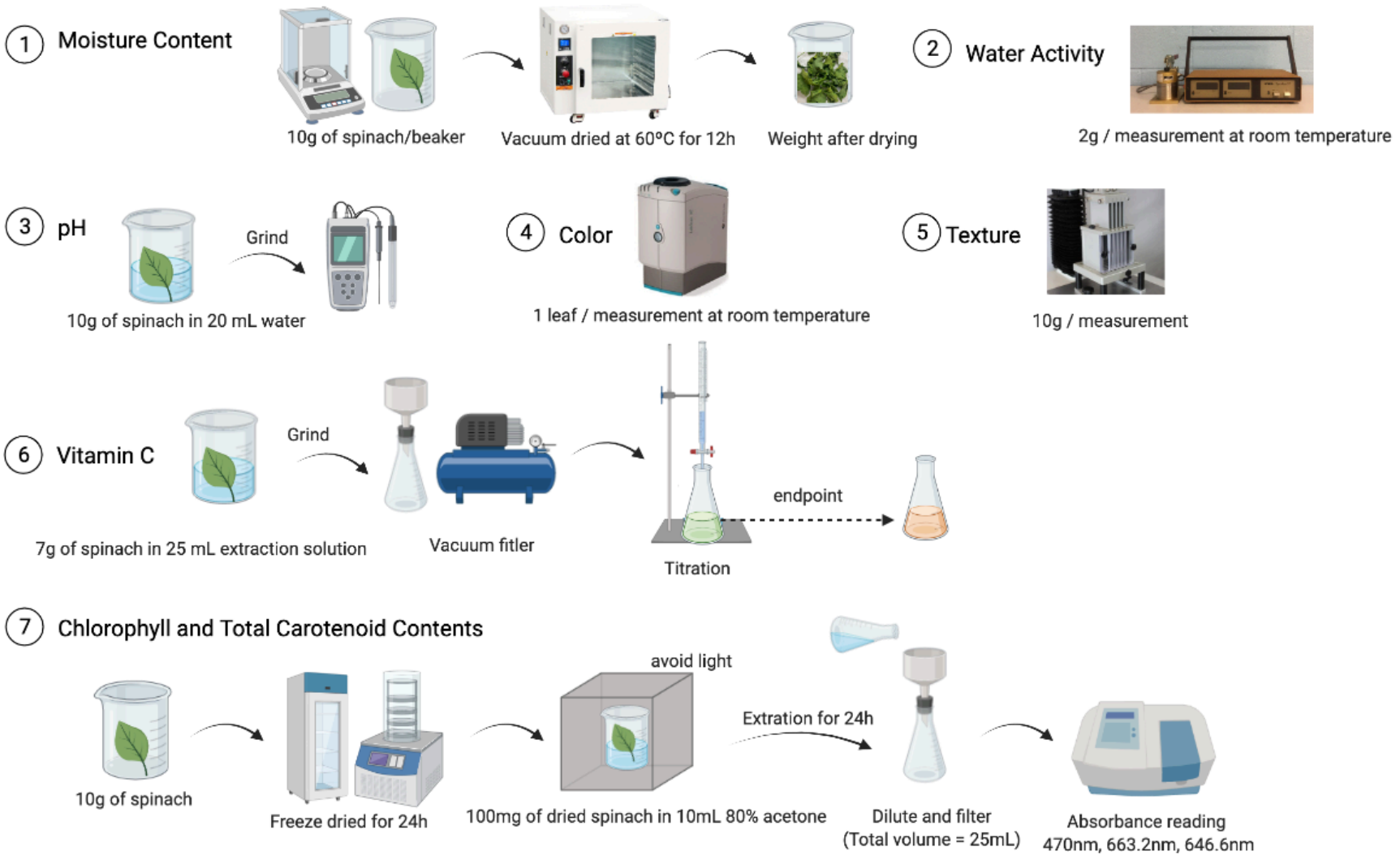

Figure 3.10 Spinach shelf life and produce quality measurement indicators and process.

3.3.3. Water Activity

Water activity (Aw) of the samples was measured with a Humidity Monitor (DT-2 Hygroskop, Rotronic AG, Switzerland) with WA 40 Probe Station. Pieces of spinach (approximately 2 g) were placed inside 2-part lidded round jars (46x16mm, Rotronic AG, Switzerland) at the base of the airtight test chamber. The measuring head enclosed the sample and formed an airtight seal with the base, the humidity of the surrounding air will be in balance with the humidity of the sample. At least 10 samples were measured per each treatment and storage time point at room temperature (Rico et al., 2008). The water activity was calculated from equilibrium relative humidity (ERH) as:

$$Aw = \text{ERH} /100 \qquad 3.8$$

3.3.4. Color

Color changes were evaluated using a LabScan® XE (16437) colorimeter (HunterLab, Inc., Reston, VA, USA) with the Universal Version 3.80 software (HunterLab, Inc., Reston, VA, USA). The measuring aperture was 36 mm and the illuminant/viewing geometry was D65/10° with an area view of 1,75" and port size of 1.20". Standard white and black plates were used to calibrate the colorimeter before sample measurements at each time.

Five leaves from different bags were measured for each treatment at each time point, three readings per leaf. The mean values were determined by the value of the total color *E* (Equation 3.8) (Dermesonluoglu et al., 2015), for the overall comparison of the color loss. Leaf color was quantified by the total color *E* and the three-dimensional standard color space (Hill, 2014).

$$E = \sqrt{L^{*2} + a^{*2} + b^{*2}} \qquad 3.9$$

Where L*, a*, b*are the color parameters of the CIELAB scale. L* represents lightness, with 0 being black of 0% reflectance or transmission, while 100 rating indicates white with 100% reflectance and clarity; a* represents red-green intensity, positive values of a* are red, while negative values are green; b* denotes yellow-blue intensity, positive values of b* are yellow, while negative values are blue ("CIELAB color space", 2021).

3.3.5. pH

10 g sample of spinach tissue was blended for 2 min in 20 mL of deionized water. The pH of the slurry was measured at room temperature using a pH Benchtop meter (AE150, Fisher Scientific™, Waltham, MA, USA). Three duplications were done for each treatment at each time point (Martín-Diana et al., 2008).

3.3.6. Texture (firmness and work)

A Kramer Shear Press with 5 blades (TA-91) attached to a TA-XT2 Texture Analyzer (Texture Technologies Corporation, Scarsdale, NY) was used to get a measure of the texture of the leaves. This probe is commonly used to quantify the firmness of leafy vegetables, which require low-strength force to penetrate (Han et al., 2004; Gomes et al., 2008). 10 grams of spinach leaves were stacked on the sample holder with the veins perpendicular to the blades (internal dimensions 82 x 63 x 89 mm^3) and forced 5 flat plungers (1.5 mm blade width) through the leaf. The blade was adjusted to a height of 65 mm above the bottom and moved at a speed of 1 mm/s.

Firmness is a descriptive term that is conventionally accepted as the maximum force reached prior to a fracture, and the work until shear is defined as the area of

maximum force to the time until shear (Figure 3.11) (Stable Micro System, 2021). The maximum force to shear the leaves in Newton and work up to shear in Joule were recorded by Exponent Version 6,1,18,0 (Stable Micro Systems, Godalming GU7 1YL, United Kingdom). Three duplications were performed for each treatment at each storage time point (0, 5, 10, and 15 days) at room temperature.

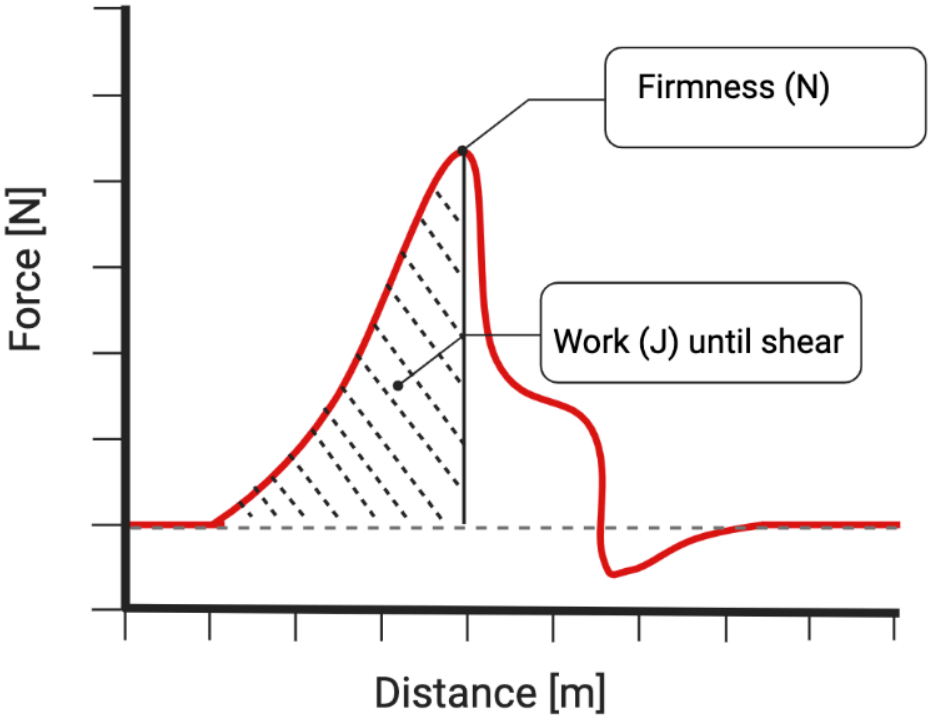

Figure 3.11 Schematic definition of firmness (N) and work (J) until shear to measure texture of spinach leaves.

3.3.7. Vitamin C

Vitamin C content was evaluated according to AOAC Official Method 967.21 (AOAC, 2006). Approximately 7 g of spinach leaves were grounded with 25 mL of

extracting solution containing 15 g metaphosphoric acid (reagent, stabilized, Acros Organics, Geel, Belgium) and 40 mL acetic acid (36%) (Glacial, $C_2H_4O_2$, 99.5-100.5%, Spectrum Chemical Manufacturing Corporation, New Brunswick, NJ, USA) in 500mL distilled water. The homogenate was vacuum-filtered (Motor Division Vacuum Pump, SA55JXGTD-4144, Emerson, St. Louis, MO, USA) with qualitative paper (Filter Paper 415, VWR, Radnor, PA, USA) and 10 mL of the filtered solution was titrated with the standard titrating solution containing 0.2 g 2,6-dichloroindophenol ($C_{12}H_6Cl_2NNaO_2$, Ward's Science, West Henrietta, NY, USA) and 0.2 g of sodium bicarbonate ($NaHCO_3$, Ward's Science, West Henrietta, NY, USA) in 1000 mL distilled water (Hughes, 1983).

The volume of titration was recorded and used to quantify the vitamin C content of the sample, the color of the solution turned light amber and did not change color within 30 seconds as the endpoint of the titration. The indophenol solution was standardized by titrating an ascorbic acid (L-Ascorbic acid, free acid, $C_6H_8O_6$, VWR, Radnor, PA, USA) standard solution (1 mg/mL) and sample blanks. Vitamin C content was expressed in mg of ascorbic acid per g of sample on a wet basis. Three repetitions for each treatment and two duplicates for each repetition were performed throughout the shelf-life study (Gomes et al., 2008).

3.3.8. Chlorophyll and Total Carotenoid Content

Spinach samples were prepared after freezing at -20°C and then crushed and freeze-dried for 24 hours. Approximately 100 mg of the sample was suspended in 10 mL of 80% acetone (v/v) (CH_3COCH_3, AR®, Macron Fine Chemicals ™, Radnor, PA, USA) and protected from light while the extraction took place for 24 hours. Extracts were filtered

with paper and the volumes was increased to 25 mL with more than 80% acetone solution. The solutions were analyzed spectrophotometrically (Genesys 10S UV-Vis Spectrophotometer, Thermo Fisher Scientific, Madison, WI, USA) at 470 nm, 646.6 nm, and 663.2 nm in a 1 cm path length cuvette. Absorbance values were used to calculate the level of carotenoids and chlorophylls present according to the method by Yang et al. (1998). The equations for calculating the chlorophyll and total carotenoid content varies according to the extraction solution and its concentration. For 80% acetone in this study:

$$\text{Chlorophyll } a \text{ (μg/mL)} = 12.25\ A_{663.2} - 2.25\ A_{646.6} \qquad 3.10$$

$$\text{Chlorophyll } b \text{ (μg/mL)} = 20.31\ A_{646.6} - 4.91\ A_{663.6} \qquad 3.11$$

$$\text{Total Chlorophyll (μg/mL)} = \text{Chlorophyll } a + \text{Chlorophyll } b \qquad 3.12$$

$$\text{Total Carotenoid (μg/mL)} = \frac{1000\ A_{470} - 2.27C_a - 81.4C_b}{227} \qquad 3.13$$

The content of total chlorophyll and total carotenoid were expressed as micrograms per gram of spinach dry weight. Three repetitions were done for each treatment at each time point and three duplications were made for each repetition.

3.3.9. Scanning Electron Microscopy

On the day of treatment (day 0), all spinach samples from different groups in the shelf life study were freeze-dried overnight without additional fixative to avoid artificial detachment of the nanoparticles from the spinach leaves (Zhang, 2016). About 5 leaves of freeze-dried samples were taken to the Texas A&M University Microscopy and Imaging Center and coated with platinum (Pt) under vacuum using a High-Resolution Sputter Coater 208 HR (Cressington Scientific Instruments UK, Watford, United Kingdom). Observations were made using a scanning electron microscope (Quanta 600 FEG, FEI

Company, Hillsboro, OR, USA) operated at an accelerating voltage of 20 kV and around 10mm working distance with the level of magnification around 608 x.

3.4. Cytotoxicity Testing

3.4.1. Maintenance of Cell Lines

HepG2 cell lines were obtained from the Texas A&M University Laboratory for Environmental Genomics cells collection (Department of Veterinary Integrative Biosciences, College Station, TX).

HepG2 were removed from liquid nitrogen and quickly resuscitated at 37°C water base. Then, 8mL of Dulbecco's Modified Eagle Medium (DMEM 1X, Gibco) was added and inoculated in a cell culture flask for 4h. After that, replaced the DMEM containing 10% fetal bovine serum (FBS) and 1% double-antibody complete medium. At 37°C and 5%, CO_2 saturated humidity, the cells adhered to the culture flask and grew in a crystal-clear elliptical shape, and the medium turned red and transparent.

When the HepG2 cells grew to 80~90% in the culture flask, discarded the culture medium in the flask, washed 3 times with PBS (pH 7.4), and added a certain volume of trypsin solution, spread it evenly on the bottom of the culture flask, and digested. After 1~2 min, discarded the trypsin and added an appropriate amount of DMEM complete medium to stop the digestion. A pipette tip was used to blow the adherent cells into the culture medium, adjusted the concentration of the cell suspension, and inoculated them into the culture flask.

3.4.2. Cytotoxicity of ZIF-8 and TC entrapped ZIF-8 nanoparticles

The cytotoxicity methods used were based on the CellTiter-Glo® 2.0 Assay.

Discarded the culture medium in the flask and digested with 4mL trypsin and collect HepG2 cells, diluted to a 10^6 cells/mL concentration and added 100 μL of the cell suspension to each well (10^5cells/well) of the 96 wells and incubated at 37℃ with 5% CO_2 and saturated humidity for 24 h (Kizhedath et al., 2019).

The cells were then exposed to ZIF-8 and 0.5TC@ZIF-8 with and without 0.1 mg/mL poly-lysine coated, ranging from 10000-1250 ug/ml for ZIF-8 and 5000-1000 ug/ml for 0.5TC@ZIF-8, respectively. Pure *trans*-Cinnamaldehyde was dissolved in warm DMEM media (Sieniawska et al., 2020). All of the solutions are containing 0.5% DMSO to remove sediment, thus the 0.5%DMSO group was set as the base (100% cell viability). Tetrabutylammonium bromide (TAB) was used as positive control and either do 1 concentration (100 μM) or a dose-response (100 μM, 10 μM, 1 μM, and 0.1 μM), depending on plate design. 0.1mg/mL PL was also measured to confirm the non-toxicity of the coating (Figure 3.12).

After 24 h exposure, the plate was equilibrated at room temperature for approximately 30 min. An equal amount (100 μL) of Cell Titer-Glo® Reagent was then added to each well. Contents were mixed for 2 min on an orbital shaker to induce cell lysis. The plate was allowed to incubate at room temperature for 10 min to stabilize the luminescent signal and then record the luminescence.

3.5. Statistical Analysis

All of the experiments carried out in this study were performed in triplicate as independent experiments unless noted otherwise. The data were expressed as mean values ± the standard deviation (SD). Statistical analysis was performed using JMP Pro 15

Statistical Discovery Software from SAS (Cary, NC) with a p-value less than .05 considered as an indication of statistical significance. Differences between variables were tested for significance by one-way analysis of variance (ANOVA). Significantly different means ($p<0.05$) were separated by the Student's t-test. Linear regression and analysis of covariance with a 95 % confidence interval were used when appropriate.

3.6. Experimental Design

The experiments in this research were conducted to test the efficacy of application methods (spraying versus rinsing) of TC@ZIF-8 nanoparticle solutions to inactivate *E.coli* O157:H7 on spinach leaves and determine whether the applied nanoparticles had a detrimental effect on the quality and shelf life of the produce.

The main hypothesis of this study was that TC@ZIF-8 can actively inhibit the growth of *E.coli* O157:H7 and do not have a detrimental effect on the quality and shelf life of fresh spinach leaves. Table 3.4 presents a summary of the indicators used to verify this hypothesis.

96 WELLS	1	2	3	4	5	6	7	8	9	10	11	12
A	0.5% DMSO	PBS	PBS	PBS	PBS	PBS	PBS	PBS	PBS	PBS	PBS	0.5% DMSO
B	0.5% DMSO	ZIF-8 10000 ug/mL	ZIF-8 7500 ug/mL	ZIF-8 5000 ug/mL	ZIF-8 2500 ug/mL	ZIF-8 1250 ug/mL	0.1 mg/mL poly lysine	POS control TAB 100um	POS control TAB 10um	POS control TAB 1um	NEG control	0.5% DMSO
C	0.5% DMSO											0.5% DMSO
D	0.5% DMSO											0.5% DMSO
E	0.5% DMSO	ZIF-8_PL 10000 ug/mL	ZIF-8_PL 7500 ug/mL	ZIF-8_PL 5000 ug/mL	ZIF-8_PL 2500 ug/mL	ZIF-8_PL 1250 ug/mL						0.5% DMSO
F	0.5% DMSO											0.5% DMSO
G	0.5% DMSO											0.5% DMSO
H	0.5% DMSO	PBS	PBS	PBS	PBS	PBS	PBS	PBS	PBS	PBS	PBS	0.5% DMSO

96 WELLS	1	2	3	4	5	6	7	8	9	10	11	12
A	0.5% DMSO	PBS	PBS	PBS	PBS	PBS	PBS	PBS	PBS	PBS	PBS	0.5% DMSO
B	0.5% DMSO	0.5TC_ZIF-8 5000 ug/mL	0.5TC_ZIF-8 4000 ug/mL	0.5TC_ZIF-8 3000 ug/mL	0.5TC_ZIF-8 2500 ug/mL	0.5TC_ZIF-8 1500 ug/mL	0.5TC_ZIF-8 1000 ug/mL	0.1 mg/mL poly lysine	POS control TAB 100um	POS control TAB 10um	NEG control	0.5% DMSO
C	0.5% DMSO											0.5% DMSO
D	0.5% DMSO											0.5% DMSO
E	0.5% DMSO	0.5TC_ZIF-8_PL 5000 ug/mL	0.5TC_ZIF-8_PL 4000 ug/mL	0.5TC_ZIF-8_PL 3000 ug/mL	0.5TC_ZIF-8_PL 2500 ug/mL	0.5TC_ZIF-8_PL 1500 ug/mL	0.5TC_ZIF-8_PL 1000 ug/mL					0.5% DMSO
F	0.5% DMSO											0.5% DMSO
G	0.5% DMSO											0.5% DMSO
H	0.5% DMSO	PBS	PBS	PBS	PBS	PBS	PBS	PBS	PBS	PBS	PBS	0.5% DMSO

96 WELLS	1	2	3	4	5	6	7	8	9	10	11	12
A	0.5% DMSO	PBS	PBS	PBS	PBS	PBS	PBS	PBS	PBS	PBS	PBS	0.5% DMSO
B	0.5% DMSO	trans-Cinnamaldehyde 5000 ug/mL	trans-Cinnamaldehyde 2500 ug/mL	trans-Cinnamaldehyde 1000 ug/mL	trans-Cinnamaldehyde 500 ug/mL	trans-Cinnamaldehyde 250 ug/mL	NEG control	POS control TAB 100um	POS control TAB 10um	POS control TAB 1um	POS control TAB 0.1um	0.5% DMSO
C	0.5% DMSO											0.5% DMSO
D	0.5% DMSO											0.5% DMSO
E	0.5% DMSO											0.5% DMSO
F	0.5% DMSO											0.5% DMSO
G	0.5% DMSO											0.5% DMSO
H	0.5% DMSO	PBS	PBS	PBS	PBS	PBS	PBS	PBS	PBS	PBS	PBS	0.5% DMSO

Figure 3.12 96 well plate designs for cytotoxicity testing.

Table 3.4 Experimental design for tests conducted in this study.

ID	Test Parameters	Treatments	Concentrations	Repititions
1	ZIF-8 nanoparticle synthesis and characterizations	ZIF-8 nanoparticles (ZIF-8) TC entrapped ZIF-8 (TC@ZIF-8) ZIF-8 with 0.1 mg/mL PL coating (ZIF-8_PL) TC entrapped ZIF-8 with 0.1 mg/mL PL coating (TC@ZIF-8_PL)	N/A	N/A
2	Encapsulation Efficiency (EE%)	0.1TC@ZIF-8 0.25TC@ZIF-8 0.5TC@ZIF-8 0.75TC@ZIF-8	0.5 mg/mL	Three repetitions three duplicates per repetition
3	Minimum Inhibitory Concentration (MIC)	ZIF-8 0.5TC@ZIF-8 ZIF-8_PL 0.5TC@ZIF-8_PL *trans* -Cinnamaldehyde (TC) poly-lysine (pL)	1250-10000 µg/mL 250-2000 µg/mL 1250-10000 µg/mL 250-2000 µg/mL 62.5-2000 µg/mL 100-500 µg/mL	Three repetitions three duplicates per repetition
4	Antimicrobial Treatments on the Total Aerobic plate Count of fresh Spinach Leaves 1) Spraying 2) Rinsing	0.5TC@ZIF-8_PL Sterilized distilled water (control) 1 mL on each side 30 s	3000 µg/mL	Three repetitions three duplicates per repetition

Table 3.5 Experimental design for tests conducted in this study(continued).

ID	Test Parameters	Treatments	Concentrations	Repititions
5	Antimicrobial Dose-response Application	ZIF-8 concentrations [mg/mL]	0.1 1 1.5 2.5	Three repetitions three duplicates per repetition
		Sterilized distilled water (control)	N/A N/A N/A N/A	
		0.1TC@ZIF-8	0.11 1.14 1.70 2.84	
		0.1TC@ZIF-8_PL	0.11 1.14 1.70 2.84	
		0.25TC@ZIF-8	0.12 1.19 1.79 2.98	
		0.25TC@ZIF-8_PL	0.12 1.19 1.79 2.98	
		0.5TC@ZIF-8	0.15 1.47 2.21 3.68	
		0.5TC@ZIF-8_PL	0.15 1.47 2.21 3.68	
		0.75TC@ZIF-8	0.14 1.41 2.11 3.52	
		0.75TC@ZIF-8_PL	0.14 1.41 2.11 3.52	
6	Inhibition of Antibacterial Treatments on E.coli O157:H7 Attached to The Surface of Spinach Leaves	Rinse Time [min]	1 5 10 20	10 g spinach each time, three duplications
		Sterilized distilled water (control)	N/A	
		0.5TC@ZIF-8_PL	3.68 mg/mL	
		Chlorine solutoin	200 ppm	
7	Spinach Shelf Life and Quality	Storage Time [day]	0 5 10 15	
		Non-treatment (negative control)	N/A	
		Chlorine solution	200 ppm	
		trans-Cinnamaldehyde	1000 μg/mL	
		0.5TC@ZIF-8_PL	3.58 mg/mL	
	1) Moisture Content (MC)			10 g spinach each time, three duplications
	2) Water Activity (Aw)			2 g spinach each time, ten duplications
	3) Color			5 leaves each time, three duplications per leaf
	4) pH			10 g spinach each time, three duplications
	5) Texture			10 g spinach each time, three duplications
	6) Vitamin C			7 g spinach each time, three repetitions, two duplicates for each repetition
	7) Chlorophyll and Total Carotenoid Content			100 mg spianch, three duplications, three duplicates for each duplication
	8) Scanning Electron Microscopy			N/A

4. RESULTS AND DISCUSSION

4.1. Characterization of ZIF-8 Nanoparticle Complexes

4.1.1. Encapsulation Efficiency of TC@ZIF-8 Nanoparticle Complexes

The encapsulation efficiency (EE%) of the TC@ZIF-8 nanoparticles increased ($p<0.05$) with increasing concentration of the antimicrobial *trans*-cinnamaldehyde, TC (Table 4.1). This result makes sense since the mass ratio of TC per solid weight increased.

The EE% increased when TC concentrations were below 0.5 and the trend gradually slowed down. The maximum EE% ($32.36 \pm 0.20\%$) occurred when the mass ratio of TC to ZIF-8 was 1:2. Similar trends were observed on a horseradish peroxide (HREP) study. The authors observed that as the concentration of horseradish peroxidase (HRP) increased from 1 to 2 mg/mL, the EE% increased from 81% to 98.4% for ZIF-8, but the continuous increase in the concentration of HRP showed even lower EE% in ZIF-8 (Wang et al., 2019). This observation is attributed to the increased number of nucleation sites at a high TC concentration, which resulted in insufficient encapsulation of TC (Wang et al., 2019).

Encapsulation efficiency of drug entrapped ZIF-8 is related to temperature, stirring time, encapsulation time, and the ratio of 2-mim to Zn^{2+} (Tiwari et al., 2017; Chowdhuri et al., 2017; Wang et al., 2018). Long encapsulation time (1 h) may be harmful to the crystallinity of the material. For instance, Tiwari et al. (2017) obtained a high EE% (83.33%) within 15 min synthesis, while Liédana et al. (2012) could only get an EE% around 28% with over 1 h synthesis. In this particular study, because of the unique oily

characteristic of TC, the compound can only be added after the ligand solution formation, which makes it challenging to get the encapsulated material in a short time.

Table 4.1 Encapsulation efficiency (EE%) values for TC@ZIF-8 nanoparticle complexes using spectrophotometer at 295 nm.

TC@ZIF-8	Encapsulation Efficiency [%]*
0.1TC@ZIF-8	11.98 ± 0.01 [a]
0.25TC@ZIF-8	16.13 ± 0.07 [b]
0.5TC@ZIF-8	32.36 ± 0.20 [d]
0.75TC@ZIF-8	29.33 ± 0.08 [c]

*Values given are averages of three replicate samples ± standard deviations;
[a,b, c, d] Means within a column, which are not followed by a common superscript letter are significantly different ($p < 0.05$).

4.2. Microbiological Study

4.2.1. Minimum Inhibitory Concentration (MIC)

The MIC of free TC determined in this study was 1000 µg/mL, which is lower than the 5000 µg/mL MIC determined by Siddiqua et al. (2015) and 2500 µg/mL MIC determined by Firmino et al. (2018) (Table 4.2). The antibacterial activity of essential oils may vary greatly depending on the number of factors such as the plant source, harvest time, developmental stage, and extraction method. These factors will significantly affect the active ingredients of the essential oil (Siddiqua et al., 2015).

The 0.5TC@ZIF-8 nanoparticle complexes were not more effective ($p>0.05$) inhibitors of *E.coli* O157:H7 growth than the ZIF-8 nanoparticles alone. However, 0.5TC@ZIF-8 enhanced the antimicrobial effect as the MIC of TC in the 0.5TC@ZIF-8 nanoparticles were lower than the MIC of free TC itself. Because of the antimicrobial effect of ZIF-8 itself, the same or even lower concentration of 0.5TC@ZIF-8 does not

necessarily enhance the antimicrobial effect of the nanoparticles. Therefore, on the basis of the same ZIF-8 nanoparticle solution concentrations, the antimicrobial dose effect of different mass ratios of TC@ZIF-8 nanoparticle solution concentrations need to be further explored.

All the antimicrobial compounds tested in this study show antimicrobial ability, except for the selected concentrations of poly-lysine. Poly-lysine-coated ZIF-8 and 0.5TC@ZIF-8 nanoparticles did not show an enhanced antimicrobial effect as found by others (Ouyang et al., 2013; Ghilini et al., 2018). Therefore, although PL helped stabilize the nanoparticles, other options must be tested to ensure they are effective antimicrobials.

Table 4.2 Minimum inhibitory concentrations against *E.coli* O157:H7 for different antimicrobial compounds after 24 h exposure

Antimicrobial Compounds	MIC [a] [μg/mL]
trans-Cinnamaldehyde	1000
poly-lysine	> 500 [b]
ZIF-8 nanoparticle solution	2500
ZIF-8_PL nanoparticle solution	5000
0.5TC@ZIF-8 nanoparticle complexes solution	2500 (800) [c]
0.5TC@ZIF-8_PL nanoparticle complexes solution	3000 (960) [c]

[a] Values are the lowest concentration of antimicrobial compounds for which a $\leqslant OD630_{NEG}$ was observed after 24 h incubation at 35°C in TSB;
[b] Values preceded by a higher than (>) means that tested concentrations were not sufficient to determine the MIC values;
[c] Values are the representative concentrations of free *trans*-cinnamaldehyde at the respective NPs concentration based on the encapsulation efficiency.

Concentration of the antimicrobial compounds below the MIC slowed the growth rate of *E.coli* O157:H7. Sub-MIC levels of antimicrobial compounds have a marked effect on *E.coli* O157:H7 growth, decreasing the final absorbance achieved at the stationary

phase (5 h and 10 h for 62.5 μg/mL and 400 μg/mL free TC , respectively) and prolonging the lag phase (Figure 4.1). While PL without antimicrobial effect was showing the same growth curve as the *E.coli* O157:H7 positive group with relatively same lag phase and final absorbance achieved (Figure 4.2). The growth curves of *E. coli* O157: H7 with 24 h exposure to other antimicrobial treatments were illustrated in Appendix C.

Recent studies reported that ZIF-8 was not thermodynamically stable in deionized (DI) water because the structure of ZIF-8 would be destroyed by DI water and then hydrolyzed into zinc and imidazolate ions or transformed into partially hydrolyzed ZIF-8 structures (Luzuriaga et al., 2019). Therefore, TSB and PBS were used as the dispersant of ZIF-8 in the antimicrobial dose-response experiments (Section 4.2.3) and the inhibition of *E.coli* O157:H7 attached to the surface of spinach leaves (Section 4.2.4) respectively. According to Luzuriaga et al. (2019), immersion in serum and cell culture medium would induce the morphological change of ZIF-8 and cause the release of the ZIF-8 drug. At the same time, the authors also measured the release of drugs encapsulated in ZIF-8 over time. After 4 hours, the release amount of green fluorescent protein (GFP) in water was almost zero while in PBS it was 5.84 μg, which is slightly higher than that at the 24h release in PBS, 5.69 μg. This is a good reference to visualize the release time of 0.5TC@ZIF-8_PL nanoparticle solution for the following study (Section 4.3).

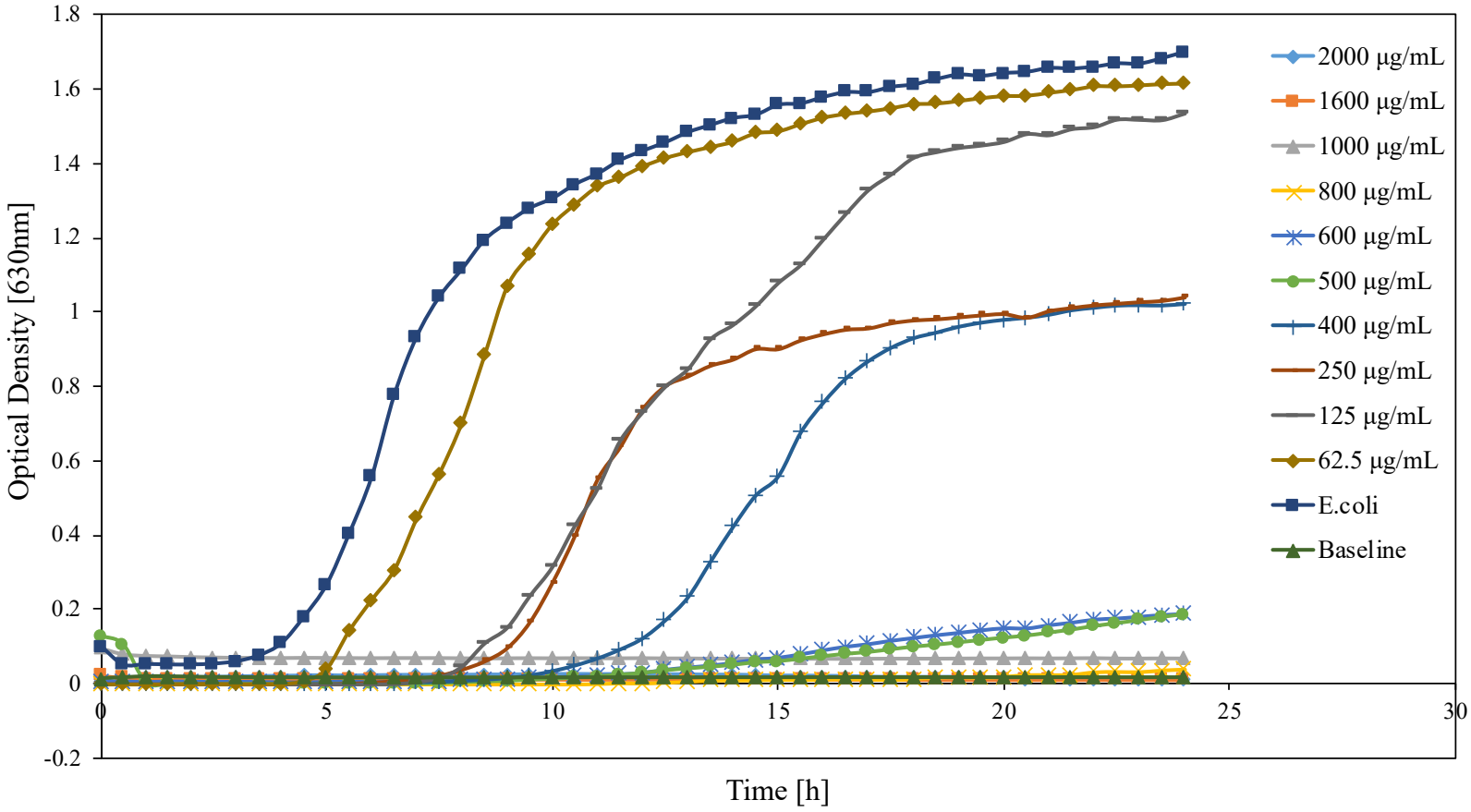

Figure 4.1 Growth Curve of *E.coli* O157:H7 with 24 h treatment with free *trans*-Cinnamaldehyde (TC).

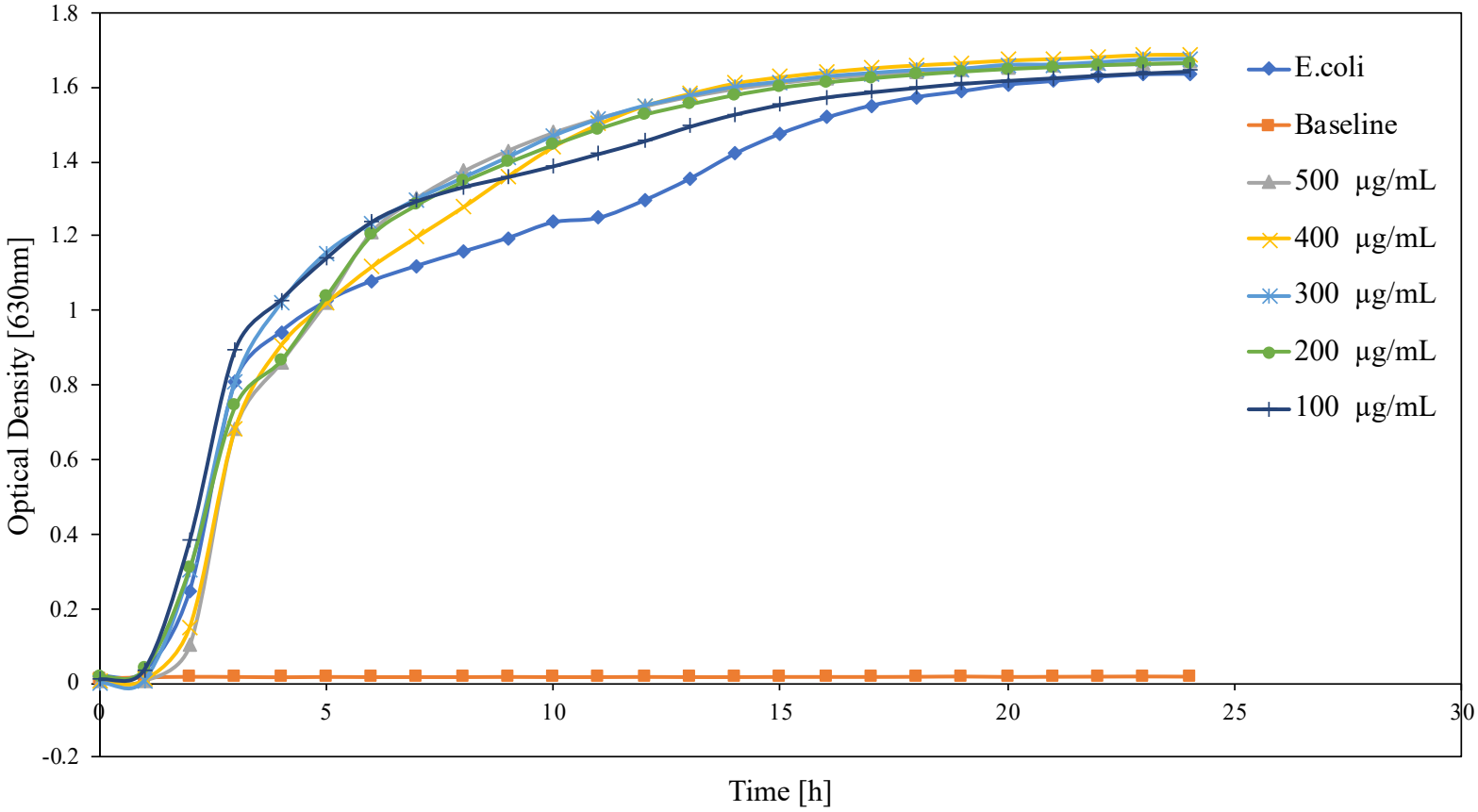

Figure 4.2 Growth curve of *E.coli* O157:H7 with 24 h treatment of poly-lysine.

4.2.2. Effects of Antimicrobial Treatment Applications Method on the Total Aerobic Plate Count (APC) of Fresh Spinach Leaves

Figure 4.3 shows the changes in the appearance of spinach leaves (control) and those leaves sprayed and rinsed with 0.5TC@ZIF-8_PL nanoparticle solution at room temperature for 5 days. Rotting of the control and spraying-treated spinach leaves began on day 3 with yellowing of the leaves, while on day 5, the rot increased, and the leaves became soggy. However, the rinsing-treated spinach leaves did not show any decay during the 5 days of storage at room temperature (~21°C) and only yellowing of leaf color was observed on the 5th day.

Table 4.3 and Figure 4.4 show the changes in total aerobic plate counts (APC) at the surface of spinach leaves in each group stored at room temperature for 5 days. All samples showed similar APC values on the day after treatment (day 0) ($p>0.05$), however, after one day, the APC values increased significantly in all groups ($p<0.05$) and then stabilized within 5 days ($p>0.05$). Although not regulated in the United States, it is generally accepted that the maximum acceptable microbial load is 7 log10 CFU/g of produce by the end-use date (Prakash et al., 2000; Artés et al., 2007). By this standard, all treated spinach samples were acceptable in terms of microbiological quality by the end of storage (5 days at room temperature). In terms of APC values, rinsing application method was more likely ($p<0.05$) to extend the shelf life of spinach stored at room temperature (Table 4.3).

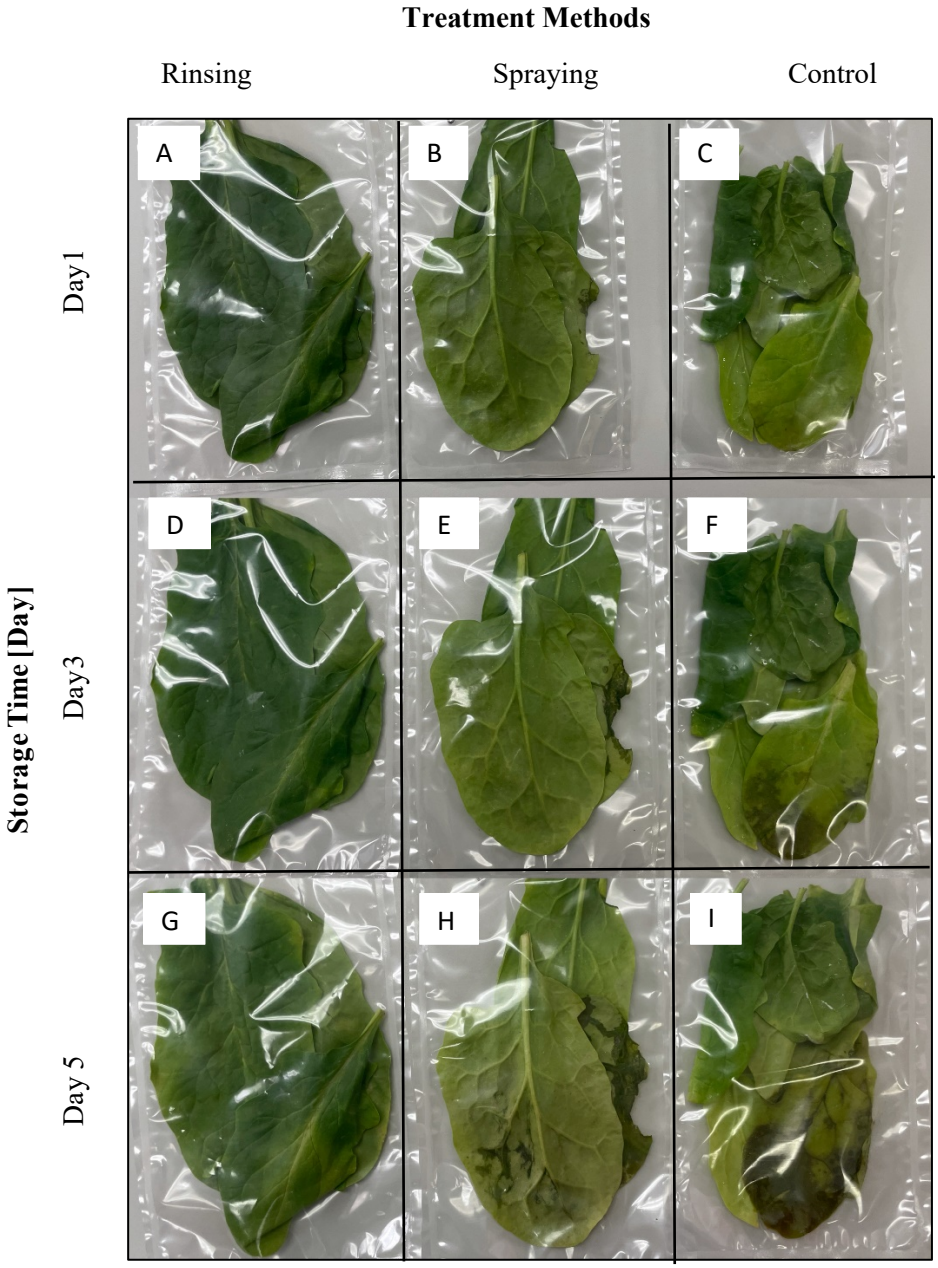

Figure 4.3 Overall appearances of fresh spinach controls and spinach samples after spraying and rinsing with 0.5 TC@ZIF-8_PL nanoparticle solution, over 5 days storage at room temperature (20-25℃).

Spinach leaves (A) spraying treated with 0.5TC@ZIF-8_PL on day 1; (B) spraying treated with 0.5TC@ZIF-8_PL on day 1; (C) control on day 1; (D) rinsing treated with 0.5TC@ZIF-8_PL on day 3; (E) spraying treated with 0.5TC@ZIF-8_PL on day 3; (F) control on day 3; (G) rinsing treated with 0.5TC@ZIF-8_PL on day 5; (H) spraying treated with 0.5TC@ZIF-8_PL on day 5; (I) control after on day 5;

Table 4.3 Total aerobic plate counts (APC) on the surface of raw spinach and spinach samples after spraying and rinsing with 0.5 TC@ZIF-8_PL nanoparticle solution, over 5 days storage at room temperature (21°C).

	Total Aerobic Plate Count [log10 CFU/g]			
Treatment Methods/Day	**0**	**1**	**3**	**5**
Control	$_{w}3.79^{a}$	$_{x}6.39^{c}$	$_{x}6.48^{c}$	$_{x}6.95^{c}$
	(0.50)	(0.48)	（0.67）	(0.46)
Spraying	$_{w}3.32^{a}$	$_{x}5.37^{b}$	$_{x}5.80^{ab}$	$_{x}6.23^{b}$
	(0.20)	(0.31)	(0.23)	(0.29)
Rinsing	$_{w}3.46^{a}$	$_{x}4.59^{a}$	$_{x}5.10^{a}$	$_{x}5.05^{a}$
	(0.29)	(0.18)	（0.20）	（0.17）

[a, b, c] Means within a column, which are not followed by a common superscript letter are significantly different ($p < 0.05$).

[w, x, y] Means within a row, which are not preceded by a common subscript letter, are significantly different ($p < 0.05$).

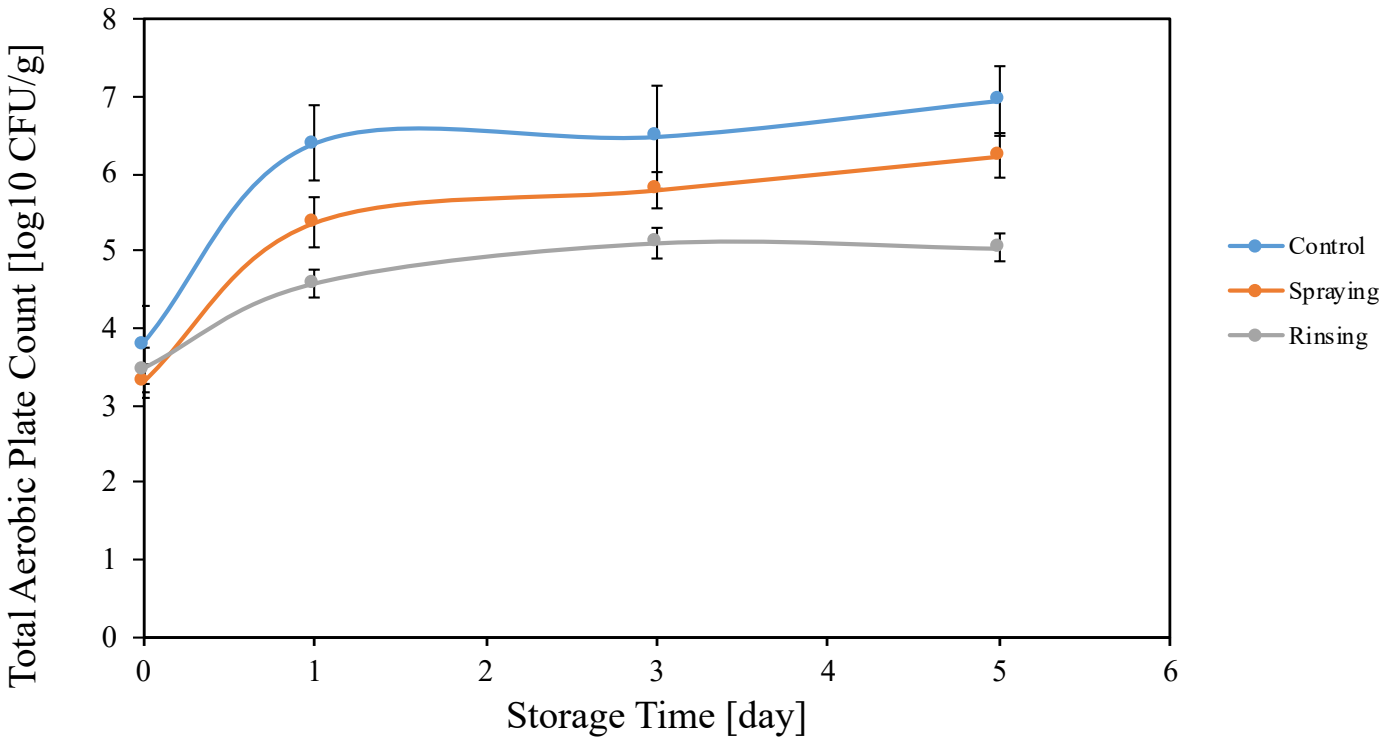

Figure 4.4 Effect of application method on the total aerobic plate counts on the surface of spinach samples with 0.5 TC@ZIF-8_PL nanoparticle solution, over 5 days storage at room temperature (21°C)

4.2.3. Antimicrobial Dose-Response Application

Figure 4.5 shows that as the concentration of ZIF-8 increases, the antimicrobial effect increases ($p < 0.05$), achieving approximately 1 to 5 log reductions for *E.coli* O157:H7 for ZIF-8 concentration ranging from 0.5 to 2.5 mg/mL. The initial *E.coli* population was 9 logs CFU/mL for the control group. At a constant ZIF-8 concentration, measured concentrations of TC-entrapped samples increased ($p > 0.05$) the log reduction, with the 0.5TC@ZIF-8 treatment the most significant ($p < 0.05$), achieving 2 to 6 log reductions depending upon the concentration of ZIF-8.

When the PL coated ZIF-8 nanoparticles were tested at the same concentration, the antimicrobial effect also increased ($p < 0.05$) with increased concentration of ZIF-8, achieving 0.5 to 2.5 log reductions (Figure 4.6). At a constant ZIF-8 concentration, measured concentrations of TC-entrapped samples increased ($p < 0.05$) the number of log reductions, with 0.5TC@ZIF-8 treatment the most significant with 3 log reductions when the ZIF-8 concentrations were 1.5 and 2.5 mg/mL. Overall, the 0.5TC@ZIF-8 nanoparticle complexes had the highest antimicrobial effect. This finding coincides with the highest encapsulation efficiency (32%) of this complex.

Appendix D shows the antimicrobial effect of the TC@ZIF-8 with and without poly-lysine coating. As Figure 4.7 shows, all the concentrations of ZIF-8 nanoparticles had significant reduction ($p < 0.05$) in their antimicrobial effect when the PL coating was applied.

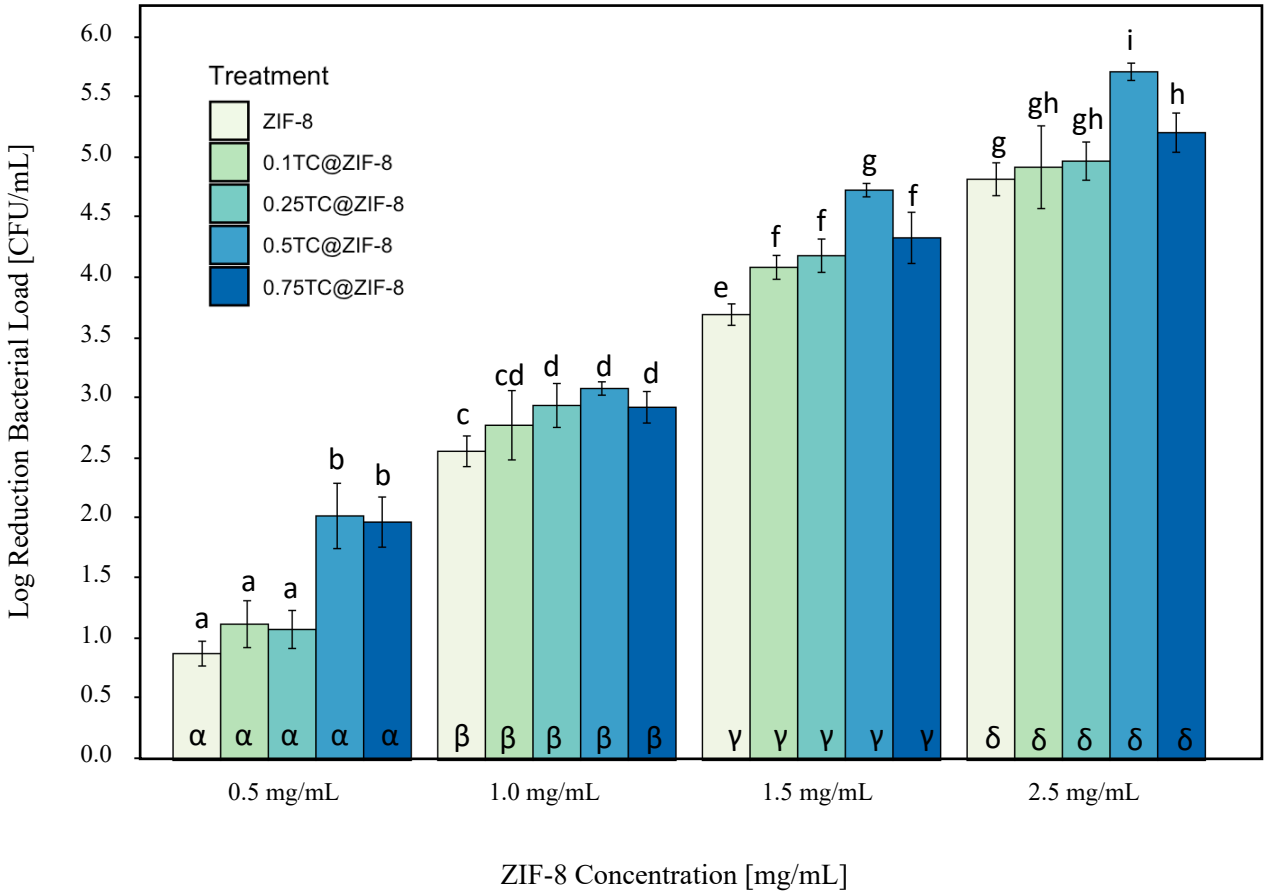

Figure 4.5 Bacteria log reductions of ZIF-8 and different ratios of TC@ZIF-8 at the same ZIF-8 concentration after 24h treatment at 35ºC. Initial *E.coli* O157:H7 population was 9 log CFU/mL.

The English letters (a, b, c, d, e, f, g, h, i) beyond the error bar means at the same ZIF-8 concentrations, which is not followed by a common letter are significantly different ($p < 0.05$).The Greek letters (α, β, γ, δ) at the bottom of the column means under the same treatment, which is not followed by a common letter are significantly different ($p<0.05$)

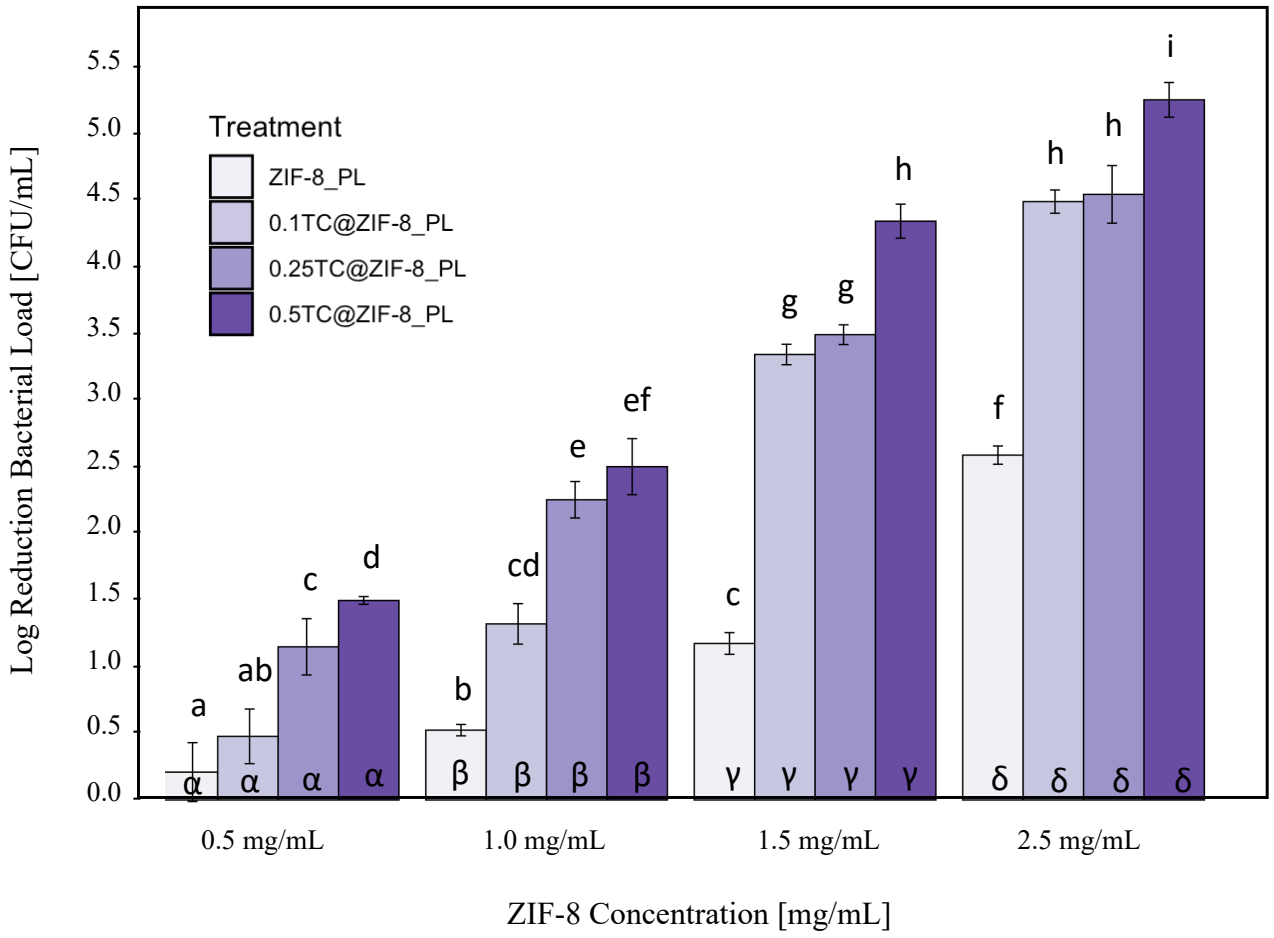

Figure 4.6 Bacteria log reductions of ZIF-8_PL and different ratios of TC@ZIF-8_PL at the same ZIF-8 concentration after 24h treatment at 35ºC. Initial *E.coli* O157:H7 population was 9 log CFU/mL.

The English letters (a, b, c, d, e, f, g, h, i) beyond the error bar means at the same ZIF-8 concentrations, which is not followed by a common letter are significantly different ($p < 0.05$).The Greek letters (α, β, γ, δ) at the bottom of the column means under the same treatment, which is not followed by a common letter are significantly different ($p<0.05$)

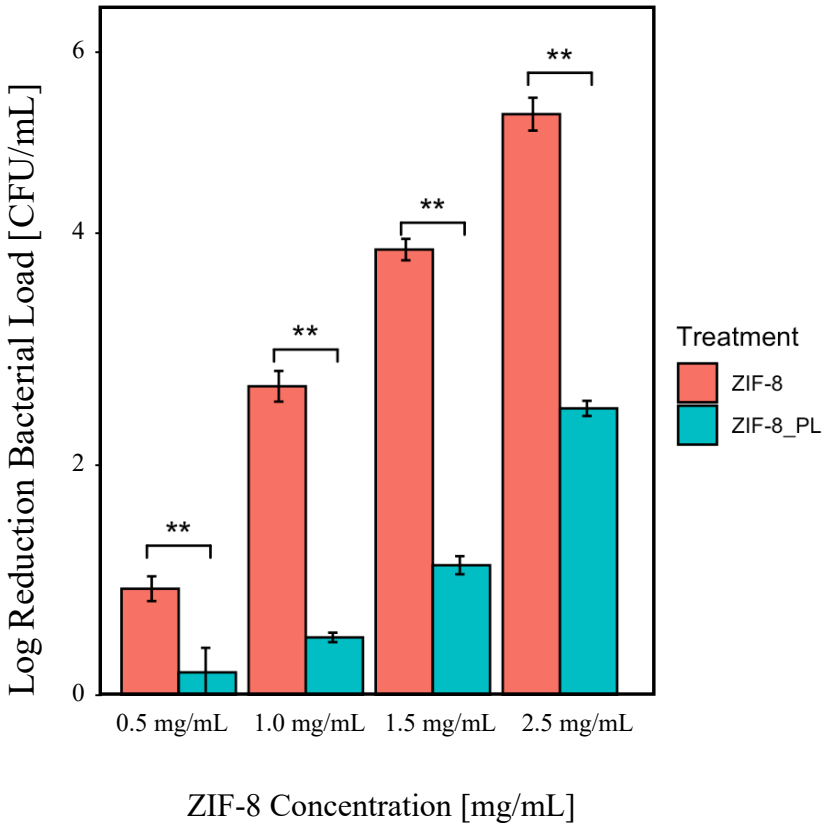

Figure 4.7 Comparison of antimicrobial log reductions of ZIF-8 nanoparticles with and without PL coating at the same ZIF-8 concentration after 24h treatment at 35ºC. Initial *E.coli* O157:H7 population was 9 log CFU/mL.
The notations beyond the error bar means at the same ZIF-8 concentrations, the significant difference between groups with/without poly-lysine coating under student's t test: · $p>0.05$, * $0.01<p<0.05$, ** $0.001<p<0.01$, *** $p<0.001$

4.2.4. Inhibition of the growth of *E.coli* O157:H7 attached to the surface of spinach leaves by antimicrobial treatments

Treatment with 0.5TC@ZIF-8 nanoparticle complexes is more effective ($p<0.05$) under the same rinse time than rinsing spinach leaves with 200 ppm chlorine. This finding was more significant ($p<0.01$) for relatively short time wash (1, 5, and 10 min) (Figure 4.8). With the increased rinse time, the antimicrobial effect of chlorine increased while there was

no difference ($p>0.05$) for 0.5TC@ZIF-8 nanoparticle complexes. These results are similar to those obtained by Keskinen et al. (2009), who reported that 200 ppm chlorine could reduce an average of 0.66 logs of *E.coli* O157:H7 after 2min treatment. Pan et al. (2014) found the results of antimicrobial treatments by different sources of free chlorine, with 1.14-1.22 log reduction in *E.coli* O157:H7 after treatment with 100 ppm NaClO for 1, 5 and 10 min, and 1.38-1.56 log reduction after washing with 50 ppm ClO_2 , both similar to the results of this study. In summary, rinsing the spinach leaves with 0.5TC@ZIF-8_PL nanoparticle complexes for 1 min is the best treatment in terms of pathogen surface.

4.3. Shelf Life and Quality Study

4.3.1. Appearance

Figure 4.9. shows the changes in appearance of spinach leaves stored at 4 ºC for 15 days. On days 0 and 5, there was no noticeable color or firmness change between the groups when touched. However, starting from the 10th day, the leaves became soft and yellowish, especially in the groups treated with 200 ppm chlorine and TC. By the 15th day, the softness of the leaves increased, moisture loss. The water droplets on the packing bags confirm this as the leaves were initially dry. Rotting occurred due to slight damage at the edges of some leaves as well as damage to the leaves during cleaning, but only in a minimal number of leaves.

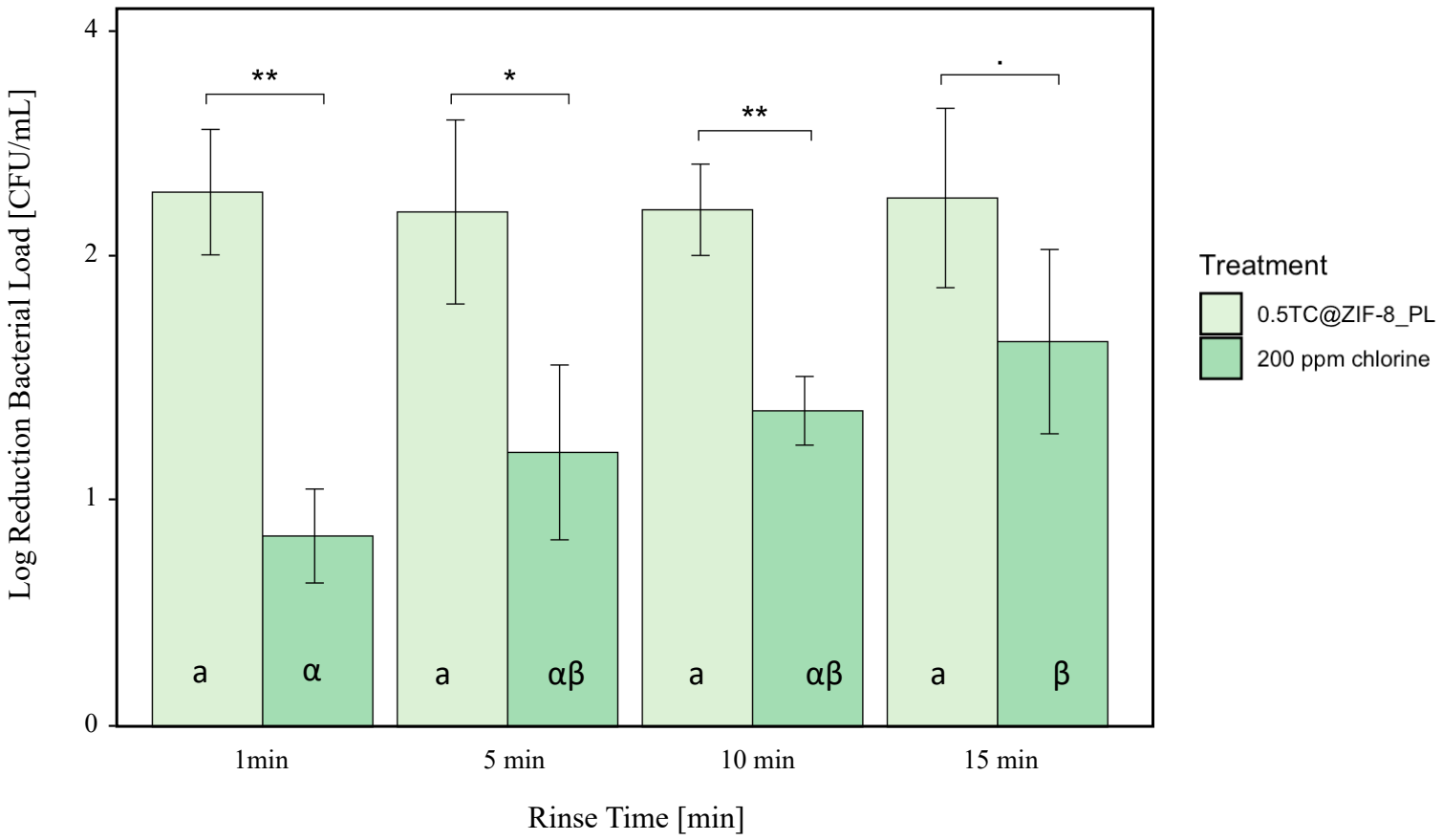

Figure 4.8 Antimicrobial effect of rinsing with 0.5TC@ZIF-8 and 200ppm chlorine solution at different rinse times

The notations beyond the error bar means at the same rinse time, the significant difference of the number of inhibited bacteria under different treatments under student's t-test: · $p>0.05$, * $0.01<p<0.05$, ** $0.001<p<0.01$;The English letters (a) and Greek alphabets (α, β) at the bottom of the column mean at the same treatments, which is not followed by a common letter are significantly different ($p < 0.05$) for rinse time.

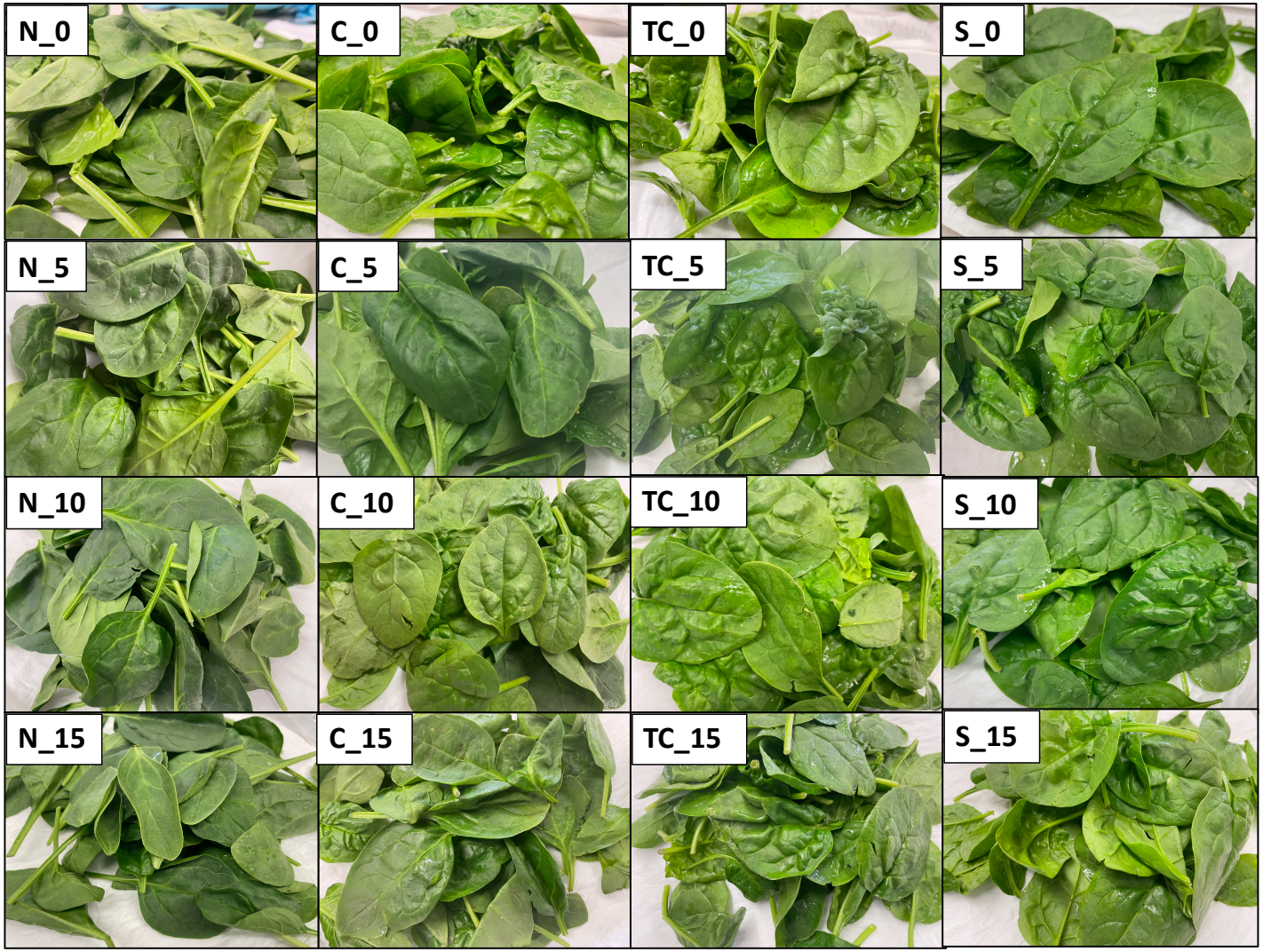

Figure 4.9 Overall appearances of fresh spinach controls (N) and spinach samples treated with chlorine (C), *trans*-Cinnamaldehyde (TC), and 0.5TC@ZIF-8_PL (S) over 15 days of storage at 4°C.

4.3.2. Moisture Content

The moisture content of all treated spinach decreased ($p<0.05$) throughout the storage time (Table 4.4). This was due to the migration of moisture from the leaves into the package, as the antimicrobial compounds do not provide any physical barrier to retain moisture. In particular, the control group showed a significant decrease on day 5 ($p<0.05$), while the chlorine, free TC, and 0.5 TC@ZIF-8_PL treatment groups showed a decrease on days 10, 15, and 10, respectively ($p<0.05$); this suggests, to some extent, that the treatment groups could alleviate the moisture loss problem of spinach during storage.

The moisture content of each treatment group was higher ($p<0.05$) than the control group, mainly because the rinsing process may have allowed some water to penetrate the cells.

4.3.3. Water Activity

All treatment groups showed higher water activity than the control group ($p<0.05$), which could be the result of water penetration into the cell walls due to rinsing during the treatment (Table 4.5). There was no change in water activity in all groups over time ($p>0.05$).

Table 4.4 Moisture content (w.b.%) of fresh spinach (control and samples) over 15 days of storage at 4°C.

	% Moisture (wet basis)			
Treatment*/Day	**0**	**5**	**10**	**15**
Control	$_{x}91.11^{a}$ (0.70)	$_{w}88.85^{a}$ (0.17)	$_{w}89.34^{a}$ （0.91）	$_{w}89.45^{a}$ (0.83)
200 ppm Chlorine	$_{wx}91.24^{a}$ (0.09)	$_{w}90.62^{b}$ （0.44）	$_{x}91.74^{b}$ （0.60）	$_{x}91.59^{b}$ （0.62）
***trans*-Cinnamaldehyde**	$_{x}92.94^{b}$ (0.76)	$_{x}92.48^{c}$ （0.07）	$_{wx}92.13^{b}$ (0.19)	$_{w}91.36^{b}$ （0.62）
0.5TC@ZIF-8_PL	$_{x}93.35^{b}$ (0.62)	$_{wx}92.91^{c}$ （0.19）	$_{w}92.25^{b}$ (0.24)	$_{w}92.24^{b}$ （0.77）

***** Treatments consisted of rinsing with sterilized water, 200 ppm chlorine, 1000 μg/mL free trans-cinnamaldehyde and 3.68 mg/mL 0.5TC@ZIF-8_PL nanoparticle complexes solution for 1 min in Section 3.3.2.

$^{a, b, c}$ Means within a column, which are not followed by a common superscript letter are significantly different ($p < 0.05$).

$_{w, x}$ Means within a row, which are not preceded by a common subscript letter, are significantly different ($p < 0.05$).

Table 4.5 Water activity of fresh spinach (control and samples) over 15 days of storage at 4°C.

	Aw			
Treatment*/Day	**0**	**5**	**10**	**15**
Control	$_{w}0.982^{a}$ (0.008)	$_{w}0.981^{a}$ (0.017)	$_{w}0.981^{a}$ (0.017)	$_{w}0.980^{a}$ (0.015)
200 ppm Chlorine	$_{w}0.992^{b}$ (0.006)	$_{w}0.994^{b}$ （0.004）	$_{w}0.990^{b}$ （0.008）	$_{w}0.988^{b}$ （0.010）
***trans*-Cinnamaldehyde**	$_{w}0.993^{b}$ (0.003)	$_{w}0.993^{b}$ (0.013)	$_{w}0.991^{b}$ （0.009）	$_{w}0.989^{b}$ （0.010）
0.5TC@ZIF-8_PL	$_{w}0.991^{b}$ (0.008)	$_{w}0.990^{b}$ (0.005)	$_{w}0.990^{b}$ (0.011)	$_{w}0.991^{b}$ (0.003)

* Treatments consisted of rinsing with sterilized water, 200 ppm chlorine, 1000 μg/mL free trans-cinnamaldehyde and 3.68 mg/mL 0.5TC@ZIF-8_PL nanoparticle complexes solution for 1 min in Section 3.3.3.

[a,b] Means within a column, which are not followed by a common superscript letter are significantly different ($p < 0.05$).

[w] Means within a row, which are not preceded by a common subscript letter, are significantly different ($p < 0.05$).

4.3.4. Color

The lightness (L* values) of the control and samples treated with chlorine did not change ($p>0.05$) with time while this parameter varied ($p<0.05$) for the groups treated with free TC and 0.5TC@ZIF-8_PL (Table 4.6). Lower *L values mean that the leaves become slightly darker as time goes by. This may occur as microbial spoilage progresses or as moisture content decreases (Prakash et al., 2000).

Table 4.6 CIELAB L*a*b* color parameters of fresh spinach (control and samples) over 15 days of storage at 4°C.

	L*			
Treatment*/Day	**0**	**5**	**10**	**15**
Control	$_{w}$24.86^{a} (1.83)	$_{w}$24.35^{a} (2.10)	$_{w}$23.58^{a} (1.94)	$_{w}$23.15^{a} (1.21)
200 ppm Chlorine	$_{w}$24.85^{a} (2.58)	$_{w}$26.07^{a} (2.45)	$_{w}$26.17^{b} (0.84)	$_{w}$26.25^{b} (0.99)
***trans*-Cinnamaldehyde**	$_{wx}$24.63^{a} (1.4)	$_{x}$25.50^{a} (1.09)	$_{x}$25.96^{b} (1.39)	$_{w}$23.46^{a} (2.05)
0.5TC@ZIF-8_PL	$_{x}$27.89^{b} (2.34)	$_{w}$25.58^{a} (1.79)	$_{wx}$26.61^{b} (1.57)	$_{w}$25.53^{b} (0.78)
	a*			
Control	$_{x}$-4.34^{ab} (0.67)	$_{wx}$-4.12^{a} (0.49)	$_{w}$-3.76^{a} (0.40)	$_{w}$-3.67^{a} (0.35)
200 ppm Chlorine	$_{w}$-4.05^{a} (0.76)	$_{x}$-5.10^{b} (0.60)	$_{x}$-4.95^{b} (0.43)	$_{x}$-4.76^{b} (0.29)
***trans*-Cinnamaldehyde**	$_{w}$-4.92^{bc} (0.37)	$_{w}$-5.07^{b} (0.34)	$_{w}$-4.89^{b} (0.53)	$_{w}$-5.11^{bc} (0.44)
0.5TC@ZIF-8_PL	$_{x}$-5.29^{c} (0.09)	$_{x}$-5.30^{b} (0.13)	$_{w}$-4.98^{b} (0.27)	$_{wx}$-5.12^{c} (0.31)
	b*			
Control	$_{x}$7.29^{a} (1.22)	$_{wx}$7.02^{a} (0.86)	$_{w}$6.19^{a} (0.70)	$_{w}$6.17^{a} (0.64)
200 ppm Chlorine	$_{w}$7.15^{a} (1.56)	$_{x}$8.99^{b} (1.42)	$_{x}$9.09^{b} (0.54)	$_{x}$8.67^{b} (0.77)
***trans*-Cinnamaldehyde**	$_{w}$8.61^{ab} (0.58)	$_{w}$8.99^{b} (0.51)	$_{w}$8.75^{b} (0.95)	$_{w}$8.85^{b} (0.88)
0.5TC@ZIF-8_PL	$_{x}$9.74^{b} (0.96)	$_{wx}$9.10^{b} (0.41)	$_{w}$8.65^{b} (0.27)	$_{w}$9.05^{b} (0.56)

***** Treatments consisted of rinsing with sterilized water, 200 ppm chlorine, 1000 μg/mL free trans-cinnamaldehyde and 3.68 mg/mL 0.5TC@ZIF-8_PL nanoparticle complexes solution for 1 min in Section 3.3.4.

^{a,b,c} Means within a column, which are not followed by a common superscript letter are significantly different ($p < 0.05$).

$_{w,x}$ Means within a row, which are not preceded by a common subscript letter, are significantly different ($p < 0.05$).

The *a values of the samples did not change ($p>0.05$) over time for TC-treated spinach while it increased for both the control group and 0.5TC@ZIF-8_PL samples and decreased ($p<0.05$) for the chlorine-treated group. According to the color changes observed in Section 4.3.1, spinach leaves began to show varying degrees of yellowing on day 10, which is also consistent with an increase in a* values. The a* values were all negative, indicating a greener of color (Archana et al., 1995). Thus, the lower the *a values, the deeper the green leaf. The decrease in green intensity is explained as chlorophyll is converted to pheophytin and other derivatives, which change from bright green to dark olive green or olive-yellow (Lu et al., 2009).

The b* values showed inverse changes compared to a* values (Table 4.6). The TC entrapped ZIF-8 nanoparticles solution did not help protect the leaves from discoloration compared to the control, while free TC and chlorine did. The apparent differences in color properties between treatments within the same day can be attributed to the heterogeneity of spinach color across leaves, as samples tend to follow the same color change trend (Bolin & Huxsoll 1991).

The overall color change was expressed as a decrease in total color (E) of spinach leaves with storage time (Figure 4.8), which indicates the loss of color in spinach leaves. This parameter did not change with time for the control and chlorine treated groups ($p>0.05$), while it decreased for the TC and 0.5TC@ZIF-8_PL treated groups showed a significant decrease ($p<0.05$) on the fifth and tenth day, respectively. It was shown that TC and 0.5TC@ZIF-8_PL treated groups started to adversely affect the color of spinach leaves on the fifth and tenth day, respectively

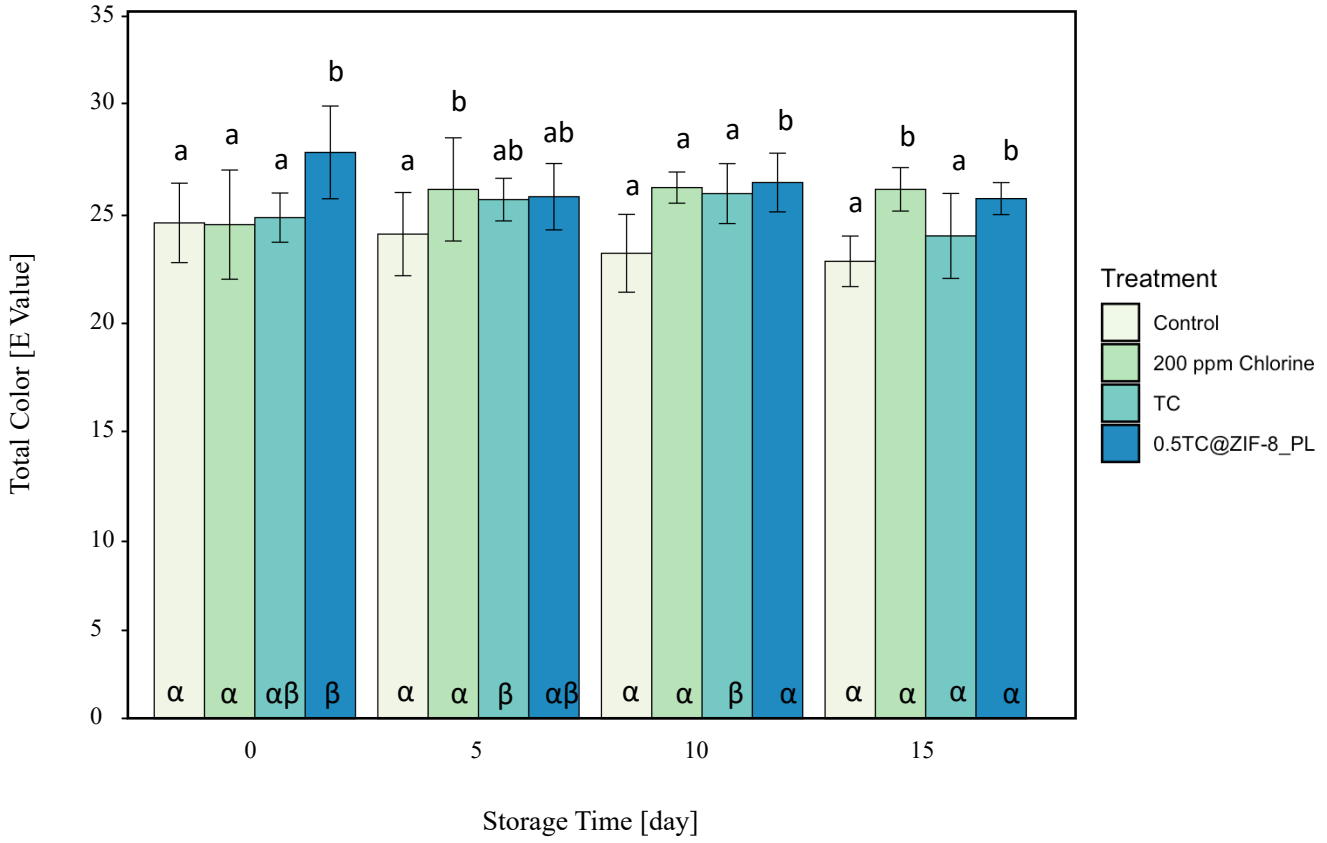

Figure 4.10 Calculated values for total color (E) by instrumentally measured color parameters L, a, and b of fresh spinach (control and samples) over 15 days of storage at 4°C.

The English letters (a, b) beyond the error bar means at the same storage day of different treatment, which is not followed by a common letter are significantly different ($p < 0.05$). The Greek letters (α, β) at the bottom of the column means under the same treatment during different storage points, which are not preceded by a common letter, are significantly different ($p < 0.05$).

4.3.5. pH

The pH for the control group decreased ($p<0.05$) during storage time while it increased ($p<0.05$) for the free TC and 0.5TC@ZIF-8_PL treated groups (Table 4.7). The chlorine-treated samples presented an increased trend first, to reach a peak at day 10 and then decrease, which was similar to the results from Martín-Diana et al. (2008). The authors reported a significant increase in pH values of fresh-cut lettuce with a peak at day 7 and then decreased at day 10 under both chlorine and green tea extract treatment. Many studies have explained the phenomenon that pH values would increase with the growth of gram-negative microbes (King & Bolin, 1989; Jacxsens et al., 2003; Gomes-Lopez et al., 2005), and the lower pH on day 15 may respond to an increase in lactic acid bacteria (Martín-Diana et al., 2008).

Table 4.7 pH values of fresh spinach (control and samples) over 15 days of storage at 4°C.

	pH			
Treatment*/Day	**0**	**5**	**10**	**15**
Control	$_{x}7.33^{a}$ (0.11)	$_{x}7.29^{a}$ (0.05)	$_{w}7.13^{a}$ （0.06）	$_{w}7.16^{a}$ （0.01）
200 ppm Chlorine	$_{w}7.29^{a}$ (0.06)	$_{wx}7.47^{b}$ (0.09)	$_{x}7.68^{c}$ (0.26)	$_{w}7.30^{ab}$ （0.16）
***trans*-Cinnamaldehyde**	$_{w}7.22^{a}$ (0.04)	$_{wx}7.44^{b}$ （0.05）	$_{x}7.60^{bc}$ (0.07)	$_{x}7.63^{c}$ (0.22)
0.5TC@ZIF-8_PL	$_{w}7.29^{a}$ (0.06)	$_{x}7.46^{b}$ (0.05)	$_{x}7.45^{ab}$ (0.06)	$_{x}7.52^{bc}$ (0.05)

***** Treatments consisted of rinsing with sterilized water, 200 ppm chlorine, 1000 μg/mL free trans-cinnamaldehyde and 3.68 mg/mL 0.5TC@ZIF-8_PL nanoparticle complexes solution for 1 min in Section 3.3.5.

^{a,b,c} Means within a column, which are not followed by a common superscript letter are significantly different ($p < 0.05$).

$_{w,x}$ Means within a row, which are not preceded by a common subscript letter, are significantly different ($p < 0.05$).

4.3.6. Texture (Firmness and work)

The maximum force and work required to shear spinach leaves increased throughout storage time for both the free TC and 0.5 TC@ZIF-8_PL treated samples ($p<0.05$), while no changes were observed for control and chlorine-treated groups ($p>0.05$) (Table 4.8, Figure 4.11 and 4.12). This increase in required force may be due to some damage in the leaves occurring when treated with the antimicrobial agents, which produce lignin and suberin inside the leaves to prevent water loss and may contribute to the hardening of the leaves, which then increases the maximum force and work for shearing (Lipton 1990; Thomson et al. 1995; Jacobsson et al. 2004). Yossa et al. (2012) also observed an increase in the maximum force required to shear spinach leaves treated with cinnamaldehyde, which was significantly higher than its initial value after 10 days of storage at 4ºC.

As spinach leaves age, their cell membranes break down, causing a slow leakage from which water and other things seep out, and the spinach subsequently becomes soggy, hard, and crispy disappearing, thus resulting in lower shear forces (Spinard et al., 2009). In contrast, in this study, no reduction in force or work was evident in all groups ($p>0.05$), indicating that the spinach was in good condition for 15 days storage at 4ºC in terms of textural characteristics.

Bacteria prefer moist environments, so once spinach leaves become slimy, they are more likely to be contaminated with microorganisms when they contact a dirty surface (Monaghan & Hutchison, 2015). Moreover, microbial decay can promote softening of the entire tissue (Baur et al., 2005). In this study, the increase ($p<0.05$) in force and work in

the TC and 0.5TC@ZIF-8_PL treated groups suggests that the spinach leaves were firmer and thus more difficult to be infected by microorganisms, which would keep the spinach fresher for longer when stored at 4ºC.

Table 4.8 The maximum force and work to shear of fresh spinach (control and samples) over 15 days of storage at 4°C.

	Force (N)			
Treatment*/Day	**0**	**5**	**10**	**15**
Control	$_{w}262.86^{c}$ (31.89)	$_{w}256.48^{b}$ (44.77)	$_{w}278.80^{b}$ （49.74）	$_{w}275.82^{c}$ （24.98）
200 ppm Chlorine	$_{w}235.15^{c}$ (25.00)	$_{w}232.23^{ab}$ (32.06)	$_{w}192.05^{a}$ (7.35)	$_{w}233.03^{bc}$ (47.20)
***trans*-Cinnamaldehyde**	$_{wx}175.61^{b}$ (18.40)	$_{x}182.34^{a}$ （27.08）	$_{x}181.86^{a}$ (25.11)	$_{x}194.73^{a}$ (12.23)
0.5TC@ZIF-8	$_{w}128.26^{a}$ (20.36)	$_{x}177.09^{a}$ (28.20)	$_{x}191.49^{a}$ （16.92）	$_{x}174.71^{ab}$ (14.35)
	Work (J)			
Control	$_{w}1.17^{c}$ (0.13)	$_{w}1.03^{a}$ (0.22)	$_{w}1.03^{b}$ （0.17）	$_{w}0.94^{c}$ （0.11）
200 ppm Chlorine	$_{w}0.84^{b}$ (0.16)	$_{w}0.91^{a}$ (0.24)	$_{w}0.85^{ab}$ (0.08)	$_{w}0.87^{b}$ (0.10)
***trans*-Cinnamaldehyde**	$_{w}0.79^{b}$ (0.05)	$_{x}0.76^{a}$ （0.12）	$_{x}0.73^{a}$ (0.09)	$_{x}0.79^{ab}$ (0.18)
0.5TC@ZIF-8	$_{w}0.53^{a}$ (0.11)	$_{x}0.82^{a}$ (0.06)	$_{x}0.76^{a}$ （0.03）	$_{x}0.72^{a}$ (0.09)

***** Treatments consisted of rinsing with sterilized water, 200 ppm chlorine, 1000 μg/mL free trans-cinnamaldehyde and 3.68 mg/mL 0.5TC@ZIF-8_PL nanoparticle complexes solution for 1 min in Section 3.3.6.

^{a,b,c} Means within a column, which are not followed by a common superscript letter are significantly different ($p < 0.05$).

$_{w,x}$ Means within a row, which are not preceded by a common subscript letter, are significantly different ($p < 0.05$).

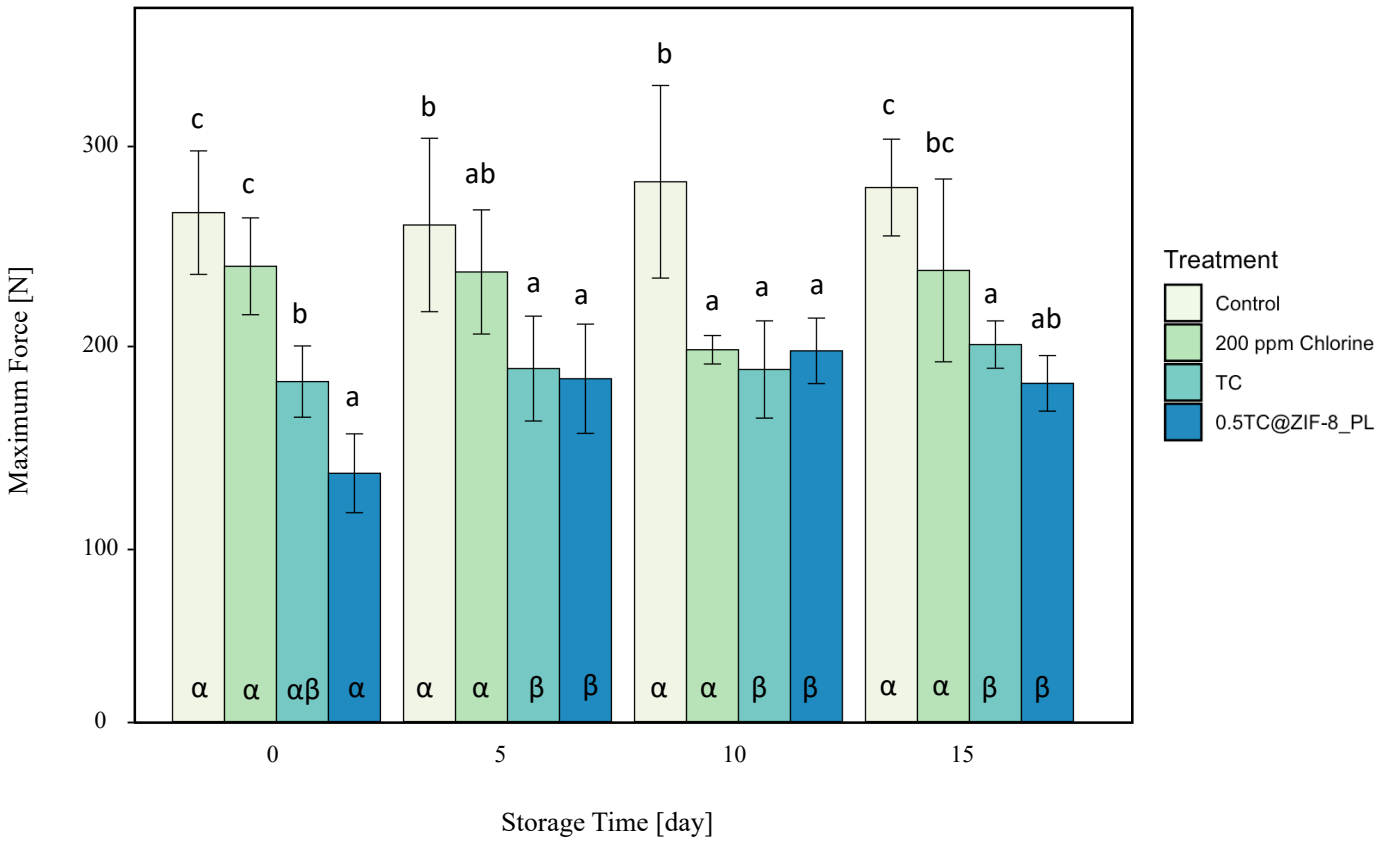

Figure 4.11 Maximum force (N) required to cut through fresh spinach (control and samples) over 15 days of storage at 4°C.

The English letters (a, b, c) beyond the error bar means at the same storage day of different treatment, which is not followed by a common letter are significantly different ($p < 0.05$). The Greek letters (α, β) at the bottom of the column means under the same treatment during different storage points, which are not preceded by a common letter, are significantly different ($p < 0.05$).

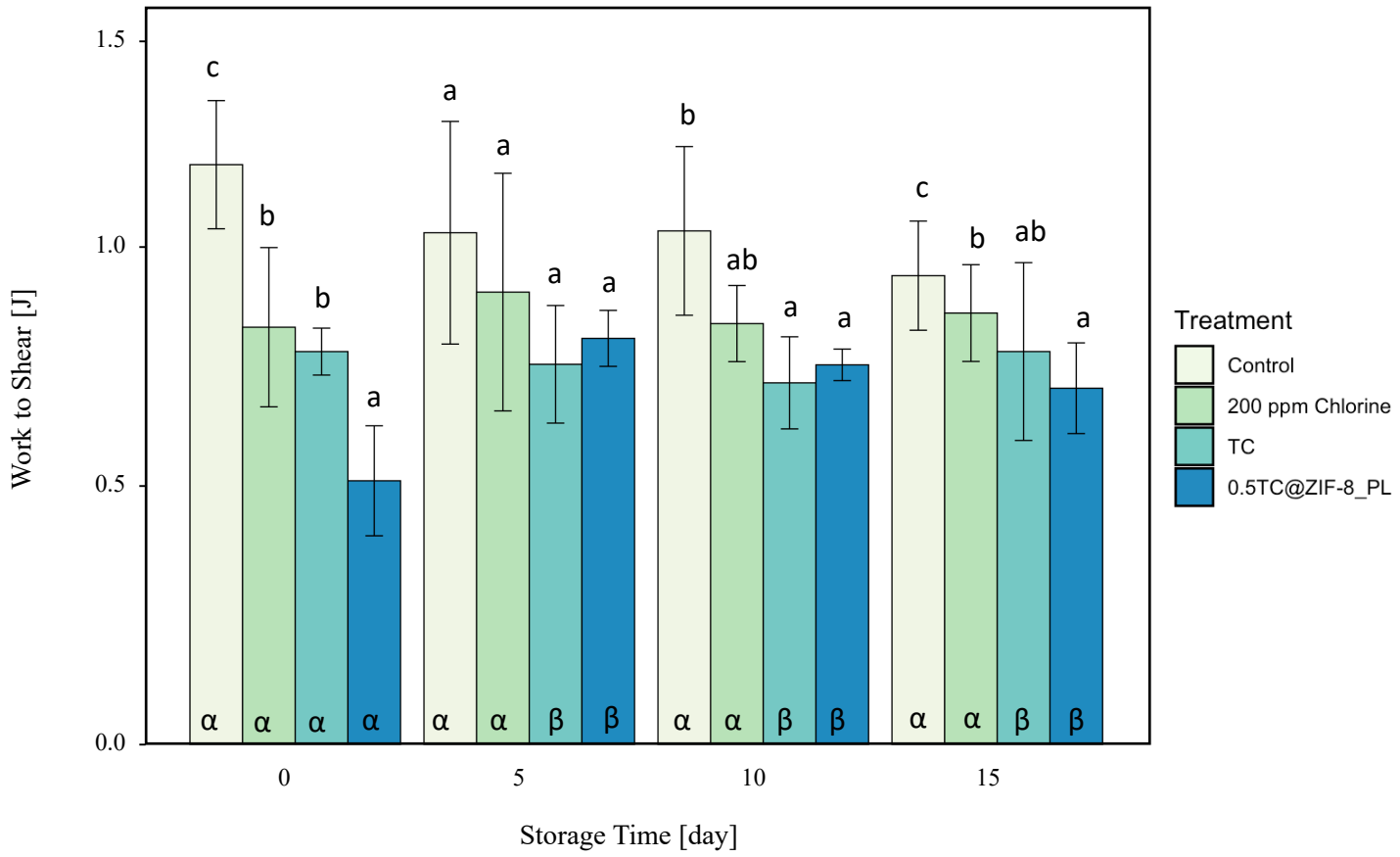

Figure 4.12 Work (J) to shear required to cut through fresh spinach (control and samples) over 15 days of storage at 4°C.
The English letters (a, b, c) beyond the error bar means at the same storage day of different treatment, which is not followed by a common letter are significantly different ($p < 0.05$). The Greek letters (α, β) at the bottom of the column means under the same treatment during different storage points, which are not preceded by a common letter, are significantly different ($p < 0.05$).

4.3.7. Vitamin C

The vitamin C content of the spinach leaves decreased ($p<0.05$) over time for all groups, especially by day 10 (Table 4.9, Figure 4.13) Compared with the control group, all treatment groups had lower ($p<0.05$) vitamin C values at each storage point, probably due to the damage of leaves during rinsing and packaging. According to the United States Department of Agriculture (USDA), a 100-gram serving of spinach contains 28.1 milligrams of vitamin C, 34 percent of the daily recommendation. Only the untreated spinach on the 0th and 5th day can meet this standard, and the others are far below.

Therefore, treatment with 0.5TC@ZIF-8_PL solution has a detrimental effect on the micronutrient quality of spinach leaves and further studies are needed.

Table 4.9 Vitamin C content of fresh spinach (control and samples) over 15 days of storage at 4°C.

	Vitamin C (mg/g)			
Treatment*/Day	**0**	**5**	**10**	**15**
Control	$_{x}0.31^{b}$ (0.06)	$_{x}0.29^{b}$ (0.04)	$_{w}0.15^{a}$ （0.03）	$_{w}0.15^{a}$ （0.02）
200 ppm Chlorine	$_{x}0.19^{b}$ (0.04)	$_{wx}0.16^{b}$ (0.03)	$_{w}0.08^{a}$ (0.01)	$_{x}0.07^{a}$ （0.03）
***trans*-Cinnamaldehyde**	$_{w}0.14^{b}$ (0.08)	$_{wx}0.14^{b}$ （0.04）	$_{x}0.11^{ab}$ (0.03)	$_{x}0.06^{a}$ (0.02)
0.5TC@ZIF-8	$_{w}0.17^{b}$ (0.02)	$_{x}0.17^{b}$ (0.03)	$_{w}0.08^{a}$ (0.01)	$_{x}0.07^{a}$ (0.01)

* Treatments consisted of rinsing with sterilized water, 200 ppm chlorine, 1000 μg/mL free trans-cinnamaldehyde and 3.68 mg/mL 0.5TC@ZIF-8_PL nanoparticle complexes solution for 1 min in Section 3.3.7.

[a, b] Means within a column, which are not followed by a common superscript letter are significantly different ($p < 0.05$).

[w, x] Means within a row, which are not preceded by a common subscript letter, are significantly different ($p < 0.05$).

The oxidation of vitamin C in green vegetables is determined by many factors, such as different tissue structures, mechanical damage during harvest, intrinsic enzymes (ascorbate oxidase), and sulfhydryl content. Ascorbic acid loss may also be enhanced by the activity of ascorbate oxidase, which is strongly dependent on the pH of the vegetable (Giannakourou & Taoukis, 2003). In this study, the pH increased significantly ($p<0.05$) over time in all experimental groups except for the control group, which remained constant. Spinach leaves tend to rapidly lose their high initial vitamin C because of the relatively high surface area and increased iron content (Giannakourou & Taoukis, 2003). Metal ions catalyze the conversion process of ascorbic acid to dehydroascorbic acid, leading to the loss of the vitamin, thus iron plays a decisive role in oxidative degradation. These changes were confirmed in the present study, where the initial vitamin C content of the treated group was much less than the control group, even less than half.

According to acceptable sensory levels, Dermesonluoglu et al. (2015) established that a 70% loss of vitamin C is considered acceptable for frozen spinach samples, while Giannakourou & Taoukis used 50% vitamin C loss values to calculate the shelf life of vegetables. According to the results (Table 4.9), the Vitamin C content of the free TC-treated group decreased significantly on day 15 ($p<0.05$), while all other groups showed a significant decrease on day 10 with a vitamin C content of approximately 50% of the vitamin C loss. This finding suggests that the antimicrobial treatments used in this study did not slow down the loss of vitamin C content.

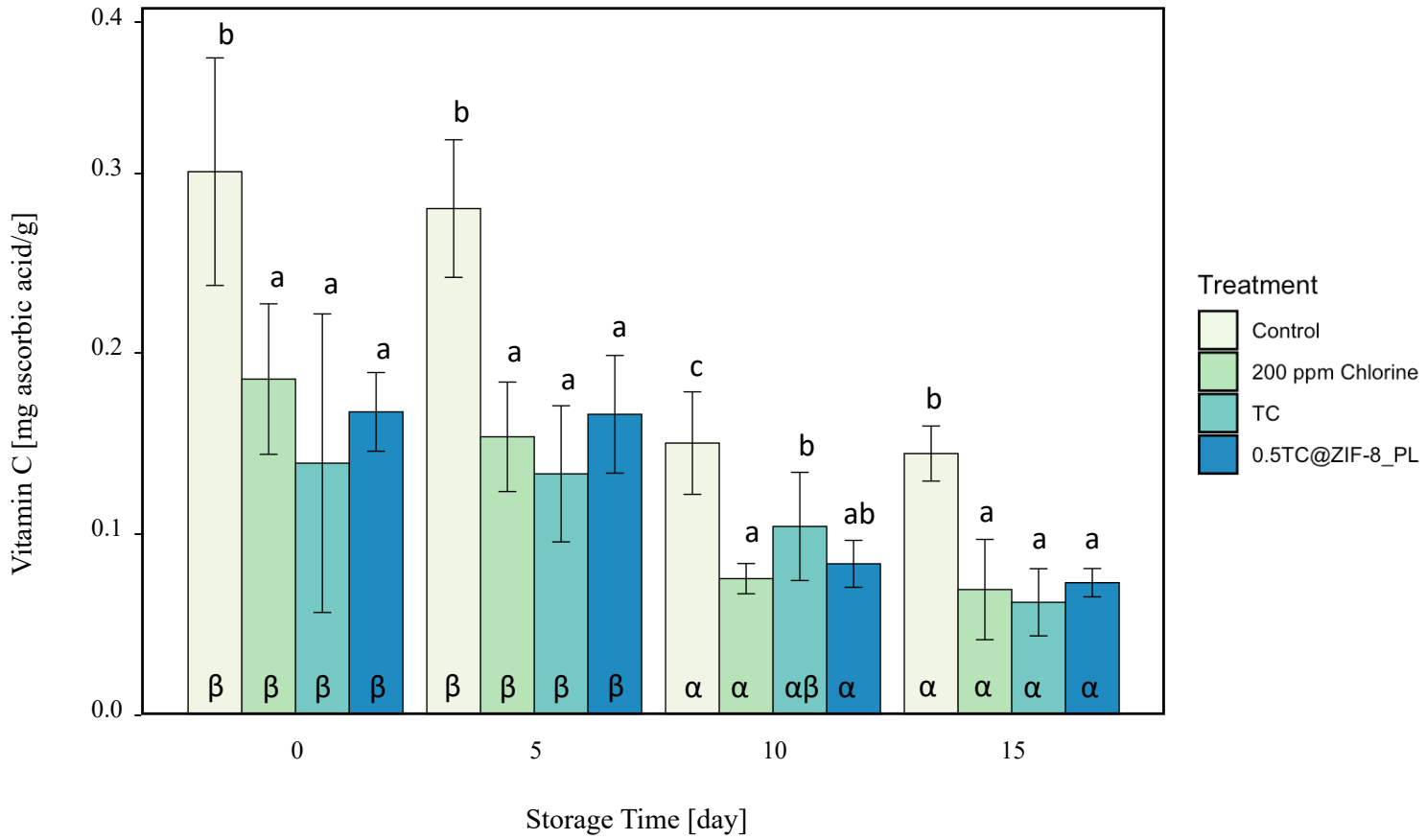

Figure 4.13 Vitamin C content (mg/g) of fresh spinach (control and samples) over 15 days of storage at 4°C.

The English letters (a, b, c) beyond the error bar means at the same storage day of different treatment, which is not followed by a common letter are significantly different ($p < 0.05$). The Greek letters (α, β) at the bottom of the column means under the same treatment during different storage points, which are not preceded by a common letter, are significantly different ($p < 0.05$)

Figure 4.14 shows that all samples followed a first-order kinetics model in terms of vitamin C degradation. There was no difference ($p>0.05$) in the rate of decay (K1) between the control and TC treated groups, but the decay rate was faster ($p<0.05$) in the chlorine and 0.5TC@ZIF-8_PL treated groups (Table 4.10). The application of antimicrobial treatments could adversely affect the vitamin content of spinach during shelf life and this result should be further investigated.

Table 4.10 First-order kinetics of Vitamin C content degradation of fresh spinach (control and samples) over 15 days of storage at 4°C

	Vitamin C (mg/g)	
	First-order rate constant	
Treatments*	**K_1 [1/day]**	**R^2**
Control	0.056 ± 0.014^{a}	0.8600
200 ppm Chlorine	0.074 ± 0.008^{c}	0.9065
***trans*-Cinnamaldehyde**	0.053 ± 0.020^{a}	0.8633
0.5TC@ZIF-8_PL	0.064 ± 0.018^{b}	0.8630

* Treatments consisted of rinsing with sterilized water, 200 ppm chlorine, 1000 μg/mL free trans-cinnamaldehyde and 3.68 mg/mL 0.5TC@ZIF-8_PL nanoparticle complexes solution for 1 min in Section 3.3.7.

[a, b, c] Means within a column, which are not followed by a common superscript letter are significantly different ($p < 0.05$).

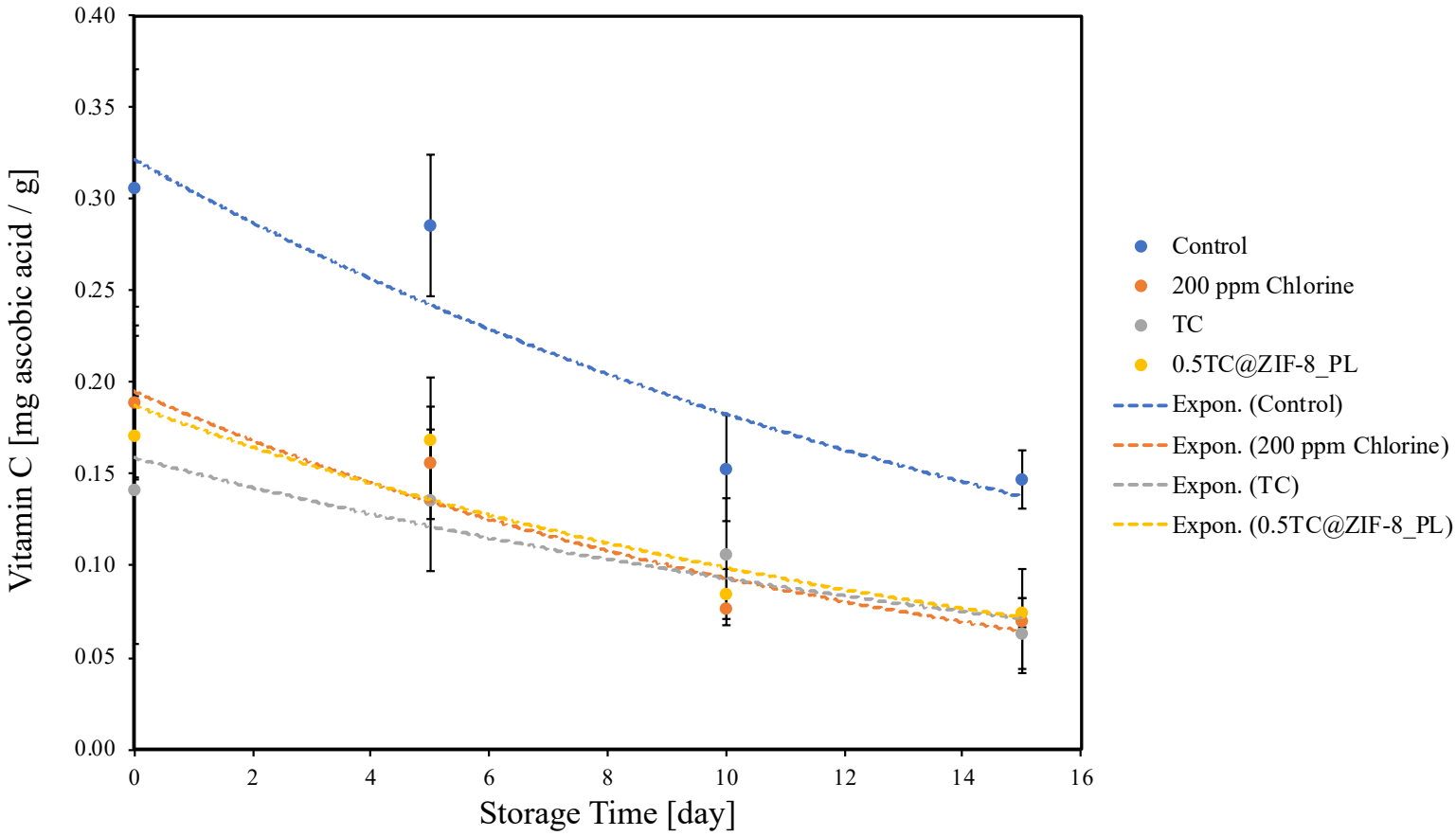

Figure 4.14 Kinetics of Vitamin C degradation in fresh spinach (control and samples) over 15 days of storage at 4°C.

4.3.8. Chlorophyll and Total Carotenoids Contents

Visually, after freeze drying, all treatment groups had lighter green color than the control group and all samples became darker during storage (Figure 4.15). Chemically, the color change is due to the conversion of chlorophyll a and b to pheophytin a and b (Canjura et al.,1991). The degradation of chlorophyll has been studied because its bright green color is generally more satisfying to consumers than the olive-brown of pheophytin (Schwartz & Lorenzo, 1991).

The total chlorophyll content among all the treatment groups was not less than for the control group, and the initial content was even higher than the control group ($p<0.05$). It is well known that the chlorophyll level changes due to the different maturity of harvested leaves exposed to sunlight (Aparicio et al., 1989). In addition, these changes may be attributed to the ability of specific green tissues to biosynthesize chlorophyll, which may be a form of chlorophyll recovery (Barth et al., 1993). With the increase in storage time, the total chlorophyll content decreased for all groups. Among them, the values for treated with chlorine and free TC decreased ($p<0.05$) on the fifth and tenth days, respectively, while the value for 0.5TC@ZIF-8_PL treated group did not show differences ($p>0.05$) during the storage period (Figure 4.16). This result was also confirmed by Hill (2014) and Gomes (2011). Overall, the change in total chlorophyll was minimal around 9 mg/g dry basis spinach. López-Ayerra et al. (1998) observed similar results as they measured the levels of pheophytin a and b in spinach and found only a slight increase during storage, which means chlorophyll loss was not high. As Schwartz et al. (1981) reported, there was a slight change after of chlorophyll in spinach during 24 days of storage.

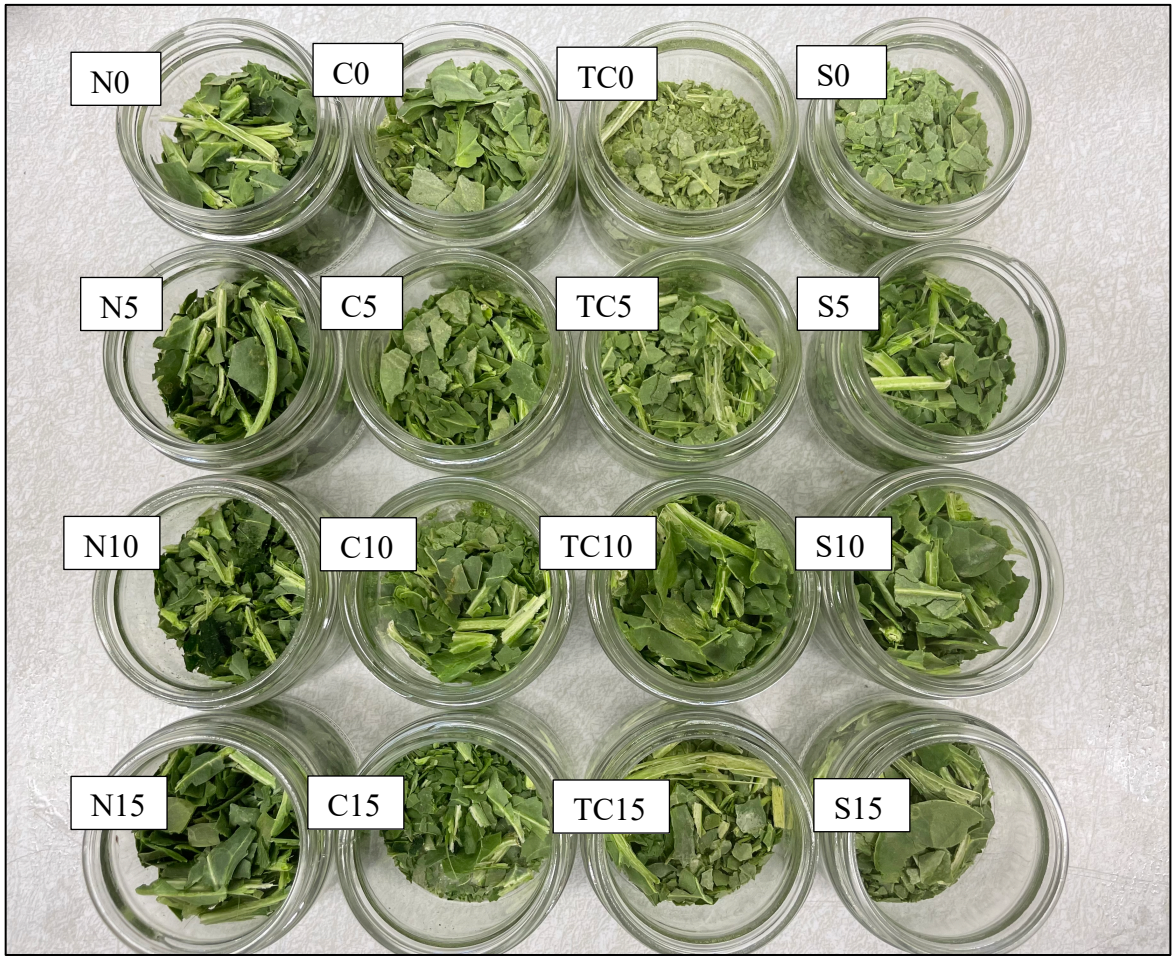

Figure 4.15 Visual observation of color in freeze-dried spinach controls (N) and spinach samples treated with chlorine (C), *trans*-Cinnamaldehyde (TC), and 0.5TC@ZIF-8_PL (S) over 15 days of storage at 4°C.

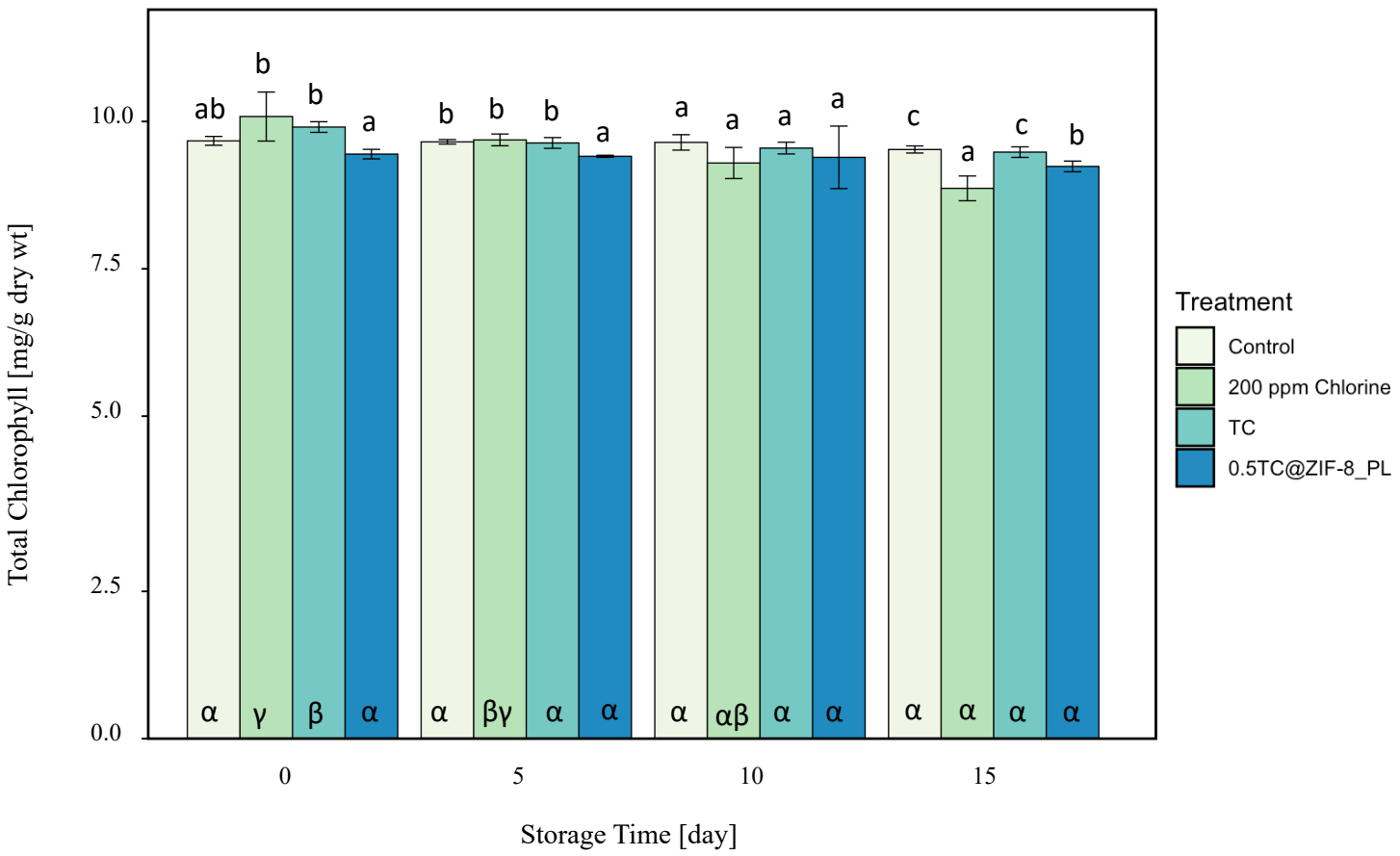

Figure 4.16 Total chlorophyll of fresh spinach (control and samples) over 15 days of storage at 4°C.

The English letters (a, b, c) beyond the error bar means at the same storage day of different treatment, which is not followed by a common letter are significantly different ($p < 0.05$). The Greek letters (α, β, γ) at the bottom of the column means under the same treatment during different storage points, which are not preceded by a common letter, are significantly different ($p < 0.05$).

Chlorophyll is easily degraded during processing and storage and depends on temperature, pH, time, enzymes, oxygen, and light (López-Ayerra et al., 1998). Therefore, a challenge for food processors is to prevent or minimize this degradation when trying to produce higher quality vegetable products (Schwarz & Lorenzo, 1991). The shelf life of green vegetables depends partly on the level of chlorophyll loss (López-Ayerra et al., 1998). Bart et al. (1993) assumed that the product is acceptable before 20% of the chlorophyll is converted to pheophytin. In this study, the percentage of chlorophyll loss for all the sample groups during cold storage was less than 4%, which is very small and does not affect the acceptable level.

The application of antimicrobial treatments could adversely affect the total chlorophyll content of spinach during shelf life and this result should be further investigated.

King et al. (2001) analyzed the chlorophyll content of fresh spinach as chlorophyll a (mg/g dry matter) content of 6.75±0.53, and chlorophyll b (mg /g dry matter) content is 2.56±0.18, which is quite similar to the values found in this study (Table 4.11). For 15 days of storage at 4ºC, the contents of chlorophyll a all increased ($p<0.05$) while contents of chlorophyll b decreased ($p<0.05$) for all groups.

As for total carotenoid contents, only the spinach samples treated with free TC and chlorine showed a continuing decrease during storage, the contents of the control group and 0.5TC@ZIF-8_PL treated group changed over time, even the content on the last day was higher than its initial value ($p<0.05$). This is due to the initial difference between each leaf and during the freezing process and the conclusion that using 0.5TC@ZIF-8_PL nanoparticle solution would not affect the total carotenoid contents (Figure 4.17). The color

of spinach is mainly related to the content of chlorophyll because this compound is the primary pigment of green vegetables and masks the bright color of carotenoids (King et al., 2001).

Table 4.11 Chlorophyll *a* and *b* of fresh spinach (control and samples) over 15 days of storage at 4°C.

	Chlorophyll a (mg/g dry wt)			
Treatment*/Day	**0**	**5**	**10**	**15**
Control	$_{w}6.87^{b}$ (0.03)	$_{w}6.90^{a}$ (0.04)	$_{x}7.01^{a}$ (0.11)	$_{x}7.06^{a}$ (0.06)
200 ppm Chlorine	$_{w}6.18^{a}$ (0.05)	$_{x}6.84^{a}$ (0.17)	$_{xy}7.08^{ab}$ (0.14)	$_{y}7.21^{b}$ (0.16)
***trans*-Cinnamaldehyde**	$_{w}6.94^{b}$ (0.05)	$_{w}6.94^{ab}$ (0.05)	$_{w}6.98^{a}$ (0.06)	$_{wx}7.27^{b}$ (0.05)
0.5TC@ZIF-8_PL	$_{w}6.94^{b}$ (0.05)	$_{w}7.00^{b}$ (0.02)	$_{wx}7.13^{b}$ (0.02)	$_{x}7.20^{b}$ (0.08)
	Chlorophyll b (mg/g dry wt)			
Control	$_{x}2.80^{b}$ (0.06)	$_{wx}2.76^{c}$ (0.05)	$_{wx}2.63^{c}$ (0.05)	$_{w}2.47^{b}$ (0.02)
200 ppm Chlorine	$_{y}2.86^{ab}$ (0.24)	$_{xy}2.61^{b}$ (0.05)	$_{wx}2.48^{b}$ (0.08)	$_{w}2.32^{a}$ (0.18)
***trans*-Cinnamaldehyde**	$_{y}2.73^{b}$ (0.08)	$_{x}2.68^{b}$ (0.06)	$_{x}2.61^{c}$ (0.05)	$_{w}2.55^{c}$ (0.04)
0.5TC@ZIF-8_PL	$_{w}2.52^{a}$ (0.03)	$_{wx}2.43^{a}$ (0.09)	$_{wx}2.39^{a}$ (0.04)	$_{w}2.27^{a}$ (0.19)

* Treatments consisted of rinsing with sterilized water, 200 ppm chlorine, 1000 μg/mL free trans-cinnamaldehyde and 3.68 mg/mL 0.5TC@ZIF-8_PL nanoparticle complexes solution for 1 min in Section 3.3.8.

$^{a, b, c}$ Means within a column, which are not followed by a common superscript letter are significantly different ($p < 0.05$).

$_{w, x, y}$ Means within a row, which are not preceded by a common subscript letter, are significantly different ($p < 0.05$).

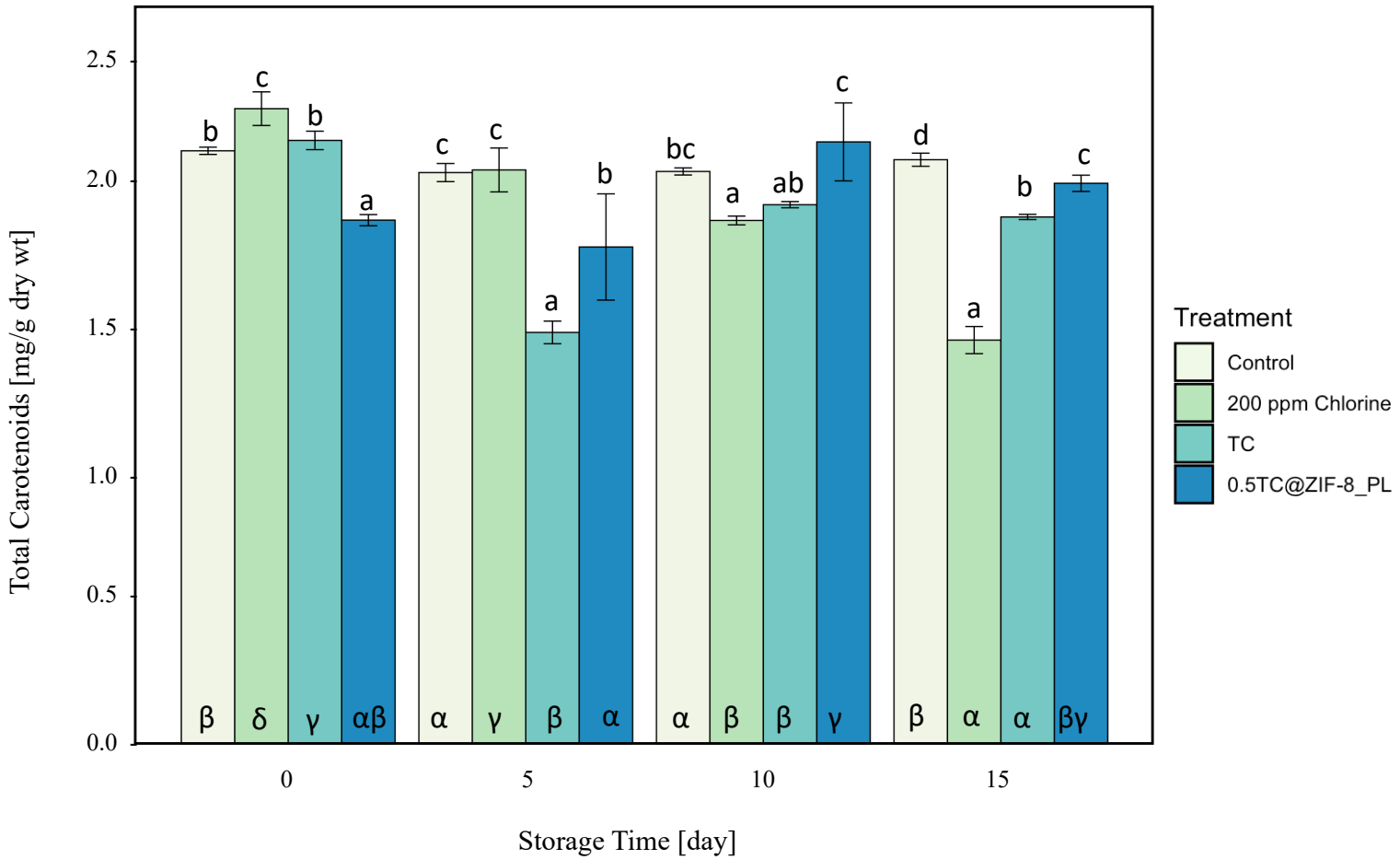

Figure 4.17 Total carotenoids of fresh spinach (control and samples) over 15 days of storage at 4°C.

The English letters (a, b, c, d) beyond the error bar means at the same storage day of different treatment, which is not followed by a common letter are significantly different ($p < 0.05$). The Greek letters (α, β, γ, δ) at the bottom of the column means under the same treatment during different storage points, which are not preceded by a common letter, are significantly different ($p < 0.05$).

4.3.9. Scanning Electron Microscopy

The SEM images of the spinach surface after treatments are shown in Figure 4.18. The micrographs clearly show that the surface of the treated spinach leaves was visually different from the surface of the untreated leaves.

There are many hexagonal compounds on the surface of the leaves treated with 200 ppm chlorine (Figure 4.18 B) compared to the control ((Figure 4.18 A), which can be inferred as a salt compound of sodium ions. As the main component of Clorox, sodium hypochlorite solution is chemically unstable and easily decomposes into hypochlorite, sodium ions, and hydroxide ions in the presence of water (Severing et al., 2019). The presence of residual crystals was also found by Zhang et al. (2016), after washing spinach leaves with 200 mg L-1 of Clorox® bleach solution, electron microscopy images showed some large regular crystal structures on the surface of spinach leaves.

As shown in Figure 4.18 C, compared to the surface of the raw spinach leaves (control), the spinach treated with free TC had a filament-like substance covering the surface. Although it could not be confirmed what kind of substance it was, it also showed that TC had some effect on the surface of spinach.

Spinach leaves treated with 0.5TC@ZIF-8_PL had nanoparticles visible to the naked eye on the surface (Figure 4.18 D). Their structure is not clear, as during the preparation of 0.5TC@ZIF-8_PL nanoparticle solution, steps such as poly lysine coating and sonication could cause damage to the structure. The presence of nanoparticles was detected on the leaf surface, indicating that the nanoparticles were attached to the spinach leaves as they acted as antimicrobials. The ideal antimicrobial treatment would be to leave

the spinach leaves as intact as possible after treatment. Thus, it is necessary to perform a subsequent treatment step or find a method that allows for more effective delivery of TC encapsulated ZIF-8 nanoparticles.

4.4. Cytotoxicity of ZIF-8 and TC entrapped ZIF-8 nanoparticles

Figure 4.19, 4.21, and 4.22 show that after 24 hours of exposure treatment, all ZIF-8 nanoparticles and *trans*-cinnamaldehyde exhibited significant ($p<0.05$) cytotoxicity to HepG2 cells. The cell survival rate of both the base solution (0.5% DMSO) and the negative control (pure DMEM medium) was around 100%, which means that all cells were alive. However, the cell survival rates for ZIF-8 and 0.5TC@ZIF-8 were below 1%, which means almost no cells survived, the same as pure *trans*-cinnamaldehyde.

There was no concentration-response for ZIF-8 and related particles ($p>0.05$). However, there was an excellent dose-response ($p<0.05$) with the positive control (TAB), which means that the cells had normal viability, showing a good dose effect. Then, due to the high toxicity of the ZIF-8 aqueous solution, it can kill almost all cells at the lowest applied concentration.

The poly-lysine coating at 0.1 mg/mL was also harmless to cells, and there was no significant difference ($p>0.05$) between ZIF-8 with and without PL coating and 0.5 TC@ZIF-8. This result demonstrates in two ways that PL coating has no significant effect ($p>0.05$) on the cytotoxicity of ZIF-8 aqueous solution.

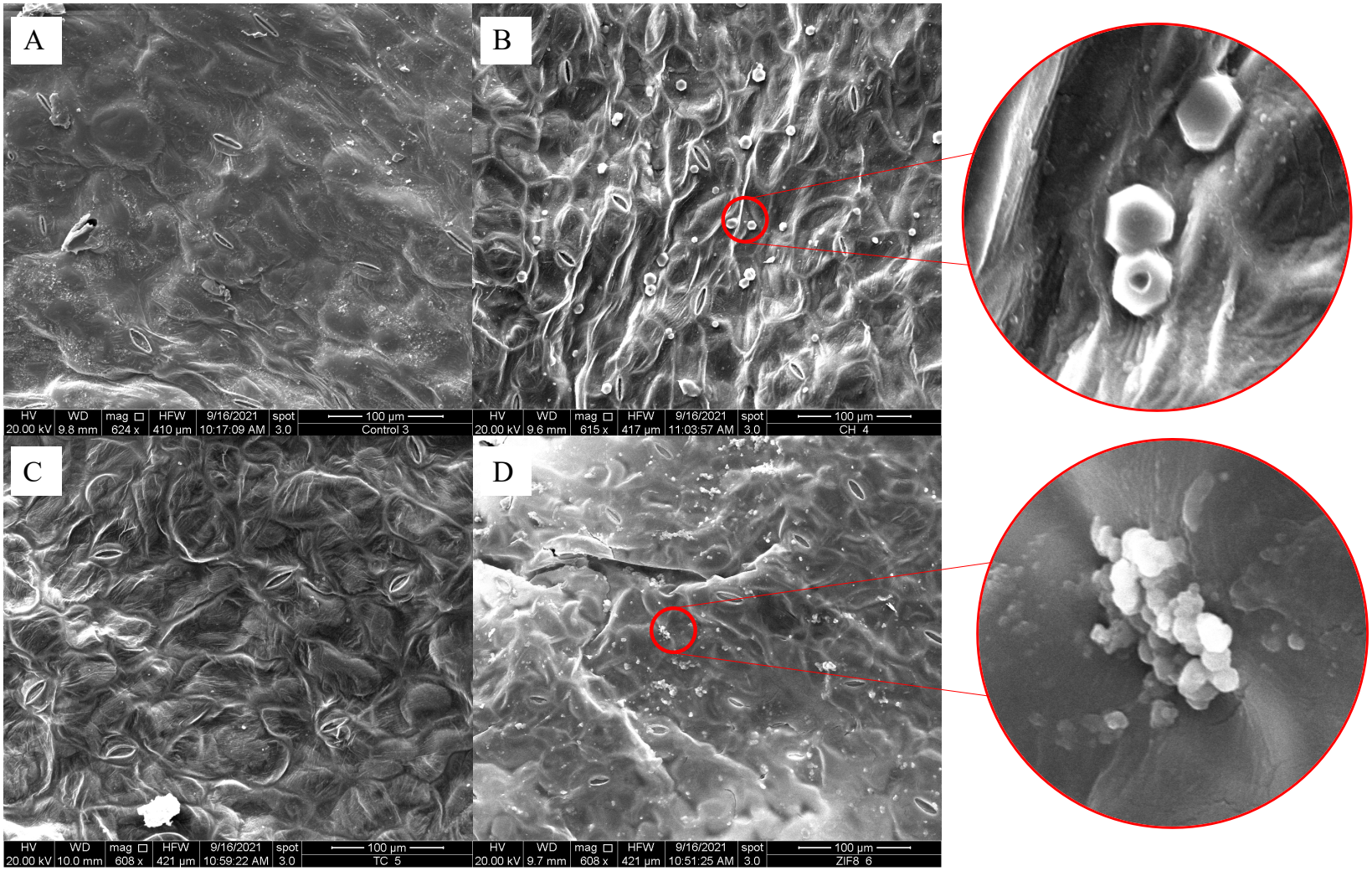

Figure 4.18 SEM images of spinach leaf surface of spinach control (A) and spinach treated with 200 ppm chlorine (B), *trans*-Cinnamaldehyde (C) and 0.5TC@ZIF-8_PL (D).

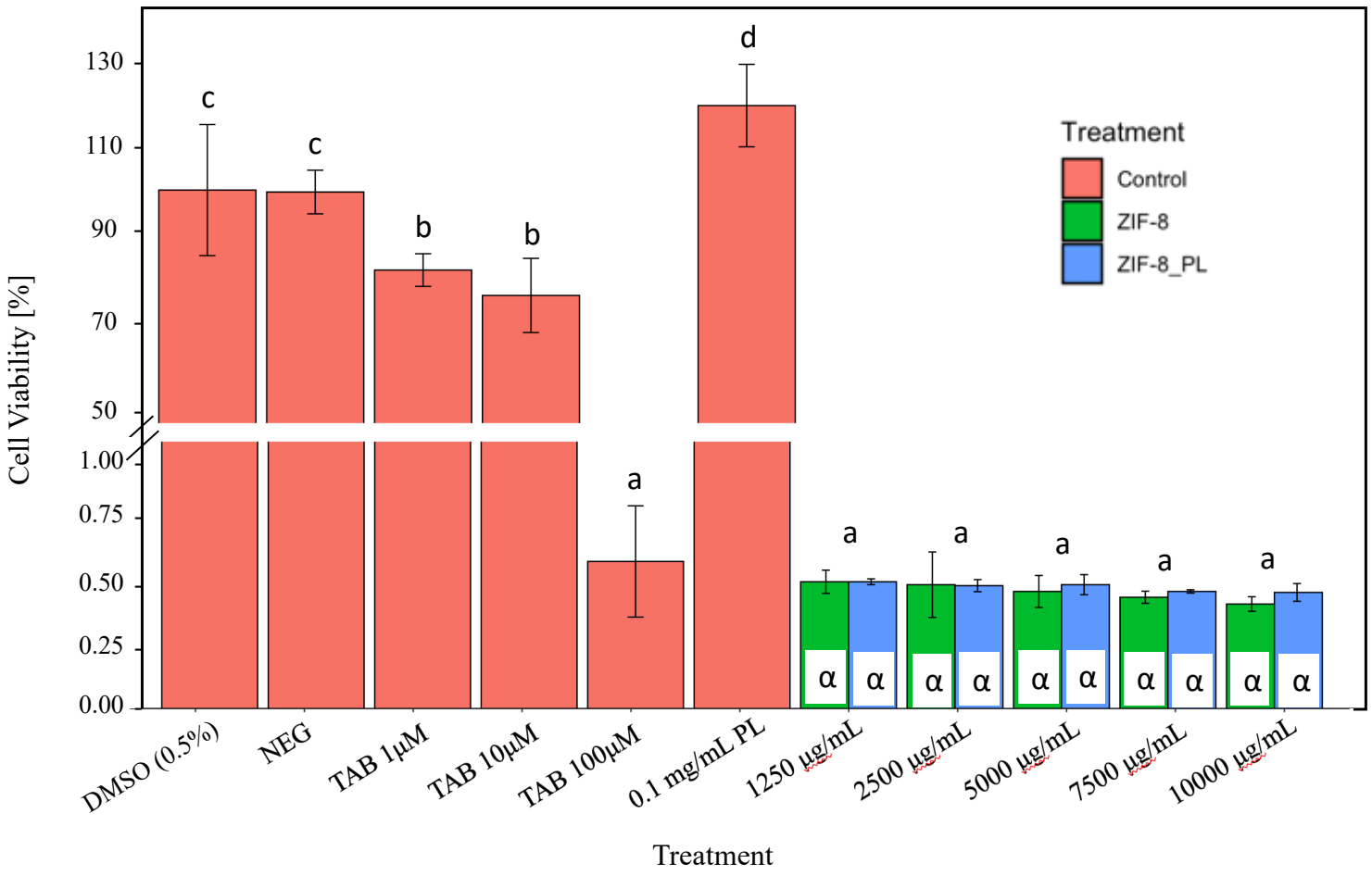

Figure 4.19 Cell Viability (%) of HepG2 cells after 24 h of ZIF-8 and ZIF-8_PL treatments.
The English letters (a, b, c) beyond the error bar means at the same plates of different treatment, which is not followed by a common letter are significantly different ($p < 0.05$). The notation on the error bar indicates the significant difference of ZIF-8 with or without PL coating under student's t-test: · $p>0.05$

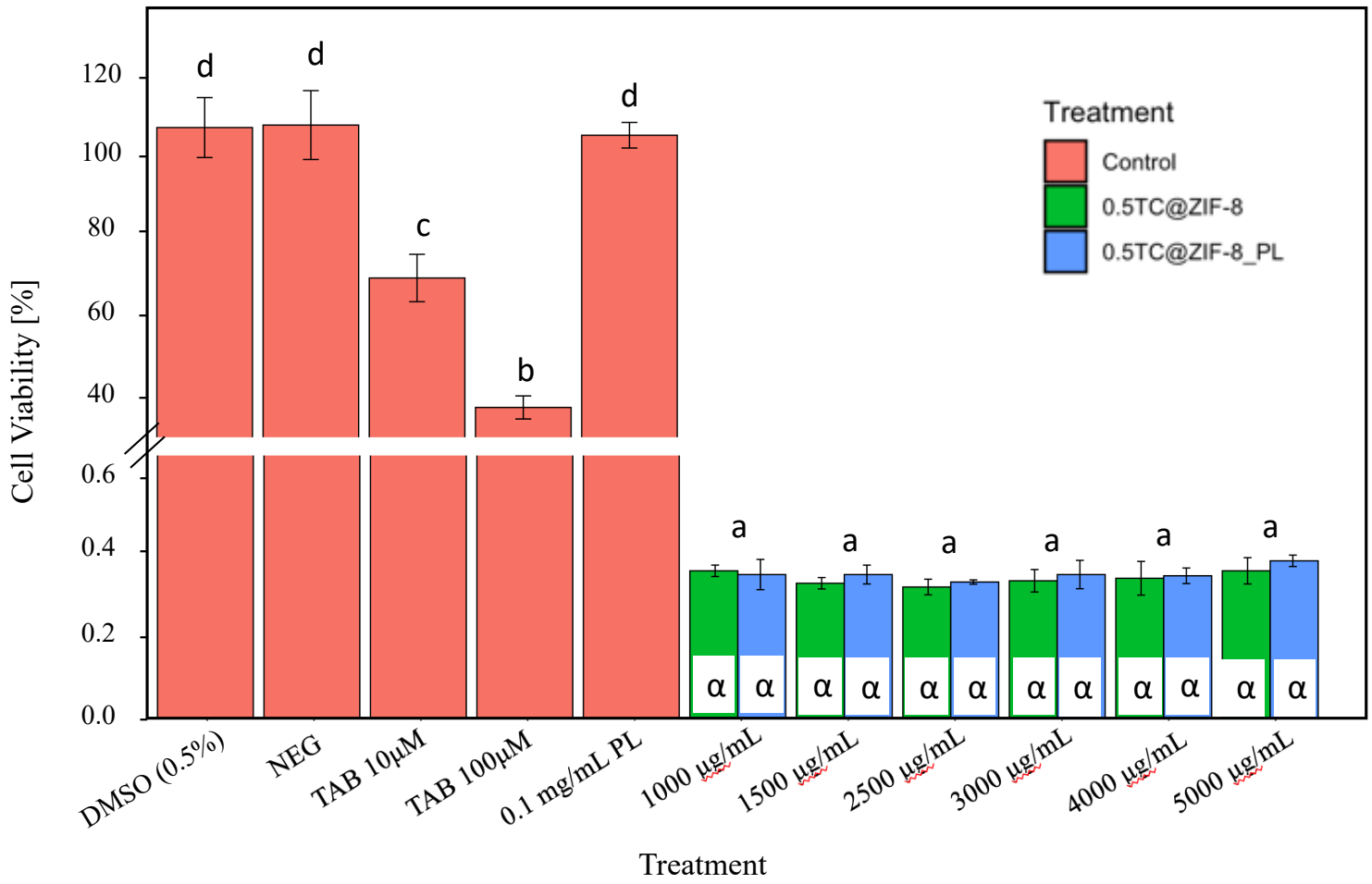

Figure 4.20 Cell Viability (%) of HepG2 cells after 24 h of 0.5TC@ZIF-8 and 0.5TC@ZIF-8_PL treatments.
The English letters (a, b, c, d) beyond the error bar means at the same plates of different treatment, which is not followed by a common letter are significantly different ($p < 0.05$). The notation on the error bar indicates the significant difference of ZIF-8 with or without PL coating under student's t-test: · $p>0.05$

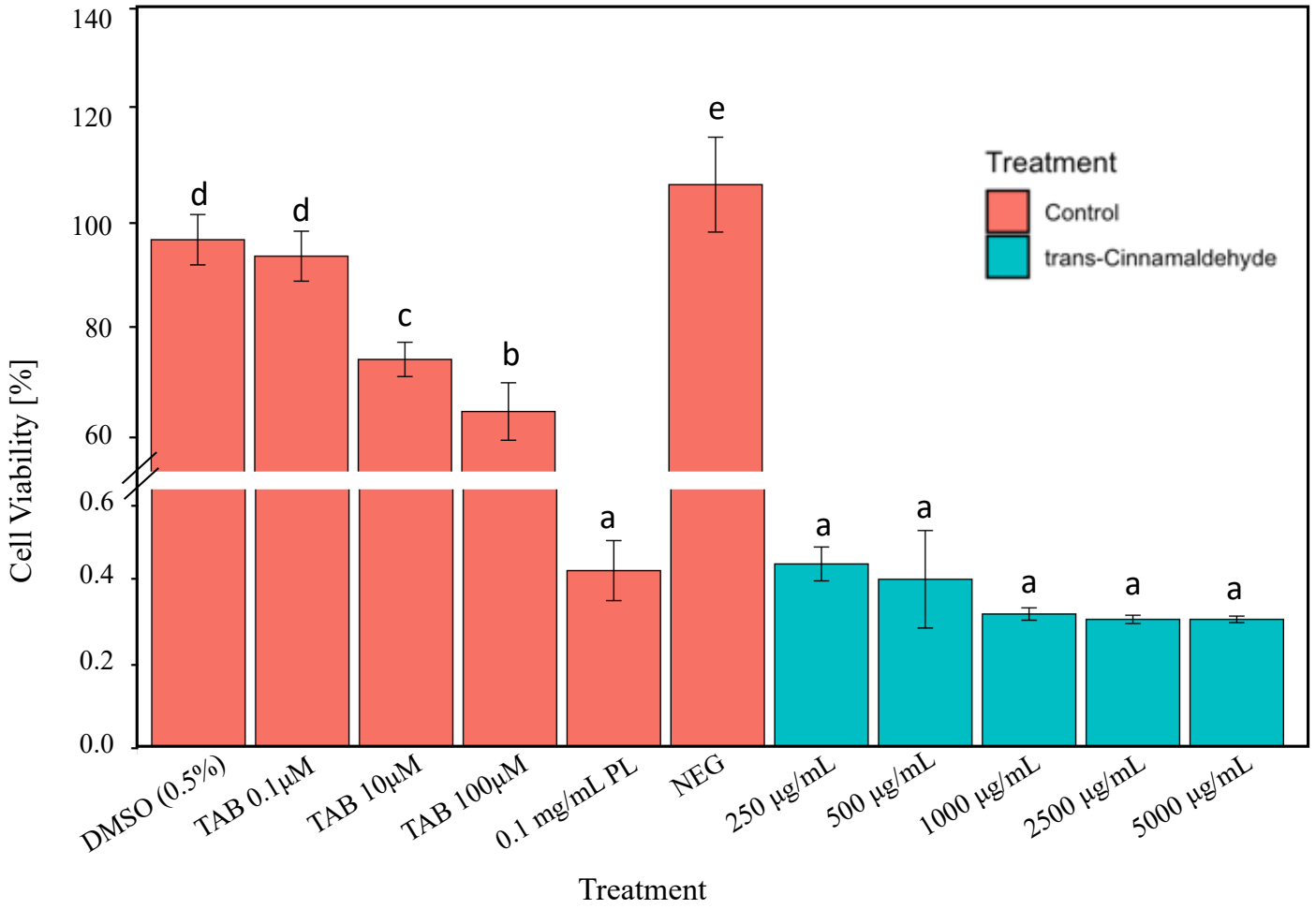

Figure 4.21 Cell Viability (%) of HepG2 cells after 24 h of *trans*-Cinnamaldehyde treatments.
The English letters (a, b, c, d, e) beyond the error bar means at the same plates of different treatment, which is not followed by a common letter are significantly different ($p < 0.05$)

Based on the cytotoxicity results, the ZIF-8 particles are harmful to a human being. Researchers have reported many tolerance limits to regard ZIF-8 and related components. Ruyra and his group reported the toxicity of ZIF-8 components in HepG2 cells in 2015, with the limitation of 200 μM both for ion metal Zn^{2+} and organic ligands 2-mim after 24 h exposure, and the toxicity limit 50 μM and 100 μM of ZIF-8 for the 24 h and 72 h exposure, respectively. These concentrations are much higher than the concentration in our experiment, but they can still maintain good cell viability. However, researchers also reported a meager cytotoxicity limit of ZIF-8 with only 30 μg/mL (Hoop et al., 2018). In their research, multiple cell lines in humans and mice from different tissues were tested for 72 h and 120 h exposure, and the cell survival rate changes with time and cell types.

In this study, the applied concentration should not be reduced to the toxicity limit level due to the minimum inhibitory concentration of microorganisms. If the level of added antimicrobial substances is insufficient (Gombas et al., 2017), washing water during processing can lead to the spread of biohazards (Davidson et al., 2013). If ZIF-8 nanoparticles are to be applied for antimicrobial treatment of food, some post-application measures for toxicity reduction are required or by adjusting the ZIF-8 composition ratio to achieve toxicity reduction.

5. CONCLUSIONS

This study explored the feasibility of using poly-lysine coated ZIF-8 nanoparticles as nanocarriers of the essential oil *trans*-cinnamaldehyde (TC), which is poorly soluble in aqueous media, for food safety applications. The following conclusions were drawn based on the specific objectives of the study:

1) The maximum encapsulation efficiency (EE%) of *trans*-Cinnamaldehyde in ZIF-8 is 32%, with a peak when the mass ratio of TC to ZIF-8 equals 0.5.
2) The poly-lysine coating limited the release of TC, with a consequent lower antimicrobial effect ($p<0.05$). Specifically, the inhibition of *E. coli* O157:H7 was reduced from 5 log CFU/mL to 2.5 log CFU/mL when using PL-coated 0.5 TC@ZIF-8 nanoparticle solution applied at a concentration of 3.68 mg/mL.
3) Encapsulation of TC in ZIF-8 enhanced ($p<0.05$) the antibacterial effect of TC and increased the stability of TC in aqueous solution.
4) 3.68 mg/mL 0.5TC@ZIF-8_PL solution inhibited the growth of *E.coli* O157:H7 by more than 2 log CFU/mL on spinach in a short time (1min). In comparison, it takes more than 20 minutes for 200 ppm chlorine to achieve the same log reduction.
5) After spraying and rinsing spinach leaves with 3.68 mg/mL 0.5TC@ZIF-8_PL, the total aerobic plate counts (APC) on the surface of spinach was reduced by 1 and 2 log CFU/g, respectively, when stored for 5 days at room temperature (~21ºC).

6) The surface of the antimicrobial-treated spinach leaves had the residual antimicrobial components under scanning electron microscopy (SEM) observation.
7) Application of 0.5TC@ZIF-8_PL alleviated moisture loss, total chlorophyll loss, and pH increase ($p<0.05$) due to the growth of gram-negative microbes when spinach was stored for 15 days at 4ºC. However, treatments did not prevent the reduction of vitamin C content and color degradation ($p>0.05$) and adversely affected spinach firmness.
8) All spinach samples followed a first-order kinetic model in terms of vitamin C and total chlorophyll degradation after 15 days of storage at 4ºC. Among them, the groups treated with 200 ppm chlorine and 0.5TC@ZIF-8_PL increased ($p<0.05$) the decay rate of vitamin C degradation. The groups treated with 200 ppm chlorine and free TC increased ($p<0.05$) the decay rate of total chlorophyll degradation.
9) ZIF-8, 0.5TC@ZIF-8 and free TC exhibited large ($p<0.05$) cytotoxicity against HepG2 cells after 24 h exposure, but PL did not show cytotoxicity ($p>0.05$).

6. FURTHER IMPACT

Even though the MOFs have been widely used in the safety and preservation of food, the application of ZIF-8 encapsulated TC in fresh vegetables is still lacking. Through the research of this experiment, we can not only confirm the antibacterial activity of ZIF-8 encapsulated TC on pathogens in spinach and maintain the quality of the product itself but also provide new ideas for food packaging and food preservation.

Monitoring food safety through nanotechnology has been widely used in many fields. Some materials such as graphene oxide (GO), carbon nanotubes (CNT), and molecularly imprinted polymers (MIP) have been used as adsorbents to extract unwanted compounds from food (González-Sálamo et al., 2016). These materials are also used as components in equipment specifically used to detect chemical and biological pollutants, remove compounds with high toxic content in the food supply chain, and minimize the distribution of contaminated products to consumers (Wang & Duncan, 2017).

Nanoparticles also have essential applications in the food preservation process. If food is improperly preserved, it is highly susceptible to contamination, especially for fresh vegetables such as spinach used in this study, so the packaging needs good thermal and mechanical properties. In many cases, introducing nanomaterials of titanium oxide, silver, or silicon dioxide coatings to make the material has antibacterial properties, thereby improving the shelf life of the product (Venkatasubbu et al., 2016). Due to excellent antibacterial activity and unique antibacterial mechanism, silver nanoparticles (AgNPs) have been widely used in food preservation (Yu et al., 2013). The application of other metal

encapsulation materials has also been proved accordingly. Although natural essential oils are valuable resources for preserving food, their practical use has always been a challenge due to the undesirable use of the aroma produced by essential oils. To avoid this effect, nanomaterials can be used as carriers to mask the odor of essential oil-based preservatives while also providing enhanced biological efficacy, bioavailability, stability, and functionality (Prakash & Kiran, 2016).

7. RECOMMENDATIONS FOR FURTHER STUDY

Moving forward, trans-cinnamaldehyde loaded ZIF-8 nanoparticle synthesis and application could be further improved by:

1) Synthesis:

i. Adjusting Zn^{2+} /2-mim ratio during synthesis to figure out if higher encapsulation efficiency of TC could be got.

ii. Use ethanol-water solution instead of absolute ethanol as a synthesis solution to reduce cost.

iii. Try to use other emulsions to enhance the stability of ZIF-8 while not worsen its antimicrobial effects.

2) Applications:

i. Try different pH of solution for dispersing ZIF-8 nanoparticles and its antimicrobial effect regard to pH.

ii. Test different microbes such as *Listeria* as a representative as gram-positive microorganisms.

iii. Try different treatment methods, such as spraying when applied antimicrobial solution on the spinach.

iv. Explore the kinetics of microorganisms growing on the surface of spinach and the kinetics of quality during storage.

v. Change the storage temperature (such as room temperature) and packaging (such as different bags) for measurement.

REFERENCES

Abduraimova, A., Molkenova, A., Duisembekova, A., Mulikova, T., Kanayeva, D., & Atabaev, T. S. (2021). Cetyltrimethylammonium bromide (CTAB)-loaded SiO2–Ag mesoporous nanocomposite as an efficient antibacterial agent. *Nanomaterials*, *11*(2), 477.

Annous, B.A., Solomon, E.B., Niemira, B.A., 2006. Biofilms on fresh produce and difficulties in decontamination. *Food Quality 13*, 80–84.

Appendini, P., & Hotchkiss, J. H. (2002). Review of antimicrobial food packaging. *Innovative Food Science & Emerging Technologies*, 3(2), 113-126.

Archana, G. N., PRAKASH, J., Asha, M. R., & CHAND, N. (1995). Effects of processing on pigments of certain selected vegetables. *Journal of food quality*, *18*(2), 91-101.

Arnade, C., Calvin, L., & Kuchler, F. (2009). Consumer response to a food safety shock: The 2006 food-borne illness outbreak of E. coli O157: H7 linked to spinach. *Applied Economic Perspectives and Policy*, *31*(4), 734-750.

Artés F, Gómez P, Artés-Hernández F. 2007. Physical, physiological and microbial deterioration of minimally fresh processed fruits and vegetables. *Food Sci Technol Int 13(3)*:177-88.

Ashakirin, S. N., Tripathy, M., Patil, U. K., & Majeed, A. A. (2017). Chemistry and bioactivity of cinnamaldehyde: a natural molecule of medicinal importance. *Int. J. Pharm. Sci. Res*, 8(6), 2333-2340.

Association of Official Analytical Chemists. (2006). Official method 967.21. Ascorbic Acid in Vitamin Preparations and Juices: 2,6-Dichloroindophenol Titrimetric Method. *Official Methods of Analysis*. *AOAC* A. International.

Au-Duong, A. N., & Lee, C. K. (2017). Iodine-loaded metal-organic framework as growth-triggered antimicrobial agent. *Materials Science and Engineering: C*, *76*, 477-482.

Bachelli, M. L. B., Amaral, R. D. Á., & Benedetti, B. C. (2013). Alternative sanitization methods for minimally processed lettuce in comparison to sodium hypochlorite. *Brazilian Journal of Microbiology*, *44*, 673-678.

Bae, T. H., Lee, J. S., Qiu, W., Koros, W. J., Jones, C. W., & Nair, S. (2010). A high-performance gas-separation membrane containing submicrometer-sized metal-organic framework crystals. *Angewandte Chemie*, *122*(51), 10059-10062.

Banach, J. L., Van Bokhorst-van De Veen, H., van Overbeek, L. S., van der Zouwen, P. S., Zwietering, M. H., & Van der Fels-Klerx, H. J. (2020). Effectiveness of a peracetic acid solution on Escherichia coli reduction during fresh-cut lettuce processing at the laboratory and industrial scales. *International journal of food microbiology*, *321*, 108537.

Barth, M. M., Kerbel, E. L., Perry, A. K., & Schmidt, S. J. (1993). Modified atmosphere packaging affects ascorbic acid, enzyme activity and market quality of broccoli. *Journal of Food Science*, *58*(1), 140-143.

Baskaran, S. A., Amalaradjou, M. A. R., Hoagland, T., & Venkitanarayanan, K. (2010). Inactivation of Escherichia coli O157: H7 in apple juice and apple cider by trans-cinnamaldehyde. *International journal of food microbiology*, *141*(1-2), 126-129.

Batish, D. R., Singh, H. P., Kohli, R. K., & Kaur, S. (2008). Eucalyptus essential oil as a natural pesticide. *Forest ecology and management*, *256*(12), 2166-2174.

Baur S, Klaiber R, Wei H, Hammes WP, Carle R. 2005. Effect of temperature and chlorination of pre-washing water on shelf-life and physiological properties of ready-to-use iceberg lettuce. *Innovative Food Sci Emerg Technol 6(2):*171-82.

Berger, C. N., Sodha, S. V., Shaw, R. K., Griffin, P. M., Pink, D., Hand, P., & Frankel, G. (2010). Fresh fruit and vegetables as vehicles for the transmission of human pathogens. *Environmental Microbiology*, *12*(9), 2385-2397.

Beuchat, L.R., 1999. Survival of enterohemorrhagic Escherichia coli O157:H7 in bovine feces applied to lettuce and the effectiveness of chlorinated water as a disinfectant. *Journal of Food Protection 62*, 845–849.

Beuchat, L.R., Adler, B.B., Lang, M.M., 2004. Efficacy of chlorine and a peroxyacetic acid sanitizer in killing Listeria monocytogenes on iceberg and romaine lettuce using simulated commercial processing conditions. *Journal of Food Protection 67*, 1238–1242.

Brandt, A. L., Castillo, A., Harris, K. B., Keeton, J. T., Hardin, M. D., & Taylor, T. M. (2010). Inhibition of *Listeria monocytogenes* by food antimicrobials applied singly and in combination. *Journal of Food Science*, *75*(9), M557-M563.

Burits, M., & Bucar, F. (2000). Antioxidant activity of Nigella sativa essential oil. *Phytotherapy Research*, 14(5), 323-328.

Canjura, F. L., Schwartz, S. J., & Nunes, R. V. (1991). Degradation kinetics of chlorophylls and chlorophyllides. *Journal of Food Science*, *56*(6), 1639-1643.

Cavanagh, H. M. A., & Wilkinson, J. M. (2002). Biological activities of lavender essential oil. *Phytotherapy Research*, 16(4), 301-308.

Centers for Disease Control and Prevention (CDC). 2018(a). *Foodborne illnesses and germs*. Retrieved at September, 2021 from: https://www.cdc.gov/foodsafety/foodborne-germs.html.

Centers for Disease Control and Prevention (CDC). 2018(b). *E. coli (Escherichia coli)*. Retrieved at September, 2021 from: https://www.cdc.gov/ecoli/general/index.html.

Centers for Disease Control and Prevention. (2006). Ongoing multistate outbreak of Escherichia coli serotype O157: H7 infections associated with consumption of fresh

spinach—United States, September 2006. *Morbidity and Mortality Weekly Report*, *55*, 1-2.

Centers for Disease Control and Prevention. (2012). Multistate Outbreak of Shiga Toxin-producing *Escherichia coli* O157:H7 Infections Linked to Organic Spinach and Spring Mix Blend (Final Update). Retrieved August 12, 2021, from: https://www.cdc.gov/ecoli/2012/O157H7-11-12/index.html

Centers for Disease Control and Prevention. Reports of Selected *E. coli* Outbreak Investigations. Retrieved August 12, 2021, from: http://www.cdc.gov/ecoli/outbreaks.html

Chatterjee, A., & Abraham, J. (2018). Microbial contamination, prevention, and early detection in the food industry. In *Microbial Contamination and Food Degradation* (pp. 21-47). Academic Press.

Chen, B., Yang, Z., Zhu, Y., & Xia, Y. (2014). Zeolitic imidazolate framework materials: recent progress in synthesis and applications. *Journal of Materials Chemistry A*, *2*(40), 16811-16831.

Chen, B., Yang, Z., Zhu, Y., & Xia, Y. (2014). Zeolitic imidazolate framework materials: recent progress in synthesis and applications. *Journal of Materials Chemistry A*, *2*(40), 16811-16831.

Chen, Y., Deng, J., Liu, F., Dai, P., An, Y., Wang, Z., & Zhao, Y. (2019). Energy-free, singlet oxygen-based chemodynamic therapy for selective tumor treatment without dark toxicity. *Advanced healthcare materials*, *8*(18), 1900366.

Chowdhuri, A. R., Das, B., Kumar, A., Tripathy, S., Roy, S., & Sahu, S. K. (2017). One-pot synthesis of multifunctional nanoscale metal-organic frameworks as an effective antibacterial agent against multidrug-resistant Staphylococcus aureus. *Nanotechnology*, *28*(9), 095102.

CIELAB color space. (2021, September 22). In *Wikipedia*. Retrieved September 26, 2021, from: https://en.wikipedia.org/wiki/CIELAB_color_space.

Cliffe, M. J., Mottillo, C., Stein, R. S., Bučar, D. K., & Friščić, T. (2012). Accelerated aging: a low energy, solvent-free alternative to solvothermal and mechanochemical synthesis of metal–organic materials. *Chemical Science*, *3*(8), 2495-2500.

Clinical and Laboratory Standards Institute (CLSI). *Performance Standards for Antimicrobial Susceptibility Testing*, 28th ed.; CLSI Supplement M100; Clinical and Laboratory Standards Institute: Wayne, PA, USA, 2018; ISBN1 978-1-68440-066-9. [Print]; ISBN2 978-1-68440-067-6. [Electronic].

Clinical and Laboratory Standards Institute (CLSI). *Performance Standards for Antimicrobial Susceptibility Testing*, 28th ed.; CLSI Supplement M100; Clinical and Laboratory Standards Institute: Wayne, PA, USA, 2018; ISBN1 978-1-68440-066-9. [Print]; ISBN2 978-1-68440-067-6. [Electronic].

Comba, S., & Sethi, R. (2009). Stabilization of highly concentrated suspensions of iron nanoparticles using shear-thinning gels of xanthan gum. *Water Research*, *43*(15), 3717-3726.

Cravillon, J., Münzer, S., Lohmeier, S. J., Feldhoff, A., Huber, K., & Wiebcke, M. (2009). Rapid room-temperature synthesis and characterization of nanocrystals of a prototypical zeolitic imidazolate framework. *Chemistry of Materials*, *21*(8), 1410-1412.

Cravillon, J., Nayuk, R., Springer, S., Feldhoff, A., Huber, K., & Wiebcke, M. (2011). Controlling zeolitic imidazolate framework nano-and microcrystal formation: insight into crystal growth by time-resolved in situ static light scattering. *Chemistry of Materials*, *23*(8), 2130-2141.

Cravillon, J., Schröder, C. A., Bux, H., Rothkirch, A., Caro, J., & Wiebcke, M. (2012). Formate modulated solvothermal synthesis of ZIF-8 investigated using time-resolved in situ X-ray diffraction and scanning electron microscopy. *CrystEngComm*, *14*(2), 492-498.

Davidson, G. R., Buchholz, A. L., & Ryser, E. T. (2013). Efficacy of commercial produce sanitizers against nontoxigenic Escherichia coli O157: H7 during processing of iceberg lettuce in a pilot-scale leafy green processing line. *Journal of food protection*, *76*(11), 1838-1845.

Deans, S. G., & Ritchie, G. (1987). Antibacterial properties of plant essential oils. *International journal of food microbiology*, *5*(2), 165-180.

Deborde, M., & Von Gunten, U. R. S. (2008). Reactions of chlorine with inorganic and organic compounds during water treatment—kinetics and mechanisms: a critical review. *Water research*, *42*(1-2), 13-51.

Del Nobile, M. A., Lucera, A., Costa, C., & Conte, A. (2012). Food applications of natural antimicrobial compounds. *Frontiers in microbiology*, 3, 287.

Dermesonluoglu, E., Katsaros, G., Tsevdou, M., Giannakourou, M., & Taoukis, P. (2015). Kinetic study of quality indices and shelf life modelling of frozen spinach under dynamic conditions of the cold chain. *Journal of Food Engineering*, *148*, 13-23.

Dima, C., Assadpour, E., Dima, S., & Jafari, S. M. (2020). Bioactive-loaded nanocarriers for functional foods: From designing to bioavailability. *Current Opinion in Food Science*, *33*, 21-29.

Dorman, H. D., & Deans, S. G. (2000). Antimicrobial agents from plants: antibacterial activity of plant volatile oils. *Journal of applied microbiology*, *88*(2), 308-316.

Eddaoudi, M., Kim, J., Rosi, N., Vodak, D., Wachter, J., O'Keeffe, M., & Yaghi, O. M. (2002). Systematic design of pore size and functionality in isoreticular MOFs and their application in methane storage. *Science*, *295*(5554), 469-472.

EUCAST Definitive Document. Methods for the determination of susceptibility of bacteria to antimicrobial agents. Terminology. *Clin. Microbiol. Infect.* 1998, *4*, 291–296

Fernández-Bertrán, J. F., Hernández, M. P., Reguera, E., Yee-Madeira, H., Rodriguez, J., Paneque, A., & Llopiz, J. C. (2006). Characterization of mechanochemically synthesized imidazolates of Ag+ 1, Zn+ 2, Cd+ 2, and Hg+ 2: Solid state reactivity of nd10 cations. *Journal of Physics and Chemistry of Solids*, *67*(8), 1612-1617.

Fernando, S. S. N., Gunasekara, T. D. C. P., & Holton, J. (2018). Antimicrobial Nanoparticles: applications and mechanisms of action.

Ferreira, C. D., & Nunes, I. L. (2019). Oil nanoencapsulation: development, application, and incorporation into the food market. *Nanoscale research letters*, *14*(1), 1-13.

Firmino, D. F., Cavalcante, T. T., Gomes, G. A., Firmino, N., Rosa, L. D., de Carvalho, M. G., & Catunda Jr, F. E. (2018). Antibacterial and antibiofilm activities of Cinnamomum sp. essential oil and cinnamaldehyde: antimicrobial activities. *The Scientific World Journal*, *2018*.

Friedman, M. (2017). Chemistry, antimicrobial mechanisms, and antibiotic activities of cinnamaldehyde against pathogenic bacteria in animal feeds and human foods. *Journal of agricultural and food chemistry*, *65*(48), 10406-10423.

Fukuzaki, S. (2006). Mechanisms of actions of sodium hypochlorite in cleaning and disinfection processes. *Biocontrol science*, *11*(4), 147-157.

Furukawa, H., Cordova, K. E., O'Keeffe, M., & Yaghi, O. M. (2013). The chemistry and applications of metal-organic frameworks. *Science*, *341*(6149).

Garay, A. L., Pichon, A., & James, S. L. (2007). Solvent-free synthesis of metal complexes. *Chemical Society Reviews*, *36*(6), 846-855.

García, L., Santos, C., Aparicio, M. P., & Gonzalo, J. C. R. (1989). Influencia de las condiciones de almacenamiento en la calidad de las judías verdes congeladas (var. Chekmate). *Revista de agroquímica y tecnología de alimentos*, *29*(2), 255-265.

Gelting, R. J., Baloch, M. A., Zarate-Bermudez, M. A., & Selman, C. (2011). Irrigation water issues potentially related to the 2006 multistate E. coli O157: H7 outbreak associated with spinach. *Agricultural Water Management*, *98*(9), 1395-1402.

Geornaras, I., Yoon, Y., Belk, K. E., Smith, G. C., & Sofos, J. N. (2007). Antimicrobial activity of ε-polylysine against Escherichia coli O157: H7, Salmonella typhimurium, and Listeria monocytogenes in various food extracts. *Journal of Food Science*, *72*(8), M330-M334.

Ghilini, F., Rodríguez González, M. C., Miñán, A. G., Pissinis, D., Creus, A. H., Salvarezza, R. C., & Schilardi, P. L. (2018). Highly stabilized nanoparticles on poly-L-lysine-coated oxidized metals: a versatile platform with enhanced antimicrobial activity. *ACS applied materials & interfaces*, *10*(28), 23657-23666.

Giannakourou, M. C., & Taoukis, P. S. (2003). Kinetic modelling of vitamin C loss in frozen green vegetables under variable storage conditions. *Food chemistry*, *83*(1), 33-41.

Gill, A. O., & Holley, R. A. (2004). Mechanisms of bactericidal action of cinnamaldehyde against Listeria monocytogenes and of eugenol against L. monocytogenes and Lactobacillus sakei. *Applied and environmental microbiology*, *70*(10), 5750-5755.

Gill, A. O., & Holley, R. A. (2006). Disruption of Escherichia coli, Listeria monocytogenes and Lactobacillus sakei cellular membranes by plant oil aromatics. *International journal of food microbiology*, *108*(1), 1-9.

Gombas, D., Luo, Y., Brennan, J., Shergill, G., Petran, R., Walsh, R., ... & Deng, K. (2017). Guidelines to validate control of cross-contamination during washing of fresh-cut leafy vegetables. *Journal of Food Protection*, *80*(2), 312-330.

Gomes, C. (2011). *Radio sensitization Strategies for Enhanced E-beam Irradiation Treatment of Fresh Produce* (Doctoral dissertation, Texas A & M University).

Gomes, C., Moreira, R. G., Castell-Perez, M. E., Kim, J., Da Silva, P., & Castillo, A. (2008). E-beam irradiation of bagged, ready-to-eat spinach leaves (Spinacea oleracea): An engineering approach. *Journal of Food Science*, *73*(2), E95-E102.

Gomez-Lopez, V. M., Devlieghere, F., Bonduelle, V., & Debevere, J. (2005). Intense light pulses decontamination of minimally processed vegetables and their shelf-life. *International journal of food microbiology*, *103*(1), 79-89.

Gómez-López, V. M., Lannoo, A. S., Gil, M. I., & Allende, A. (2014). Minimum free chlorine residual level required for the inactivation of Escherichia coli O157: H7 and trihalomethane generation during dynamic washing of fresh-cut spinach. *Food Control*, *42*, 132-138.

Gómez-López, V. M., Marín, A., Medina-Martínez, M. S., Gil, M. I., & Allende, A. (2013). Generation of trihalomethanes with chlorine-based sanitizers and impact on microbial, nutritional and sensory quality of baby spinach. *Postharvest Biology and Technology*, *85*, 210-217.

González-Sálamo, J., Socas-Rodríguez, B., Hernández-Borges, J., & Rodríguez-Delgado, M. Á. (2016). Nanomaterials as sorbents for food sample analysis. *TrAC Trends in Analytical Chemistry*, *85*, 203-220.

Gutierrez, J., Barry-Ryan, C., & Bourke, P. (2009). Antimicrobial activity of plant essential oils using food model media: efficacy, synergistic potential and interactions with food components. *Food microbiology*, 26(2), 142-150.

Gyawali, R., & Ibrahim, S. A. (2014). Natural products as antimicrobial agents. *Food control*, 46, 412-429.

Han, J., Gomes-Feitosa, C. L., Castell-Perez, E., Moreira, R. G., & Silva, P. F. (2004). Quality of packaged romaine lettuce hearts exposed to low-dose electron beam irradiation. *LWT-Food Science and Technology*, *37*(7), 705-715.

Hanušová, K., Dobiáš, J., & Klaudisová, K. (2009). Effect of packaging films releasing antimicrobial agents on stability of food products. *Czech J. Food Sci*, 27, 347-349.

Helrich, K. (1990). *Official methods of analysis of the Association of Official Analytical Chemists*. Association of official analytical chemists.

Herman, K. M., Hall, A. J., & Gould, L. H. (2015). Outbreaks attributed to fresh leafy vegetables, United States, 1973–2012. *Epidemiology & Infection*, *143*(14), 3011-3021.

Hill, L. E. (2014). *Nanoencapsulation Strategies for Antimicrobial Controlled Release to Enhance Fresh and Fresh-Cut Produce Safety* (Doctoral dissertation).

Ho, P. H., Salles, F., Di Renzo, F., & Trens, P. (2020). One-pot synthesis of 5-FU@ ZIF-8 and ibuprofen@ ZIF-8 nanoparticles. *Inorganica Chimica Acta*, *500*, 119229.

Hoop, M., Walde, C. F., Riccò, R., Mushtaq, F., Terzopoulou, A., Chen, X. Z., ... & Pané, S. (2018). Biocompatibility characteristics of the metal organic framework ZIF-8 for therapeutical applications. *Applied Materials Today*, *11*, 13-21.

Horcajada, P., Chalati, T., Serre, C., Gillet, B., Sebrie, C., Baati, T., ... & Chang, J. S. (2010). Porous metal–organic-framework nanoscale carriers as a potential platform for drug delivery and imaging. *Nature materials*, *9*(2), 172-178.

Hrudey, S. E. (2009). Chlorination disinfection by-products, public health risk tradeoffs and me. *Water research*, *43*(8), 2057-2092.

Hughes, D. E. (1983). Titrimetric determination of ascorbic acid with 2, 6-dichlorophenol indophenol in commercial liquid diets. *Journal of pharmaceutical sciences*, *72*(2), 126-129.

Iddir, M., Brito, A., Dingeo, G., Fernandez Del Campo, S. S., Samouda, H., La Frano, M. R., & Bohn, T. (2020). Strengthening the immune system and reducing inflammation and oxidative stress through diet and nutrition: considerations during the COVID-19 crisis. *Nutrients*, *12*(6), 1562.

Jacobsson, A., Nielsen, T., Sjoholm, I., (2004). Effects of type of packaging material on shelf-life of fresh broccoli by means of changes in weight, colour and texture. *European Food Research and Technology* 218, 158-163.

Jacxsens, L., Devlieghere, F., Ragaert, P., Vanneste, E., & Debevere, J. (2003). Relation between microbiological quality, metabolite production and sensory quality of equilibrium modified atmosphere packaged fresh-cut produce. International *journal of food microbiology*, *83*(3), 263-280.

Jaworska, G. (2005). Nitrates, nitrites, and oxalates in products of spinach and New Zealand spinach: Effect of technological measures and storage time on the level of nitrates, nitrites, and oxalates in frozen and canned products of spinach and New Zealand spinach. *Food chemistry*, *93*(3), 395-401.

Jia, Z., Liu, Z., & He, F. (2003). Synthesis of nanosized BaSO4 and CaCO3 particles with a membrane reactor: effects of additives on particles. *Journal of colloid and interface science*, *266*(2), 322-327.

Kalemba, D. A. A. K., & Kunicka, A. (2003). Antibacterial and antifungal properties of essential oils. *Current medicinal chemistry*, *10*(10), 813-829.

Kannappan, S., Jayaraman, T., Rajasekar, P., Ravichandran, M. K., & Anuradha, C. V. (2006). Cinnamon bark extract improves glucose metabolism and lipid profile in the fructose-fed rat. *Singapore medical journal*, *47*(10), 858.

Kathuria, A., Abiad, M. G., & Auras, R. (2021). PLLA-ZIF-8 metal organic framework composites for potential use in food applications: Production, characterization and migration studies. *Packaging Technology and Science*.

Kawashima, L. M., & Soares, L. M. V. (2003). Mineral profile of raw and cooked leafy vegetables consumed in Southern Brazil. *Journal of Food Composition and Analysis*, *16*(5), 605-611.

Keskinen, L. A., Burke, A., & Annous, B. A. (2009). Efficacy of chlorine, acidic electrolyzed water and aqueous chlorine dioxide solutions to decontaminate Escherichia coli O157: H7 from lettuce leaves. *International journal of food microbiology*, *132*(2-3), 134-140.

Khan, I., Saeed, K., & Khan, I. (2019). Nanoparticles: Properties, applications and toxicities. *Arabian journal of chemistry*, *12*(7), 908-931.

Kim, J. G., Luo, Y., Saftner, R. A., & Gross, K. C. (2005). Delayed modified atmosphere packaging of fresh-cut Romaine lettuce: Effects on quality maintenance and shelf-life. *Journal of the American Society for Horticultural Science*, *130*(1), 116-123.

King, A. D., & Bolin, H. R. (1989). Physiological and microbiological storage stability of minimally processed fruits and vegetables. Food Technology, 43(2).

King, V. A. E., Liu, C. F., & Liu, Y. J. (2001). Chlorophyll stability in spinach dehydrated by freeze-drying and controlled low-temperature vacuum dehydration. *Food research international*, *34*(2-3), 167-175.

Kizhedath, A., Wilkinson, S., & Glassey, J. (2019). Assessment of hepatotoxicity and dermal toxicity of butylparaben and methylparaben using HepG2 and HDFn in vitro models. *Toxicology in Vitro*, *55*, 108-115.

Knobloch, K., Pauli, A., Iberl, B., Weigand, H., & Weis, N. (1989). Antibacterial and antifungal properties of essential oil components. *Journal of Essential Oil Research*, 1(3), 119-128.

Kohsari, I., Shariatinia, Z., & Pourmortazavi, S. M. (2016). Antibacterial electrospun chitosan-polyethylene oxide nanocomposite mats containing ZIF-8 nanoparticles. *International journal of biological macromolecules*, *91*, 778-788.

Kowalska-Krochmal, B., & Dudek-Wicher, R. (2021). The minimum inhibitory concentration of antibiotics: Methods, interpretation, clinical relevance. *Pathogens*, *10*(2), 165.

Kowalska-Krochmal, B., & Dudek-Wicher, R. (2021). The minimum inhibitory concentration of antibiotics: Methods, interpretation, clinical relevance. *Pathogens, 10(2),* 165.

Kreno, L. E., Hupp, J. T., & Van Duyne, R. P. (2010). Metal− organic framework thin film for enhanced localized surface plasmon resonance gas sensing. *Analytical chemistry*, *82*(19), 8042-8046.

Kwon, J. A., Yu, C. B., & Park, H. D. (2003). Bacteriocidal effects and inhibition of cell separation of cinnamic aldehyde on Bacillus cereus. *Letters in applied microbiology*, *37*(1), 61-65.

Lam, S. J., Wong, E. H., Boyer, C., & Qiao, G. G. (2018). Antimicrobial polymeric nanoparticles. *Progress in polymer science*, *76*, 40-64.

Lee, J., Farha, O. K., Roberts, J., Scheidt, K. A., Nguyen, S. T., & Hupp, J. T. (2009). Metal–organic framework materials as catalysts. *Chemical Society Reviews*, *38*(5), 1450-1459.

Lee, N. Y., Ko, W. C., & Hsueh, P. R. (2019). Nanoparticles in the treatment of infections caused by multidrug-resistant organisms. *Frontiers in pharmacology*, *10*, 1153.

Lee, W. N., & Huang, C. H. (2019). Formation of disinfection byproducts in wash water and lettuce by washing with sodium hypochlorite and peracetic acid sanitizers. *Food Chemistry: X*, *1*, 100003.

Li, M., Tao, Y., Shu, Y., LaRochelle, J. R., Steinauer, A., Thompson, D., ... & Liu, D. R. (2015). Discovery and characterization of a peptide that enhances endosomal escape of delivered proteins in vitro and in vivo. *Journal of the American Chemical Society*, *137*(44), 14084-14093.

Li, Y., Liang, F., Bux, H., Yang, W., & Caro, J. (2010). Zeolitic imidazolate framework ZIF-7 based molecular sieve membrane for hydrogen separation. *Journal of Membrane Science*, *354*(1-2), 48-54.

Li, Y., Xu, N., Zhou, J., Zhu, W., Li, L., Dong, M., ... & Xie, Z. (2018). Facile synthesis of a metal–organic framework nanocarrier for NIR imaging-guided photothermal therapy. *Biomaterials science*, *6*(11), 2918-2924.

Li, Y., Zheng, Y., Lai, X., Chu, Y., & Chen, Y. (2018). Biocompatible surface modification of nano-scale zeolitic imidazolate frameworks for enhanced drug delivery. *RSC advances*, *8*(42), 23623-23628.

Liang, K., Ricco, R., Doherty, C. M., Styles, M. J., Bell, S., Kirby, N., ... & Falcaro, P. (2015). Biomimetic mineralization of metal-organic frameworks as protective coatings for biomacromolecules. *Nature communications*, *6*(1), 1-8.

Liao, W., Badri, W., Dumas, E., Ghnimi, S., Elaissari, A., Saurel, R., & Gharsallaoui, A. (2021). Nanoencapsulation of Essential Oils as Natural Food Antimicrobial Agents: An Overview. *Applied Sciences*, *11*(13), 5778.

Liédana, N., Galve, A., Rubio, C., Téllez, C., & Coronas, J. (2012). CAF@ ZIF-8: one-step encapsulation of caffeine in MOF. *ACS applied materials & interfaces*, *4*(9), 5016-5021.

Lin, J. B., Lin, R. B., Cheng, X. N., Zhang, J. P., & Chen, X. M. (2011). Solvent/additive-free synthesis of porous/zeolitic metal azolate frameworks from metal oxide/hydroxide. *Chemical Communications*, *47*(32), 9185-9187.

Lin, Z. J., Lü, J., Hong, M., & Cao, R. (2014). Metal–organic frameworks based on flexible ligands (FL-MOFs): structures and applications. *Chemical Society Reviews*, *43*(16), 5867-5895.

Lipton, W. J. (1990). Postharvest biology of fresh asparagus. *Horticultural reviews*, *12*(2), 65-155.

Lisiewska, Z., Gębczyński, P., Bernaś, E., & Kmiecik, W. (2009). Retention of mineral constituents in frozen leafy vegetables prepared for consumption. *Journal of food composition and analysis*, *22*(3), 218-223.

Lismont, M., Dreesen, L., & Wuttke, S. (2017). Metal-organic framework nanoparticles in photodynamic therapy: current status and perspectives. *Advanced Functional Materials*, *27*(14), 1606314.

Liu, J., Li, S., Fang, Y., & Zhu, Z. (2019). Boosting antibacterial activity with mesoporous silica nanoparticles supported silver nanoclusters. *Journal of colloid and interface science*, *555*, 470-479.

López-Ayerra, B., Murcia, M. A., & Garcia-Carmona, F. (1998). Lipid peroxidation and chlorophyll levels in spinach during refrigerated storage and after industrial processing. *Food chemistry*, *61*(1-2), 113-118.

López-Gálvez, F., Allende, A., Truchado, P., Martínez-Sánchez, A., Tudela, J. A., Selma, M. V., & Gil, M. I. (2010). Suitability of aqueous chlorine dioxide versus sodium hypochlorite as an effective sanitizer for preserving quality of fresh-cut lettuce while avoiding by-product formation. *Postharvest Biology and Technology*, *55*(1), 53-60.

Loquercio, A. S. (2014). *Preparation and Characterization of Chitosan-Alginate Nanoparticles for Trans-Cinnamaldehyde Entrapment* (Doctoral dissertation).

Lu, G., & Hupp, J. T. (2010). Metal− organic frameworks as sensors: a ZIF-8 based Fabry− Pérot device as a selective sensor for chemical vapors and gases. *Journal of the American Chemical Society*, *132*(23), 7832-7833.

Lu, G., Li, S., Guo, Z., Farha, O. K., Hauser, B. G., Qi, X., ... & Huo, F. (2012). Imparting functionality to a metal–organic framework material by controlled nanoparticle encapsulation. *Nature chemistry*, *4*(4), 310-316.

Lu, J. L., Pan, S. S., Zheng, X. Q., Dong, J. J., Borthakur, D., & Liang, Y. R. (2009). Effects of lipophillic pigments on colour of the green tea infusion. *International journal of food science & technology*, *44*(12), 2505-2511.

Luksiene, Z. (2017). Nanoparticles and their potential application as antimicrobials in the food industry. In *Food Preservation* (pp. 567-601). Academic press.

Luna-Guevara, J. J., Arenas-Hernandez, M. M., Martínez de la Peña, C., Silva, J. L., & Luna-Guevara, M. L. (2019). The role of pathogenic E. coli in fresh vegetables: Behavior, contamination factors, and preventive measures. *International journal of microbiology*, *2019*.

Luo, Y., Nou, X., Yang, Y., Alegre, I., Turner, E., Feng, H., ... & Conway, W. (2011). Determination of free chlorine concentrations needed to prevent Escherichia coli O157: H7 cross-contamination during fresh-cut produce wash. *Journal of food protection, 74(3)*, 352-358.

Luzuriaga, M. A., Benjamin, C. E., Gaertner, M. W., Lee, H., Herbert, F. C., Mallick, S., & Gassensmith, J. J. (2019). ZIF-8 degrades in cell media, serum, and some—but not all—common laboratory buffers. *Supramolecular chemistry*, *31*(8), 485-490.

Lynch, M. F., Tauxe, R. V., & Hedberg, C. W. (2009). The growing burden of foodborne outbreaks due to contaminated fresh produce: risks and opportunities. *Epidemiology & Infection*, *137*(3), 307-315. Jiang, H. L., Liu, B., Akita, T., Haruta, M., Sakurai, H., & Xu, Q. (2009). Au@ ZIF-8: CO oxidation over gold nanoparticles deposited to metal− organic framework. *Journal of the American Chemical Society*, *131*(32), 11302-11303.

Lynch, M. F., Tauxe, R. V., & Hedberg, C. W. (2009). The growing burden of foodborne outbreaks due to contaminated fresh produce: risks and opportunities. *Epidemiology & Infection*, *137*(3), 307-315.

Marino, M., Bersani, C., & Comi, G. (2001). Impedance measurements to study the antimicrobial activity of essential oils from Lamiaceae and Compositae. *International journal of food microbiology*, 67(3), 187-195.

Marsich, L., Bonifacio, A., Mandal, S., Krol, S., Beleites, C., Sergo, V. 2012. Poly-L-lysine-Coated Silver Nanoparticles as Positively Charged Substrates for Surface-Enhanced Raman Scattering. Langmuir, 28, 13166-13171.

Martín-Diana, A. B., Rico, D., & Barry-Ryan, C. (2008). Green tea extract as a natural antioxidant to extend the shelf-life of fresh-cut lettuce. *Innovative Food Science & Emerging Technologies*, *9*(4), 593-603.

Martins, G. A., Byrne, P. J., Allan, P., Teat, S. J., Slawin, A. M., Li, Y., & Morris, R. E. (2010). The use of ionic liquids in the synthesis of zinc imidazolate frameworks. *Dalton Transactions*, *39*(7), 1758-1762.

Merisko-Liversidge, E. M., & Liversidge, G. G. (2008). Drug nanoparticles: formulating poorly water-soluble compounds. *Toxicologic pathology*, *36*(1), 43-48.

Mohanraj, V. J., & Chen, Y. (2006). Nanoparticles-a review. *Tropical journal of pharmaceutical research*, *5*(1), 561-573.

Moleyar, V., & Narasimham, P. (1992). Antibacterial activity of essential oil components. *International journal of food microbiology*, 16(4), 337-342.

Monaghan, J., & Hutchison, M. (2015). *Monitoring microbial food safety of fresh produce*. AHDB Horticulture.

Nowak, E., Kammerer, S., & Küpper, J. H. (2018). ATP-based cell viability assay is superior to trypan blue exclusion and XTT assay in measuring cytotoxicity of anticancer drugs Taxol and Imatinib, and proteasome inhibitor MG-132 on human hepatoma cell line HepG2. *Clinical hemorheology and microcirculation*, *69*(1-2), 327-336.

Nthenge, A.K., Weese, J.S., Carter, M., Wei, C., Huang, T., 2007. Efficacy of gamma radiation and aqueous chlorine on Escherichia coli O157:H7 in hydroponically grown lettuce plants. *Journal of Food Protection 70*, 748–752.

Nychas, G. J. E. (1995). Natural antimicrobials from plants. In *New methods of food preservation* (pp. 58-89). Springer, Boston, MA.

Olaimat, A. N., & Holley, R. A. (2012). Factors influencing the microbial safety of fresh produce: a review. *Food microbiology*, *32*(1), 1-19.

Ouyang, Y., Cai, X., Shi, Q., Liu, L., Wan, D., Tan, S., & Ouyang, Y. (2013). Poly-l-lysine-modified reduced graphene oxide stabilizes the copper nanoparticles with higher water-solubility and long-term additively antibacterial activity. *Colloids and surfaces B: Biointerfaces*, *107*, 107-114.

Painter, J. A., Hoekstra, R. M., Ayers, T., Tauxe, R. V., Braden, C. R., Angulo, F. J., & Griffin, P. M. (2013). Attribution of foodborne illnesses, hospitalizations, and deaths to food commodities by using outbreak data, United States, 1998–2008. *Emerging infectious diseases*, *19*(3), 407.

Pan, X., & Nakano, H. (2014). Effects of chlorine-based antimicrobial treatments on the microbiological qualities of selected leafy vegetables and wash water. Food Science and Technology Research, 20(4), 765-774.

Pan, Y., Liu, Y., Zeng, G., Zhao, L., & Lai, Z. (2011). Rapid synthesis of zeolitic imidazolate framework-8 (ZIF-8) nanocrystals in an aqueous system. *Chemical Communications*, *47*(7), 2071-2073.

Pandey, A. K., Chávez-González, M. L., Silva, A. S., & Singh, P. (2021). Essential oils from the genus Thymus as antimicrobial food preservatives: Progress in their use as nanoemulsions-a new paradigm. *Trends in Food Science & Technology*.

Parish, M.E., Beuchat, L.R., Suslow, T.V., Harris, L.J., Garrett, E.H., Farber, J.N., Busta, F.F., 2003. Methods to reduce/eliminate pathogens from fresh and fresh-cut produce. *Comprehensive Reviews in Food Science and Food Safety 2*, 161–173.

Park, K. S., Ni, Z., Côté, A. P., Choi, J. Y., Huang, R., Uribe-Romo, F. J., ... & Yaghi, O. M. (2006). Exceptional chemical and thermal stability of zeolitic imidazolate

frameworks. *Proceedings of the National Academy of Sciences*, *103*(27), 10186-10191.

Parnham, E. R., & Morris, R. E. (2007). Ionothermal synthesis of zeolites, metal–organic frameworks, and inorganic–organic hybrids. *Accounts of chemical research*, *40*(10), 1005-1013.

Pateiro, M., Munekata, P. E., Sant'Ana, A. S., Domínguez, R., Rodríguez-Lázaro, D., & Lorenzo, J. M. (2021). Application of essential oils as antimicrobial agents against spoilage and pathogenic microorganisms in meat products. *International journal of food microbiology*, *337*, 108966.

Peller, M., Böll, K., Zimpel, A., & Wuttke, S. (2018). Metal–organic framework nanoparticles for magnetic resonance imaging. *Inorganic Chemistry Frontiers*, *5*(8), 1760-1779.

Petri, E., Rodríguez, M., & García, S. (2015). Evaluation of combined disinfection methods for reducing Escherichia coli O157: H7 population on fresh-cut vegetables. *International journal of environmental research and public health*, *12*(8), 8678-8690.

Petri, E., Virto, R., MOTTURA, M., & PARRA, J. (2021). Comparison of Peracetic Acid and Chlorine Effectiveness during Fresh-Cut Vegetable Processing at Industrial Scale. *Journal of Food Protection*, *84*(9), 1592-1602.

Polylysine. (2020, April 17). In *Wikipedia*. Retrieved August 13, 2021, from: https://en.wikipedia.org/wiki/Polylysine .

Prakash A, Guner A, Caporaso F, Foley D. 2000. Effects of Low-dose Gamma Irradiation on the Shelf Life and Quality Characteristics of Cut Romaine Lettuce Packaged under Modified Atmosphere. *J Food Sci 65(3)*:549-53.

Prakash, A., Guner, A. R., Caporaso, F., & Foley, D. M. (2000). Effects of low-dose gamma irradiation on the shelf life and quality characteristics of cut romaine lettuce packaged under modified atmosphere. *Journal of Food Science*, *65*(3), 549-553.

Prakash, B., & Kiran, S. (2016). Essential oils: a traditionally realized natural resource for food preservation. *Current Science*, *110*(10), 1890-1892.

Qin, B., Nagasaki, M., Ren, M., Bajotto, G., Oshida, Y., & Sato, Y. (2003). Cinnamon extract (traditional herb) potentiates in vivo insulin-regulated glucose utilization via enhancing insulin signaling in rats. *Diabetes research and clinical practice*, *62*(3), 139-148.

Qin, Z., Huang, Y., Wang, Q., Qi, J., Xing, X., & Zhang, Y. (2010). Controllable synthesis of well-dispersed and uniform-sized single crystalline zinc hydroxystannate nanocubes. *CrystEngComm*, *12*(12), 4156-4160.

Rafiee, Z., Nejatian, M., Daeihamed, M., & Jafari, S. M. (2019). Application of curcumin-loaded nanocarriers for food, drug and cosmetic purposes. *Trends in Food Science & Technology*, *88*, 445-458.

Rico, D., Martín-Diana, A. B., Barry-Ryan, C., Frías, J. M., Henehan, G. T., & Barat, J. M. (2008). Use of neutral electrolysed water (EW) for quality maintenance and shelf-life extension of minimally processed lettuce. *Innovative food science & emerging technologies*, *9*(1), 37-48.

Rowe, M. D., Thamm, D. H., Kraft, S. L., & Boyes, S. G. (2009). Polymer-modified gadolinium metal-organic framework nanoparticles used as multifunctional nanomedicines for the targeted imaging and treatment of cancer. *Biomacromolecules*, *10*(4), 983-993.

Ruyra, À., Yazdi, A., Espín, J., Carné-Sánchez, A., Roher, N., Lorenzo, J., ... & Maspoch, D. (2015). Synthesis, culture medium stability, and in vitro and in vivo zebrafish embryo toxicity of metal–organic framework nanoparticles. *Chemistry–A European Journal*, *21*(6), 2508-2518.

Schmidt, S. J., & Fontana Jr, A. J. (2020). E: Water Activity Values of Select Food Ingredients and Products. *Water activity in foods: Fundamentals and applications*, 573-591.

Schwartz, S. J., & Lorenzo, T. V. (1991). Chlorophyll stability during continuous aseptic processing and storage. *Journal of Food Science*, *56*(4), 1059-1062.

Serpen, A., Gökmen, V., Bahçeci, K. S., & Acar, J. (2007). Reversible degradation kinetics of vitamin C in peas during frozen storage. European Food Research and Technology, 224(6), 749-753.

Severing, A. L., Rembe, J. D., Koester, V., & Stuermer, E. K. (2019). Safety and efficacy profiles of different commercial sodium hypochlorite/hypochlorous acid solutions (NaClO/HClO): antimicrobial efficacy, cytotoxic impact and physicochemical parameters in vitro. *Journal of Antimicrobial Chemotherapy*, *74*(2), 365-372.

Shahbandeh, M. (2021). U.S. per capita consumption of fresh vegetables by type 2020. Retrieved August 12, 2021, from: https://www.statista.com/statistics/257345/per-capita-consumption-of-fresh-vegetables-in-the-us-by-type/

Shan, C., Yang, H., Han, D., Zhang, Q., Ivaska, A., & Niu, L. (2009). Water-soluble graphene covalently functionalized by biocompatible poly-L-lysine. *Langmuir*, *25*(20), 12030-12033.

Shreaz, S., Wani, W. A., Behbehani, J. M., Raja, V., Irshad, M., Karched, M., ... & Hun, L. T. (2016). Cinnamaldehyde and its derivatives, a novel class of antifungal agents. Fitoterapia, 112, 116-131.

Siddiqua, S., Anusha, B. A., Ashwini, L. S., & Negi, P. S. (2015). Antibacterial activity of cinnamaldehyde and clove oil: effect on selected foodborne pathogens in model food systems and watermelon juice. *Journal of food science and technology*, *52*(9), 5834-5841.

Sieniawska, E., Sawicki, R., Golus, J., & Georgiev, M. I. (2020). Untargeted metabolomic exploration of the Mycobacterium tuberculosis stress response to cinnamon essential oil. *Biomolecules*, *10*(3), 357.

Singh, H. D., Wang, G., Uludağ, H., & Unsworth, L. D. (2010). Poly-L-lysine-coated albumin nanoparticles: stability, mechanism for increasing in vitro enzymatic resilience, and siRNA release characteristics. *Acta biomaterialia*, *6*(11), 4277-4284.

Sinha, N., Hui, Y. H., Evranuz, E. Ö., Siddiq, M., & Ahmed, J. (2010). *Handbook of vegetables and vegetable processing*. John Wiley & Sons.

Sivapalasingam, S., Friedman, C. R., Cohen, L., & Tauxe, R. V. (2004). Fresh produce: a growing cause of outbreaks of foodborne illness in the United States, 1973 through 1997. *Journal of food protection*, *67*(10), 2342-2353.

Skandamis, P., Tsigarida, E., & Nychas, G. E. (2002). The effect of oregano essential oil on survival/death of Salmonella typhimurium in meat stored at 5 C under aerobic, VP/MAP conditions. *Food Microbiology*, *19*(1), 97-103.

Slavin, J. L., & Lloyd, B. (2012). Health benefits of fruits and vegetables. *Advances in nutrition*, *3*(4), 506-516.

Spinardi, A., Cocetta, G., Baldassarre, V., Ferrante, A., & Mignani, I. (2009, April). Quality changes during storage of spinach and lettuce baby leaf. In *VI International Postharvest Symposium 877* (pp. 571-576).

Srividya, N., Ghoora, M. D., & Padmanabh, P. R. (2017). Antimicrobial nanotechnology: Research implications and prospects in food safety. In *Food Preservation* (pp. 125-165). Academic Press.

Stock, N., & Biswas, S. (2012). Synthesis of metal-organic frameworks (MOFs): routes to various MOF topologies, morphologies, and composites. *Chemical reviews*, *112*(2), 933-969.

Stuart, D., Shennan, C., & Brown, M. (2006). Food safety versus environmental protection on the Central California coast: exploring the science behind an apparent conflict.

Sun, C. Y., Qin, C., Wang, X. L., Yang, G. S., Shao, K. Z., Lan, Y. Q., ... & Wang, E. B. (2012). Zeolitic imidazolate framework-8 as efficient pH-sensitive drug delivery vehicle. *Dalton Transactions*, *41*(23), 6906-6909.

Taheri, M., Ashok, D., Sen, T., Enge, T. G., Verma, N. K., Tricoli, A., ... & Tsuzuki, T. (2021). Stability of ZIF-8 nanopowders in bacterial culture media and its implication for antibacterial properties. *Chemical Engineering Journal*, *413*, 127511.

Taheri, M., Ashok, D., Sen, T., Enge, T. G., Verma, N. K., Tricoli, A., ... & Tsuzuki, T. (2021). Stability of ZIF-8 nanopowders in bacterial culture media and its implication for antibacterial properties. *Chemical Engineering Journal*, *413*, 127511.

Tan, J., Wang, D., Cao, H., Qiao, Y., Zhu, H., & Liu, X. (2018). Effect of local alkaline microenvironment on the behaviors of bacteria and osteogenic cells. *ACS applied materials & interfaces*, *10*(49), 42018-42029.

Tanaka, S., Kida, K., Okita, M., Ito, Y., & Miyake, Y. (2012). Size-controlled synthesis of zeolitic imidazolate framework-8 (ZIF-8) crystals in an aqueous system at room temperature. *Chemistry Letters*, *41*(10), 1337-1339.

Tao, B., Zhao, W., Lin, C., Yuan, Z., He, Y., Lu, L., ... & Cai, K. (2020). Surface modification of titanium implants by ZIF-8@ Levo/LBL coating for inhibition of bacterial-associated infection and enhancement of in vivo osseointegration. *Chemical Engineering Journal*, *390*, 124621.

The European Committee on Antimicrobial Susceptibility Testing (EUCAST). Clinical Breakpoints—Bacteria (v 10.0). 2020. Retrieved at October, 2021 from: **https://www.eucast.org/fileadmin/src/media/PDFs/EUCAST_files/Breakpoint_tables/v_10.0_Breakpoint_Tables.pdf** .

The Food Industry Association. (2020). The power of produce 2021. Retrieved September 18, 2021, from: https://www.fmi.org/forms/store/ProductFormPublic/power-of-produce-2021

Thomson, N., Evert, R. F., & Kelman, A. (1995). Wound healing in whole potato tubers: a cytochemical, fluorescence, and ultrastructural analysis of cut and bruise wounds. *Canadian Journal of Botany*, *73*(9), 1436-1450.

Tiwari, A., Singh, A., Garg, N., & Randhawa, J. K. (2017). Curcumin encapsulated zeolitic imidazolate frameworks as stimuli responsive drug delivery system and their interaction with biomimetic environment. *Scientific reports*, *7*(1), 1-12.

Tranchemontagne, D.J., R. Hunt, J. R., & Yaghi, O. M. (2008). Room temperature synthesis of metal-organic frameworks: MOF-5, MOF-74, MOF-177, MOF-199, and IRMOF-0, *Tetrahedron, 64(36),* 8553-8557.

Transport Information Service. Cinnamon. Retrieved August 13, 2021, from: https://www.tis-gdv.de/tis_e/ware/gewuerze/zimt/zimt.htm/.

Turner, K., Moua, C. N., Hajmeer, M., Barnes, A., & Needham, M. (2019). Overview of leafy greens–related food safety incidents with a California link: 1996 to 2016. *Journal of Food Protection*, *82*(3), 405-414.

Van Haute, S., Tryland, I., Veys, A., & Sampers, I. (2015). Wash water disinfection of a full-scale leafy vegetables washing process with hydrogen peroxide and the use of a commercial metal ion mixture to improve disinfection efficiency. *Food Control*, *50*, 173-183.

Varier, K. M., Gudeppu, M., Chinnasamy, A., Thangarajan, S., Balasubramanian, J., Li, Y., & Gajendran, B. (2019). Nanoparticles: antimicrobial applications and its prospects. *In Advanced nanostructured materials for environmental remediation* (pp. 321-355). Springer, Cham.

Vasconcelos, N. G., Croda, J., & Simionatto, S. (2018). Antibacterial mechanisms of cinnamon and its constituents: A review. *Microbial pathogenesis*, *120*, 198-203.

Venkatasubbu, G. D., Baskar, R., Anusuya, T., Seshan, C. A., & Chelliah, R. (2016). Toxicity mechanism of titanium dioxide and zinc oxide nanoparticles against food pathogens. *Colloids and Surfaces B: Biointerfaces*, *148*, 600-606.

Venna, S. R., & Carreon, M. A. (2010). Highly permeable zeolite imidazolate framework-8 membranes for CO2/CH4 separation. *Journal of the American Chemical Society*, *132*(1), 76-78.

Venna, S. R., Jasinski, J. B., & Carreon, M. A. (2010). Structural evolution of zeolitic imidazolate framework-8. *Journal of the American Chemical Society*, *132*(51), 18030-18033.

Venna, S. R., Jasinski, J. B., & Carreon, M. A. (2010). Structural evolution of zeolitic imidazolate framework-8. *Journal of the American Chemical Society*, *132*(51), 18030-18033.

Visvalingam, J., Hernandez-Doria, J. D., & Holley, R. A. (2013). Examination of the genome-wide transcriptional response of Escherichia coli O157: H7 to cinnamaldehyde exposure. *Applied and environmental microbiology*, *79*(3), 942-950.

Wang, C., Sudlow, G., Wang, Z., Cao, S., Jiang, Q., Neiner, A., ... & Singamaneni, S. (2018). Metal-Organic Framework Encapsulation Preserves the Bioactivity of Protein Therapeutics. *Advanced healthcare materials*, *7*(22), 1800950.

Wang, J., Wang, Y., Zhang, Y., Uliana, A., Zhu, J., Liu, J., & Van der Bruggen, B. (2016). Zeolitic imidazolate framework/graphene oxide hybrid nanosheets functionalized thin film nanocomposite membrane for enhanced antimicrobial performance. *ACS applied materials & interfaces*, *8*(38), 25508-25519.

Wang, L., Hu, C., & Shao, L. (2017). The antimicrobial activity of nanoparticles: present situation and prospects for the future. *International journal of nanomedicine*, *12*, 1227.

Wang, L., Zhi, W., Lian, D., Wang, Y., Han, J., & Wang, Y. (2019). HRP@ ZIF-8/DNA Hybrids: Functionality Integration of ZIF-8 via Biomineralization and Surface Absorption. ACS Sustainable Chemistry & Engineering, 7(17), 14611-14620.

Wang, S., McGuirk, C. M., d'Aquino, A., Mason, J. A., & Mirkin, C. A. (2018). Metal–organic framework nanoparticles. *Advanced Materials*, *30*(37), 1800202.

Wang, T., Li, S., Zou, Z., Hai, L., Yang, X., Jia, X., ... & Wang, K. (2018). A zeolitic imidazolate framework-8-based indocyanine green theranostic agent for infrared fluorescence imaging and photothermal therapy. *Journal of Materials Chemistry B*, *6*(23), 3914-3921.

Wang, Y. W., Cao, A., Jiang, Y., Zhang, X., Liu, J. H., Liu, Y., & Wang, H. (2014). Superior antibacterial activity of zinc oxide/graphene oxide composites originating

from high zinc concentration localized around bacteria. *ACS applied materials & interfaces*, *6*(4), 2791-2798.

Wang, Y., & Duncan, T. V. (2017). Nanoscale sensors for assuring the safety of food products. *Current opinion in biotechnology*, *44*, 74-86.

Wei, X., Xu, D., Ge, K., Qi, S., & Chen, Y. (2020). Two-dimensional ultrathin multilayers ZIF-8 nanosheets with sustained antibacterial Efficacy for Aeromonas Hydrophila. *Journal of Inorganic and Organometallic Polymers and Materials*, *30*(10), 3862-3868.

Weiss, J., Gaysinsky, S., Davidson, M., & McClements, J. (2009). Nanostructured encapsulation systems: food antimicrobials. In *Global issues in food science and technology* (pp. 425-479). Academic Press.

Whipps, J. M., Hand, P., Pink, D. A., & Bending, G. D. (2008). Human pathogens and the phyllosphere. *Advances in applied microbiology*, *64*, 183-221.

Wuttke, S., Lismont, M., Escudero, A., Rungtaweevoranit, B., & Parak, W. J. (2017). Positioning metal-organic framework nanoparticles within the context of drug delivery–a comparison with mesoporous silica nanoparticles and dendrimers. *Biomaterials*, *123*, 172-183.

Xu, D., You, Y., Zeng, F., Wang, Y., Liang, C., Feng, H., & Ma, X. (2018). Disassembly of hydrophobic photosensitizer by biodegradable zeolitic imidazolate framework-8 for photodynamic cancer therapy. *ACS applied materials & interfaces*, *10*(18), 15517-15523.

Yang, C. M., Chang, K. W., Yin, M. H., & Huang, H. M. (1998). Methods for the determination of the chlorophylls and their derivatives. *Taiwania*, *43*(2), 116-122.

Yang, L., & Lu, H. (2012). Microwave-assisted ionothermal synthesis and characterization of zeolitic imidazolate framework-8. *Chinese Journal of Chemistry*, *30*(5), 1040-1044.

Yang, Y., Guo, Z., Huang, W., Zhang, S., Huang, J., Yang, H., ... & Gu, S. (2020). Fabrication of multifunctional textiles with durable antibacterial property and efficient oil-water separation via in situ growth of zeolitic imidazolate framework-8 (ZIF-8) on cotton fabric. *Applied Surface Science*, *503*, 144079.

Yao, J., & Wang, H. (2014). Zeolitic imidazolate framework composite membranes and thin films: synthesis and applications. *Chemical Society Reviews*, *43*(13), 4470-4493.

Yossa, N., Patel, J., Millner, P., & Lo, Y. M. (2012). Essential oils reduce Escherichia coli O157: H7 and Salmonella on spinach leaves. *Journal of food protection*, *75*(3), 488-496.

Yousefi, M., Ehsani, A., & Jafari, S. M. (2019). Lipid-based nano delivery of antimicrobials to control food-borne bacteria. *Advances in colloid and interface science*, *270*, 263-277.

Yu, S. J., Yin, Y. G., & Liu, J. F. (2013). Silver nanoparticles in the environment. *Environmental Science: Processes & Impacts*, *15*(1), 78-92.

Yuan, C., Wang, Y., Liu, Y., & Cui, B. (2019). Physicochemical characterization and antibacterial activity assessment of lavender essential oil encapsulated in hydroxypropyl-beta-cyclodextrin. *Industrial crops and products*, *130*, 104-110.

Yuan, P., Ding, X., Yang, Y. Y., & Xu, Q. H. (2018). Metal nanoparticles for diagnosis and therapy of bacterial infection. *Advanced healthcare materials*, *7*(13), 1701392.

Zabetakis, I., Lordan, R., Norton, C., & Tsoupras, A. (2020). COVID-19: the inflammation link and the role of nutrition in potential mitigation. *Nutrients,* 12(5), 1466.

Zhang, H., Zhao, M., Lin, Y. S. (2019). Stability of ZIF-8 in water under ambient conditions. Microporous and Mesoporous Materials. 279, 201–210.

Zhang, Y., Zhang, X., Song, J., Jin, L., Wang, X., & Quan, C. (2019). Ag/H-ZIF-8 Nanocomposite as an Effective Antibacterial Agent Against Pathogenic Bacteria. *Nanomaterials*, *9*(11), 1579.

Zhang, Z. (2016). Investigate the Interactions between Silver Nanoparticles and Leafy Vegetables Using Surface Enhanced Raman Spectroscopic Mapping Technique.

Zhao, J., Li, Y., Liu, Q., & Gao, K. (2010). Antimicrobial activities of some thymol derivatives from the roots of Inula hupehensis. *Food chemistry*, *120*(2), 512-516.

Zheng, H., Zhang, Y., Liu, L., Wan, W., Guo, P., Nyström, A. M., & Zou, X. (2016). One-pot synthesis of metal–organic frameworks with encapsulated target molecules and their applications for controlled drug delivery. *Journal of the American chemical society*, *138*(3), 962-968.

ZIF Metal Organic Framework. In *ChemTube3D*. Retrieved September 26, 2021, from: https://www.chemtube3d.com/mof-zif8/.

APPENDIX A

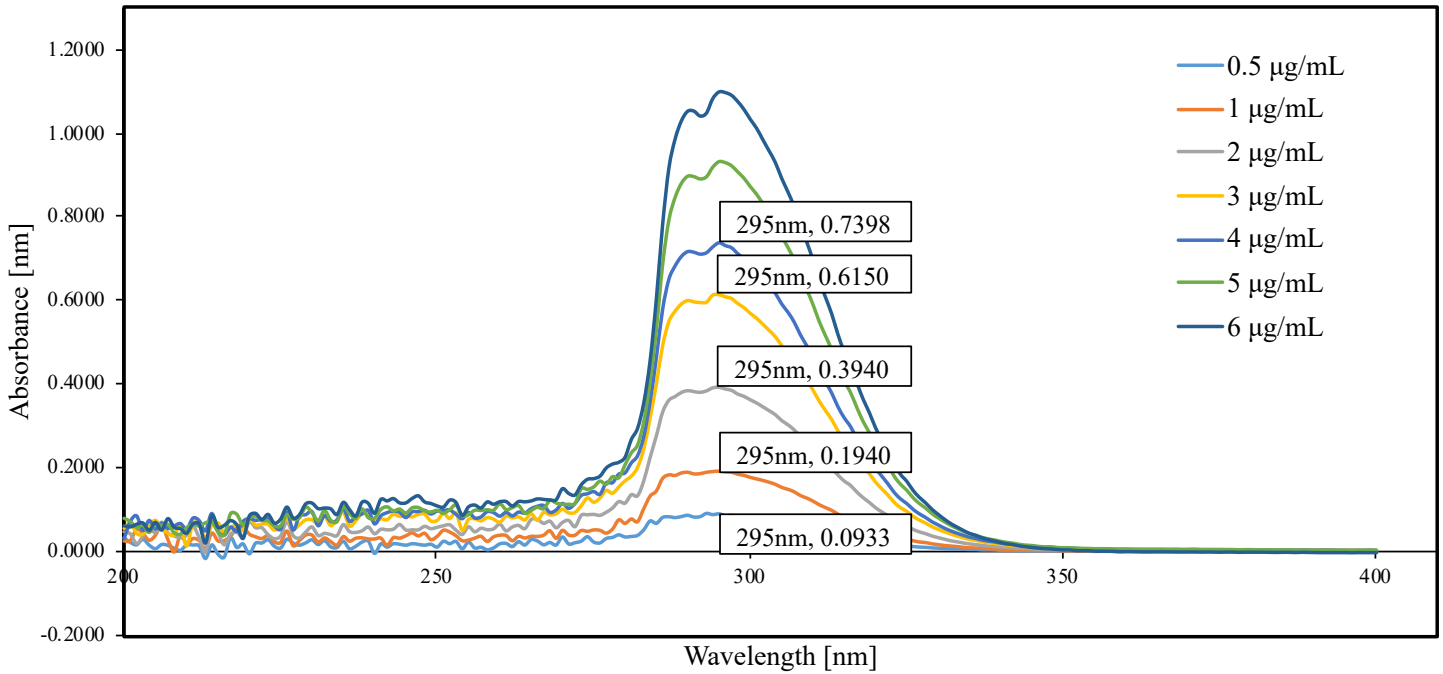

Figure 1. The absorbances obtained by scanning the UV–vis spectra (Genesys 10S UV Vis, Thermo Scientific, Madison, WI, USA) ranging from 200nm to 400 nm of TC dissolved in 0.1 M HCI. For all TC concentrations that reaches the maximum absorbance when wavelength at 295nm.

APPENDIX B

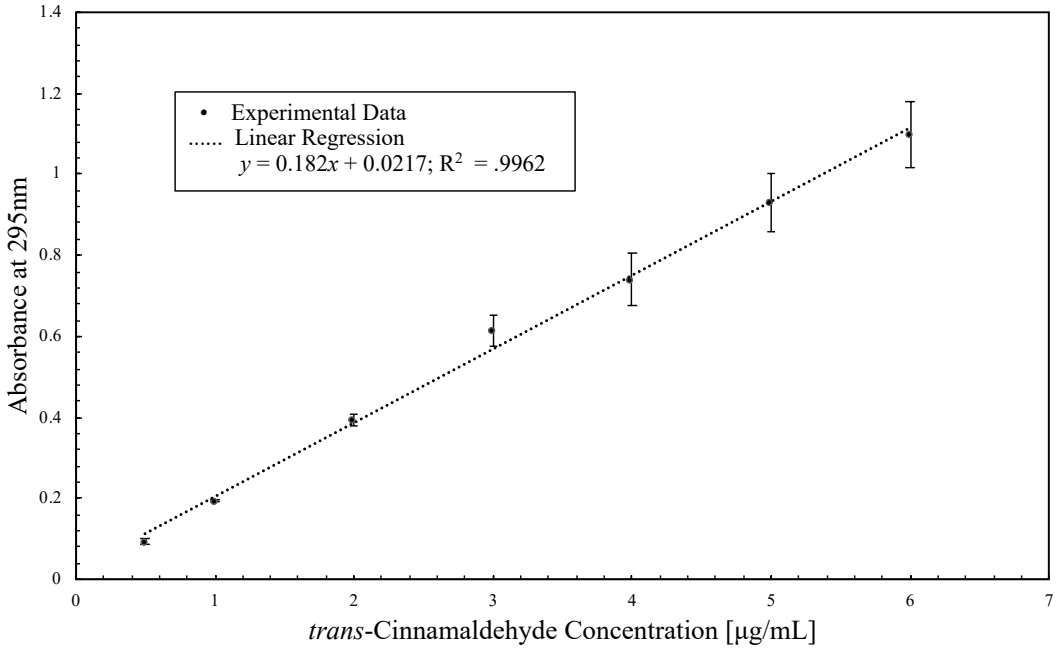

Figure 2. Standard calibration curve of *trans*-cinnamaldehyde for determination of encapsulation efficiency of TC@ZIF-8. TC (0.5-6.0 µg/ml) was dissolved in ZIF-8 Blank (ZIF-8 dissolved in 0.1 M HCl) and measured spectrophotometrically at 295 nm in triplicate to obtain absorbance (Genesys 10S UV-Vis, Thermo Scientific, Madison, WI, USA). Regression followed equation $y = 0.182x+0.0217$ ($R^2 = .9976$).

APPENDIX C

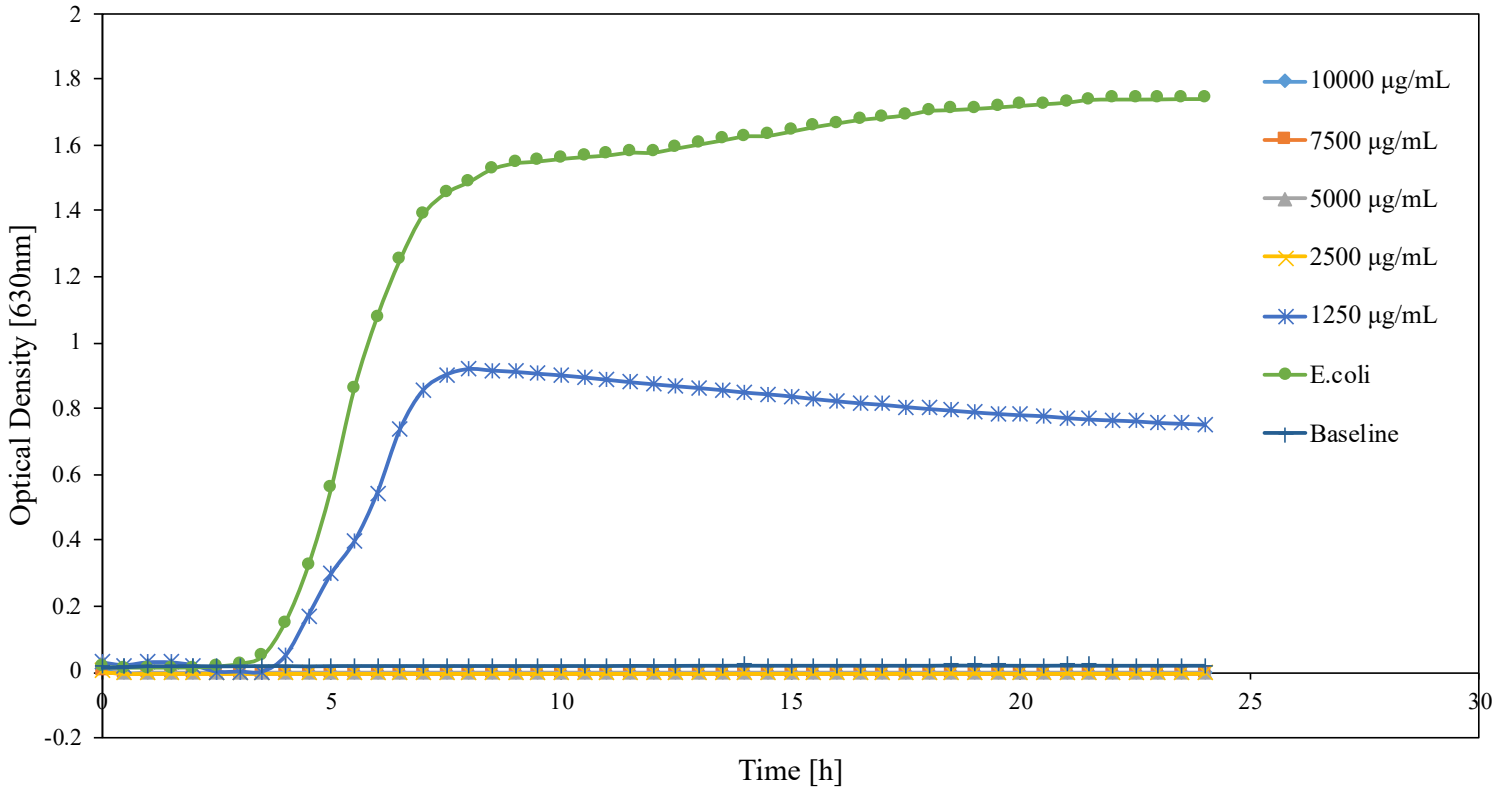

Figure C1. Growth curve of *E.coli* O157:H7 with 24 h treatment of ZIF-8 nanoparticle solutions.

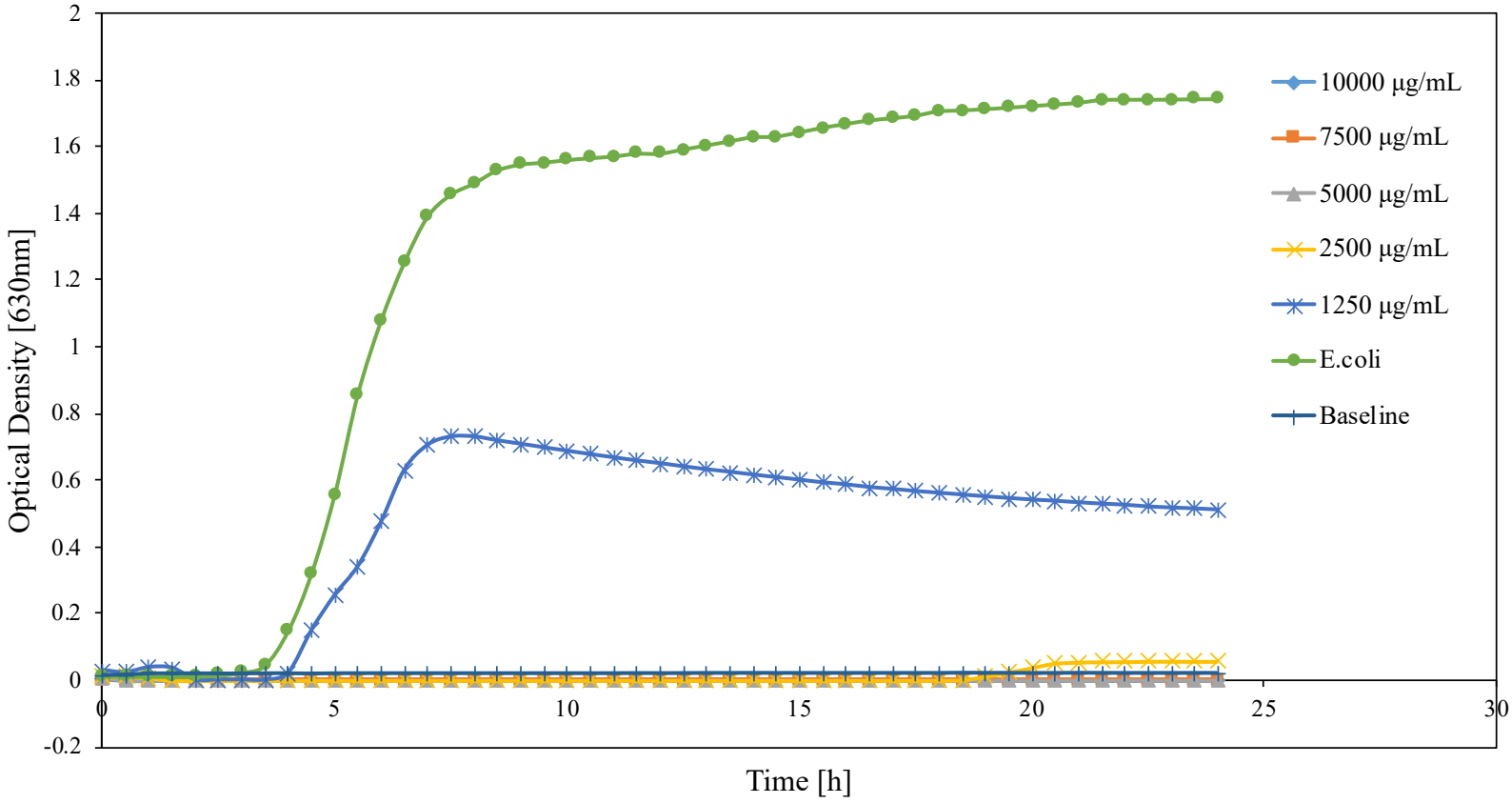

Figure C2. Growth curve of *E.coli* O157:H7 with 24 h treatment of ZIF-8_PL nanoparticle solutions.

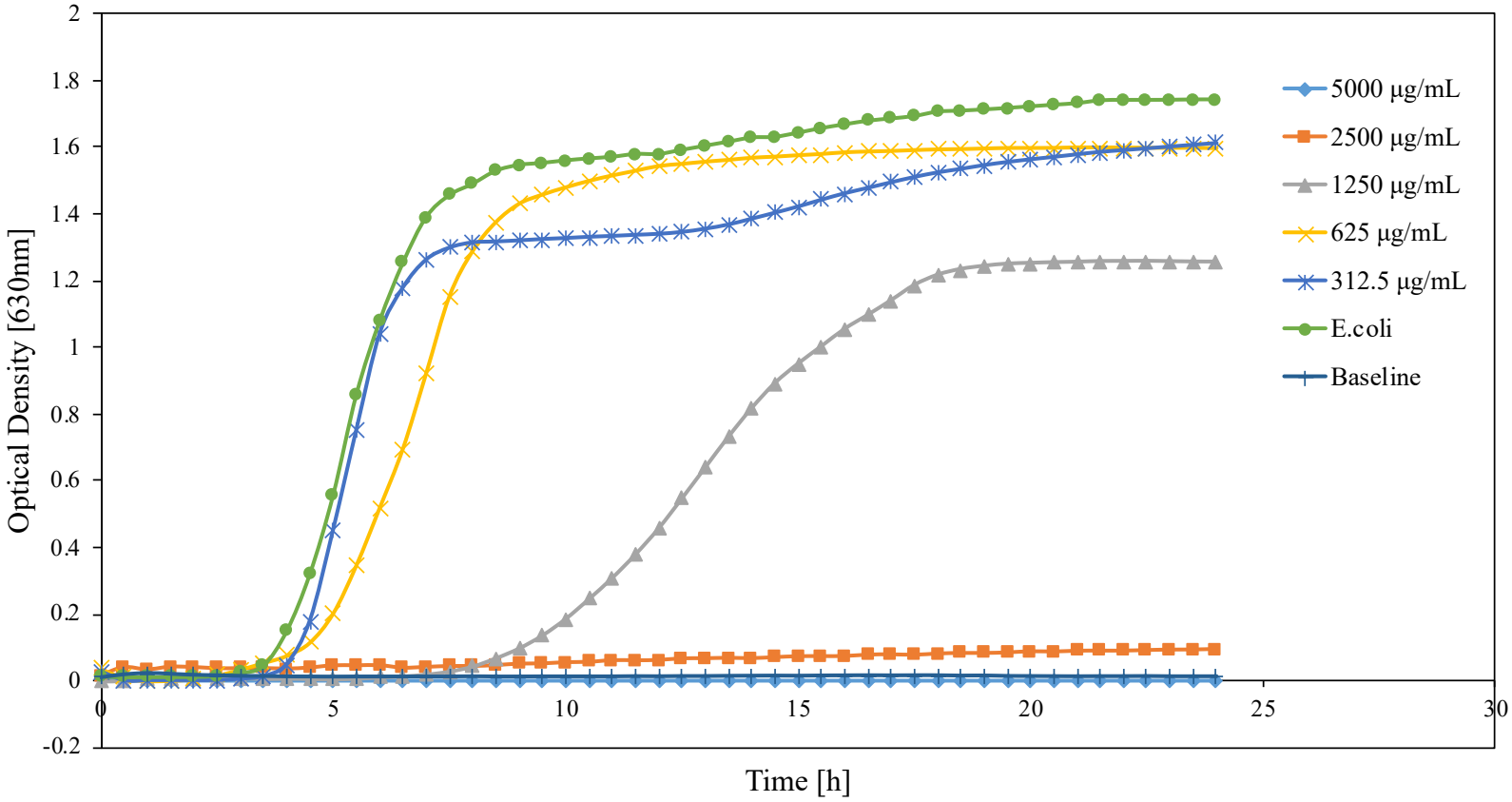

Figure C3. Growth curve of *E.coli* O157:H7 with 24 h treatment of 0.5TC@ZIF-8 nanoparticle solutions

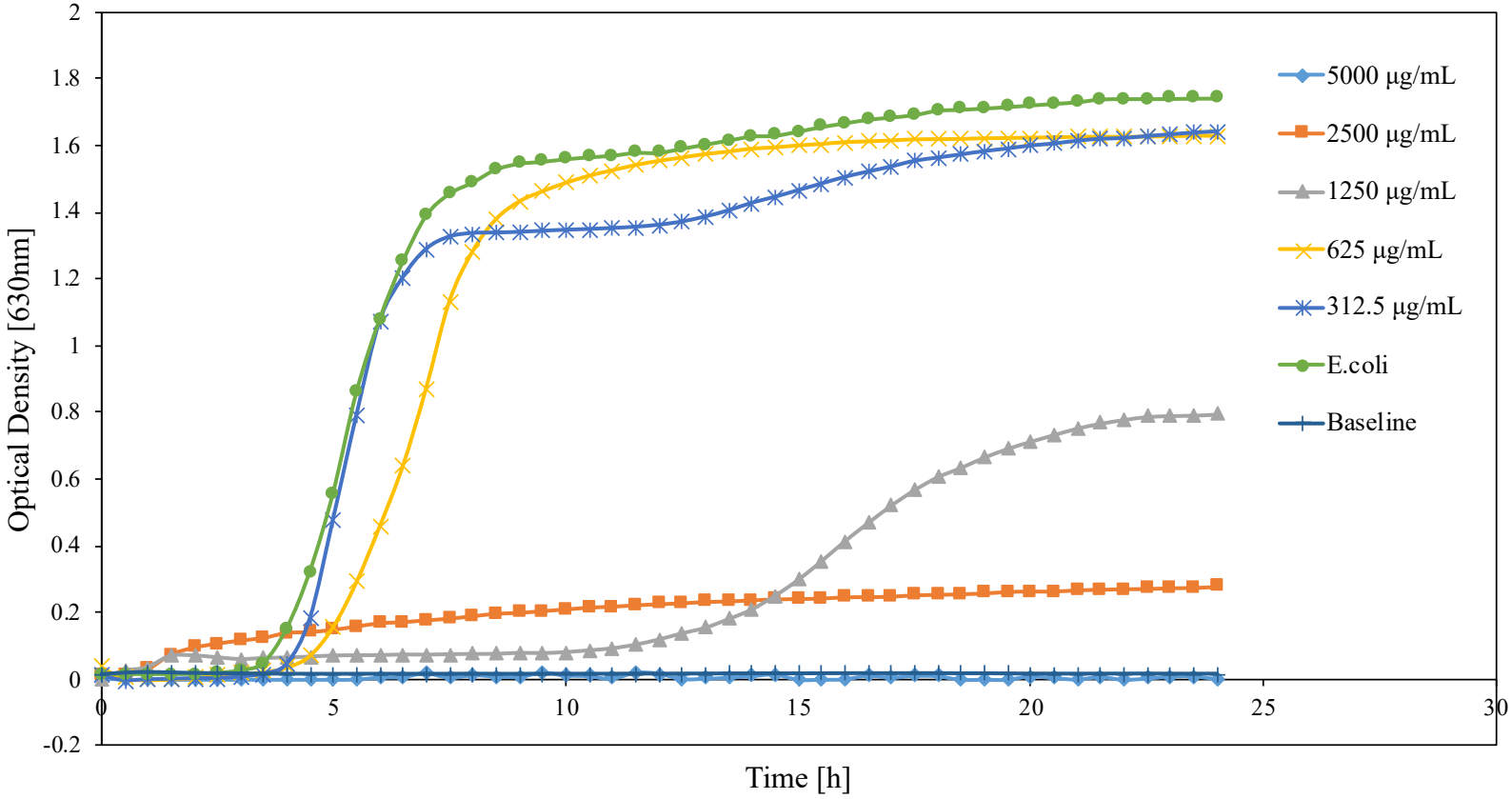

Figure C4. Growth curve of *E.coli* O157:H7 with 24 h treatment of 0.5TC@ZIF-8_PL nanoparticle solutions

APPENDIX D

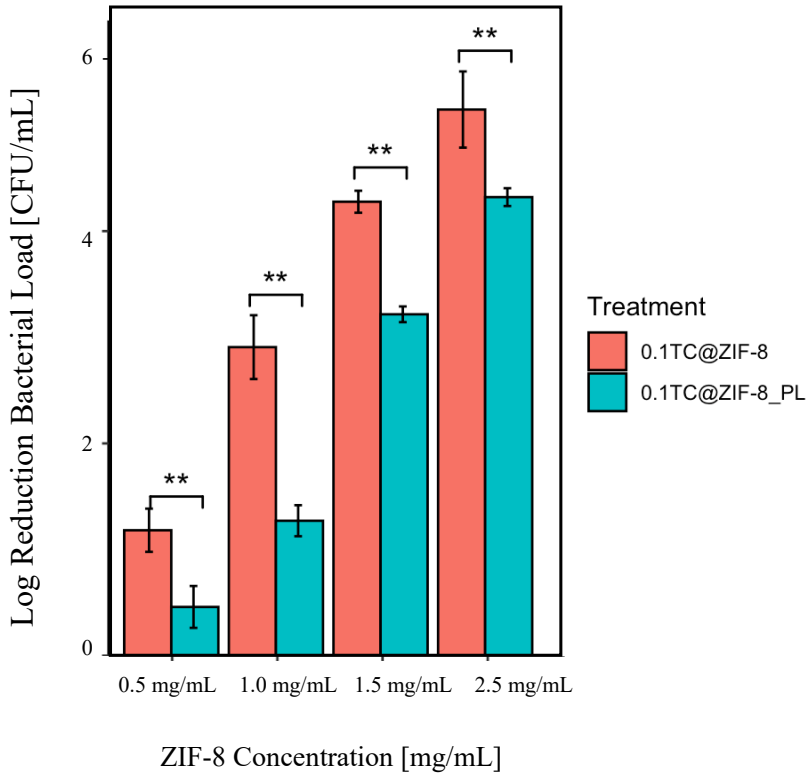

Figure D1. Comparison of antimicrobial log reductions of 0.1TC@ZIF-8 nanoparticles with and without PL coating at the same ZIF-8 concentration after 24h treatment at 35ºC. Initial *E.coli* O157:H7 population was 9 log CFU/mL.
The notations beyond the error bar means at the same ZIF-8 concentrations, the significant difference between groups with/without poly-lysine coating under student's t test: · $p>0.05$, * $0.01<p<0.05$, ** $0.001<p<0.01$, *** $p<0.001$

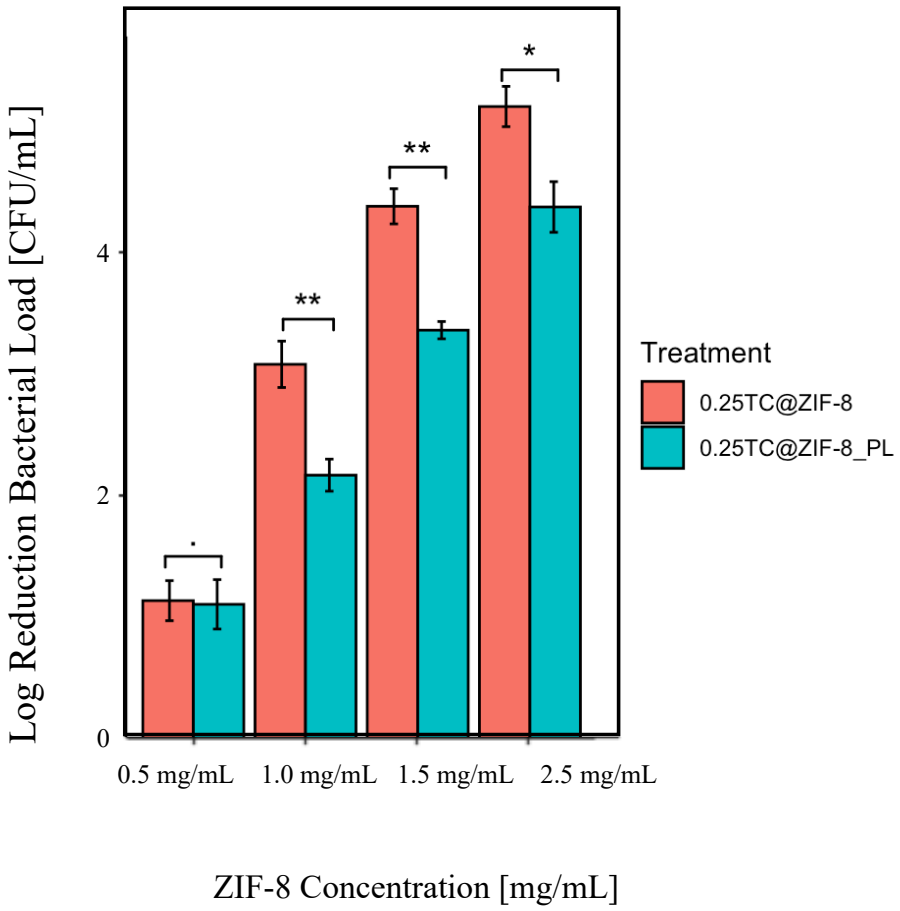

Figure D2. Comparison of antimicrobial log reductions of 0.25TC@ZIF-8 nanoparticles with and without PL coating at the same ZIF-8 concentration after 24h treatment at 35ºC. Initial *E.coli* O157:H7 population was 9 log CFU/mL.
The notations beyond the error bar means at the same ZIF-8 concentrations, the significant difference between groups with/without poly-lysine coating under student's t test: · $p>0.05$, * $0.01<p<0.05$, ** $0.001<p<0.01$, *** $p<0.001$

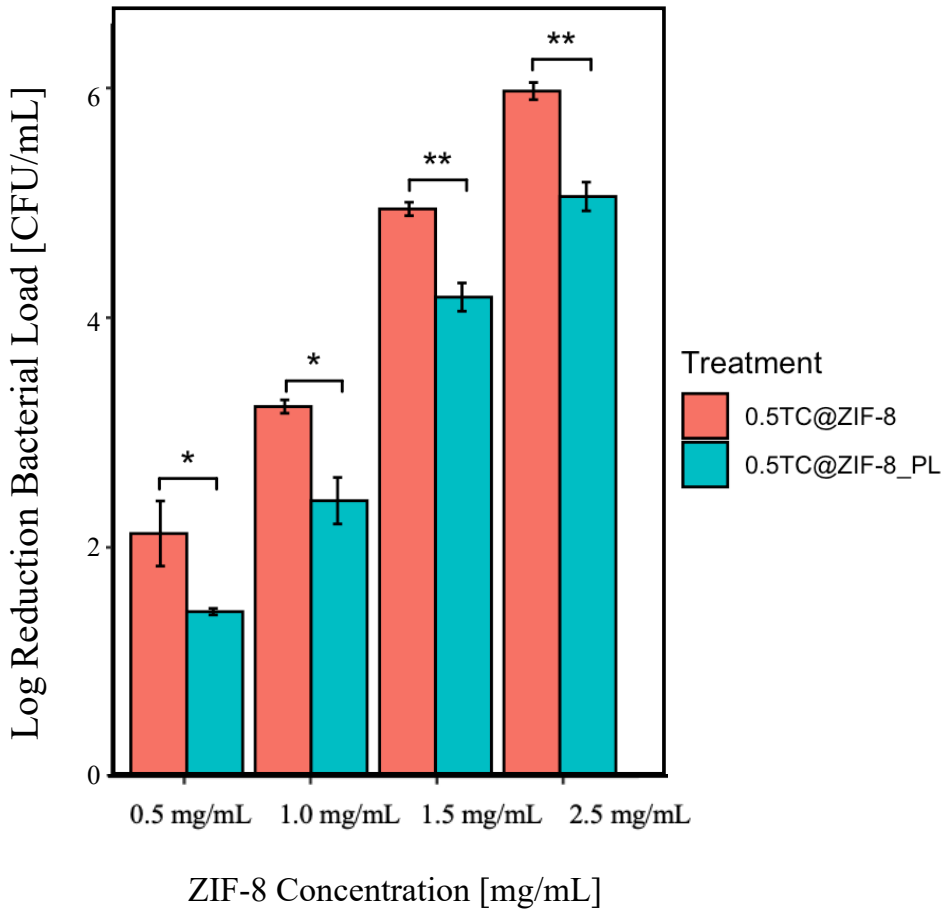

Figure D3. Comparison of antimicrobial log reductions of 0.5TC@ZIF-8 nanoparticles with and without PL coating at the same ZIF-8 concentration after 24h treatment at 35ºC. Initial *E.coli* O157:H7 population was 9 log CFU/mL.
The notations beyond the error bar means at the same ZIF-8 concentrations, the significant difference between groups with/without poly-lysine coating under student's t test: · $p>0.05$, * $0.01<p<0.05$, ** $0.001<p<0.01$, *** $p<0.001$